INPC 2013

INTERNATIONAL NUCLEAR PHYSICS CONFERENCE

FIRENZE, ITALY 2-7 JUNE 2013

Pasquale Di Nezza

INFN Frascati

LNF General Seminar 13/6/13

25^{th} three annual international conference

33 (3) plenary talks

88 (6) invited talks

217 (19) parallel talks

>400 posters

Topics

- ✧ Nuclear structure (C.Curceanu)
- ✧ Nuclear reactions
- ✧ Hot and dense nuclear matter (L.Cunqueiro)
- ✧ Fundamental symmetries and interactions in nuclei
- ✧ Hadron structure (M.Mirazita)
- ✧ Nuclear astrophysics
- ✧ Neutrinos and nuclei
- ✧ Hadrons in nuclei
- ✧ Nuclear physics based applications
- ✧ New facilities and instrumentation

Hadron Structure

Meson Spectroscopy in the World

- Many experiments in the world have studied and are studying the meson spectrum in the light-quark sector using different production processes

- proton-antiproton annihilation:
  Crystal Barrel at CERN, Panda at GSI, ...
- $e^+ e^-$ annihilation:
  LEP, Babar at SLAC, Belle at KEK, CLEO at Cornell, KLOE at Frascati, BES at Beijing, KLOE-II, Belle II at SuperKEKB,…
- proton-proton scattering:
  WA experiments at CERN, GAMS at Protvino, LHC, …
- pion beams on fixed target:
  E852 at BNL, VES at Protvino, COMPASS at Cern, …
- photoproduction experiments:
  CLAS at Jefferson Lab, GlueX and CLAS12 at Jefferson Lab

Scalar Mesons

Scalars are fundamental states because they represent the Higgs sector of strong interaction:

- same quantum numbers of the QCD vacuum
- responsible for chiral symmetry breaking

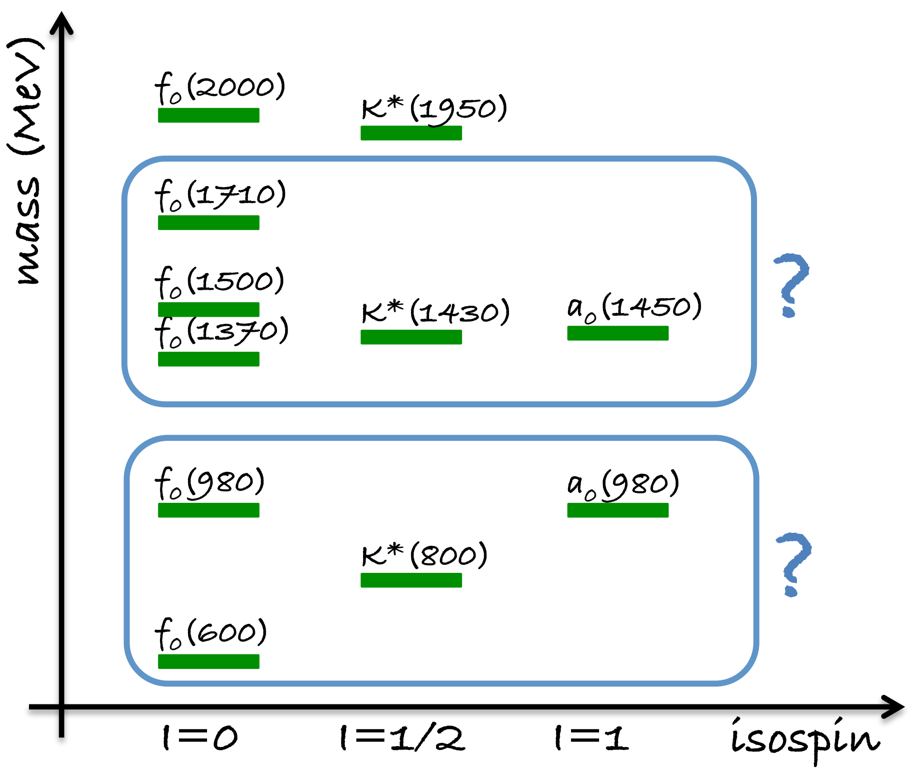

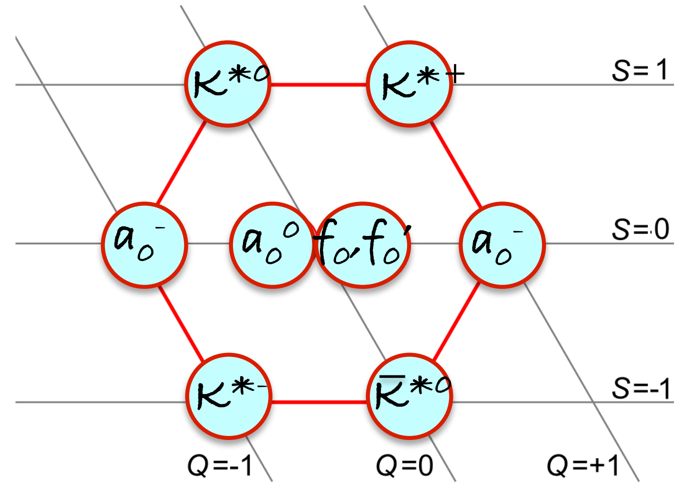

- The scalar meson nonet should be composed by a_0(I=1),K* (I=1/2), f_0 and f_0'(I=0), with the a_0 as lightest state and the f_0' showing a large strange content
- At present, given the I=1 and I=1/2 states that have been identified, there is an excess of I=0 states

Higher mass scalars

Abundance of I=0 states with unexpected decay patterns between 1.3 and 2 GeV led to speculate about the presence of a glueball in this sector

$f_0(1370)$
$f_0(1500)$
$f_0(1710)$
$f_0(2100)$
…

- Lower two states seen first by Crystal Barrel
- Higher mass states seen by WA102 and BES
- Discrepancies between different experimental observations
- *High statistics/high precision data needed!*

New high statistics data set from BESIII in Beijing:

- clear structures in the ηη mass spectrum from J/ψ radiative decays
- full partial wave analysis to isolate S wave contribution
- $f_0(1710)$ and $f_0(2100)$ are dominant scalars
- $f_0(1500)$ exists (8.2 σ)
- $f_0(1710)$ and $f_0(2100)$ strength ~10x larger than $f_0(1500)$

Additional data expected in the near future from this and other experiments can lead to a full understanding of the scalar sector

BES, arXiv:1301.0053, to appear in PRD

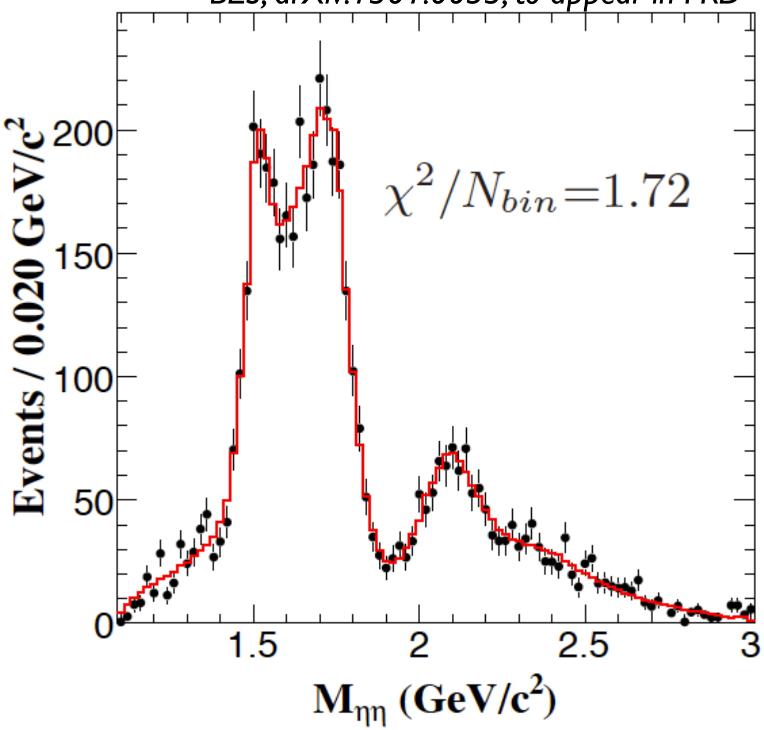

Beyond the quark model…Exotics

QCD tells us that bound states have to be color neutral but does not prohibit the existence of state with unconventional quark-gluon configurations as tetraquarks, glueballs or hybrids

- Several phenomenological models predict the existence of such states and give indications of masses and decays
- Supporting evidence is provided by Lattice QCD calculations
- Experimental evidence has been searched in many laboratories
  - X(3872) observed at B-factories interpreted as tetraquark
  - Indication of hybrids below 2 GeV reported by several experiments
  - …

- If unambiguously confirmed, these state would provide the mean to further investigates aspects of QCD as confinement and gluonic excitations

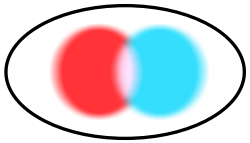

regular meson

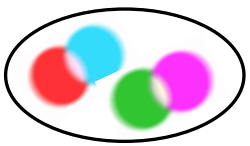

tetraquarks

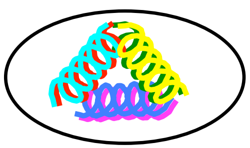

glueball

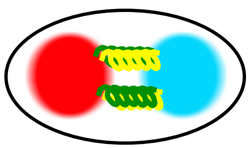

hybrid

J. Dudek et al., Phys. Rev. D84, 074023 (2011)

Lattice QCD

Predictions of the meson spectrum from Lattice QCD are now available

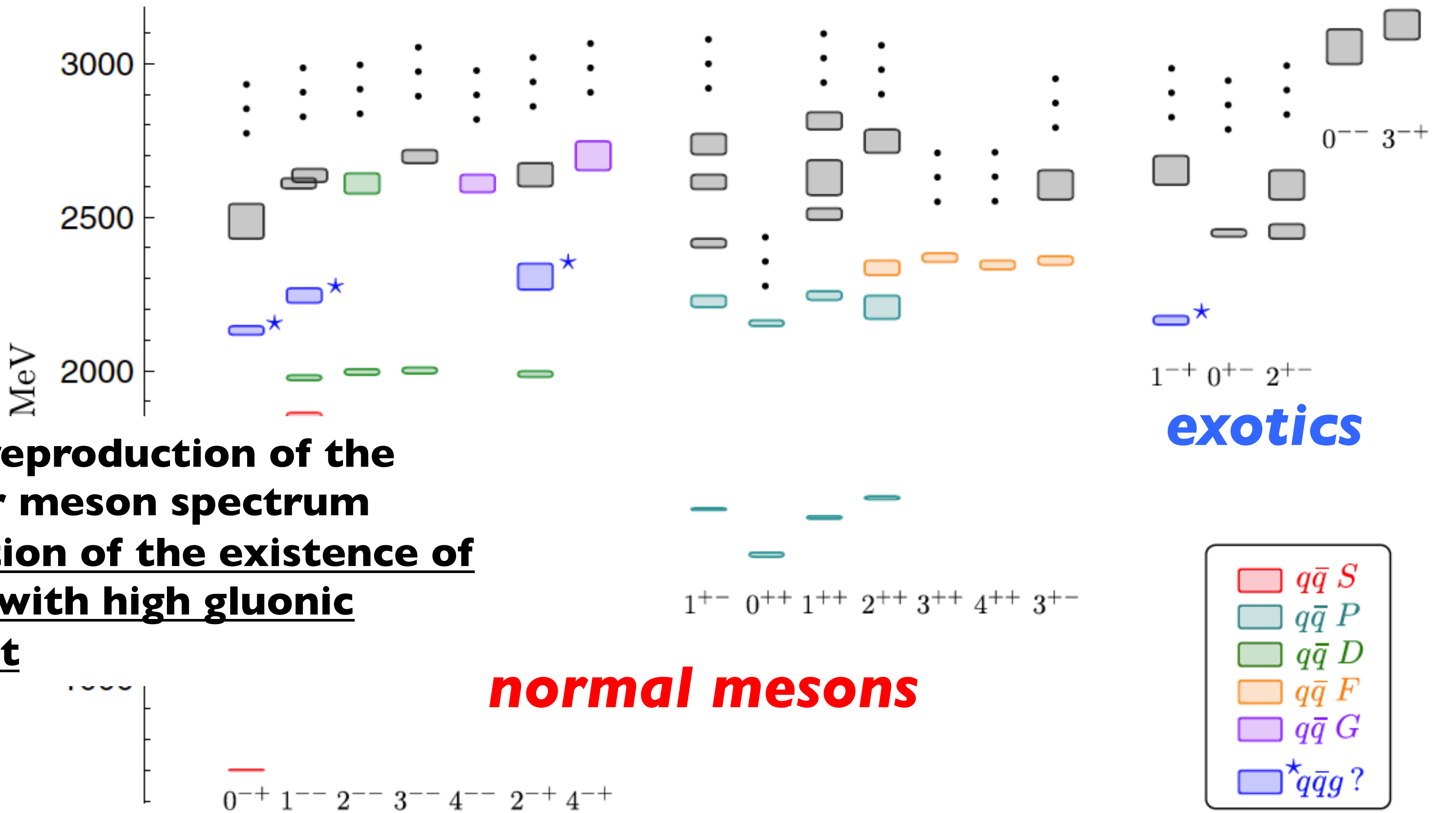

- **Good reproduction of the regular meson spectrum**
- **Indication of the existence of states with high gluonic content**

isovector mesons, m_π~700 MeV

The exotic $\pi_1(1600)$

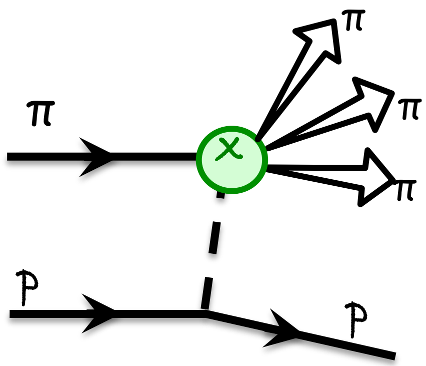

Exotic signal reported by BNL-E852 experiment in the analysis of the 3 pion final state

Opposite findings reported by the CLAS Collaboration in photo-production

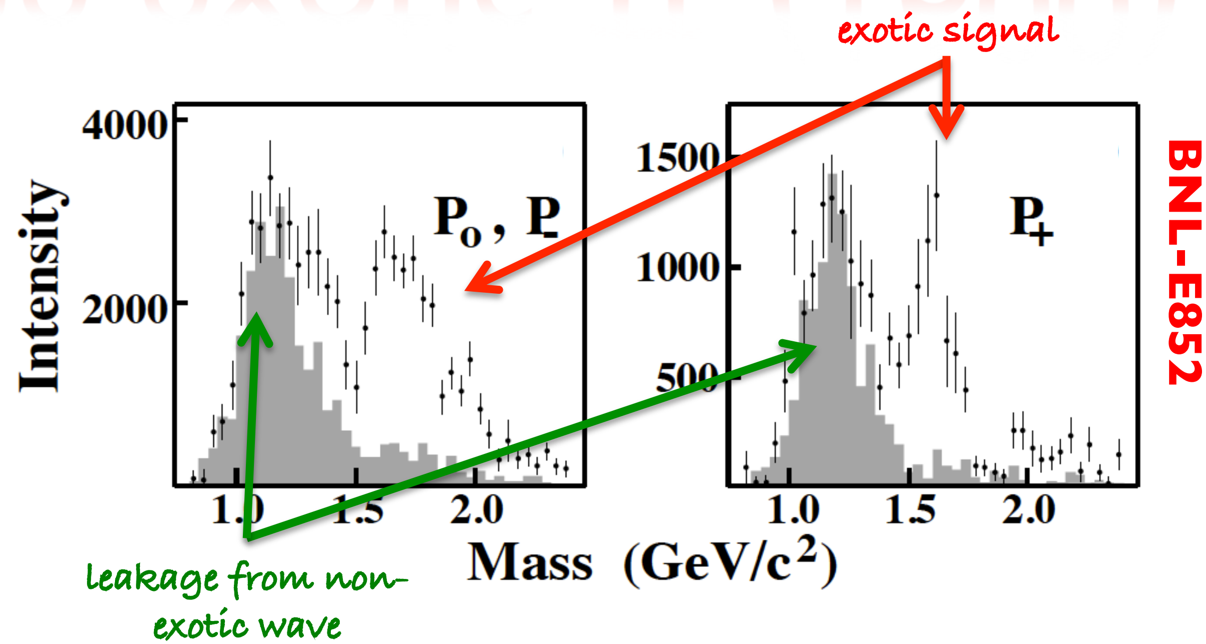

P_+ or $M^{\varepsilon}=1^+$ natural-parity exchange

$P_{0,-}$ or $M^{\varepsilon}=0^-,1^-$ unnatural-parity exchange

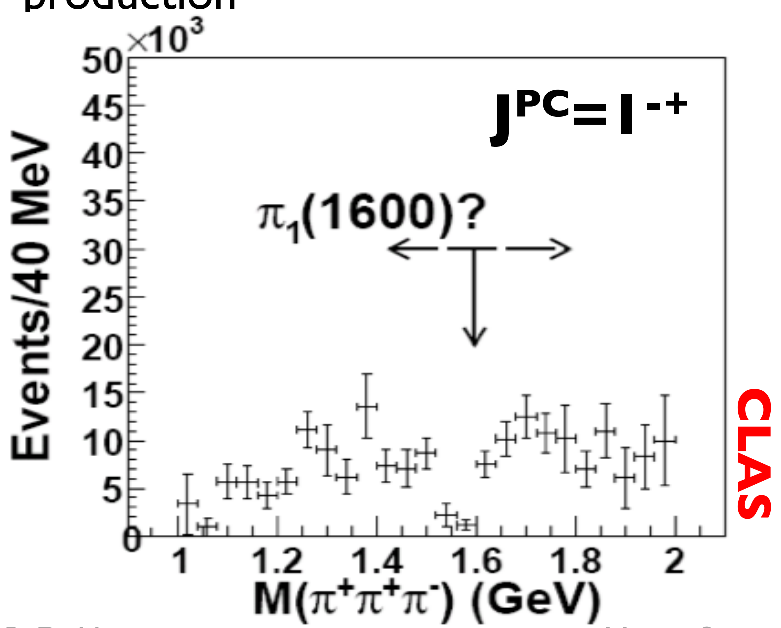

Significant intensity in the 1^{-+} wave with clear phase motion with respect to the 2^{-+}

$$M = \left(1.593 \pm 0.080^{+0.029}_{-0.047}\right) GeV$$

$$\Gamma = \left(0.168 \pm 0.020^{+0.150}_{-0.012}\right) GeV$$

The Nucleon Spin Puzzle

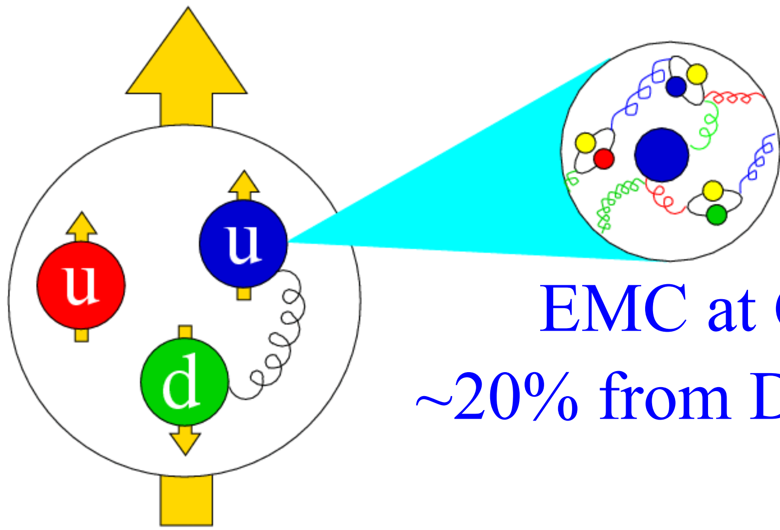

EMC at CERN (85):

~20% from Deep Inelastic Scattering (DIS)

$$\int_{0.05}^{0.2} \Delta g(x)\,dx = 0.1 \pm^{0.06}_{0.07}$$

RHIC Spin & SIDIS

DIS (DSSV-2009)

$$\int_{0.001}^{1} \Delta\Sigma(x)\,dx = 0.366 \pm^{0.042}_{0.062}$$

Proton's spin

$$\frac{1}{2} \equiv \underbrace{\frac{1}{2}\sum(q_f^{+} - q_f^{-}) + L_q}_{J_q} + \underbrace{\Delta G + L_g}_{J_g}$$

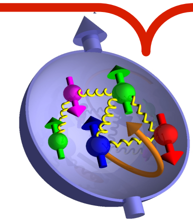

Understanding of the orbital motion of partons crucial!!!

Spin "pizza"

$$\frac{1}{2} \equiv \frac{\Delta q}{2} + L_q + \Delta G + L_g$$

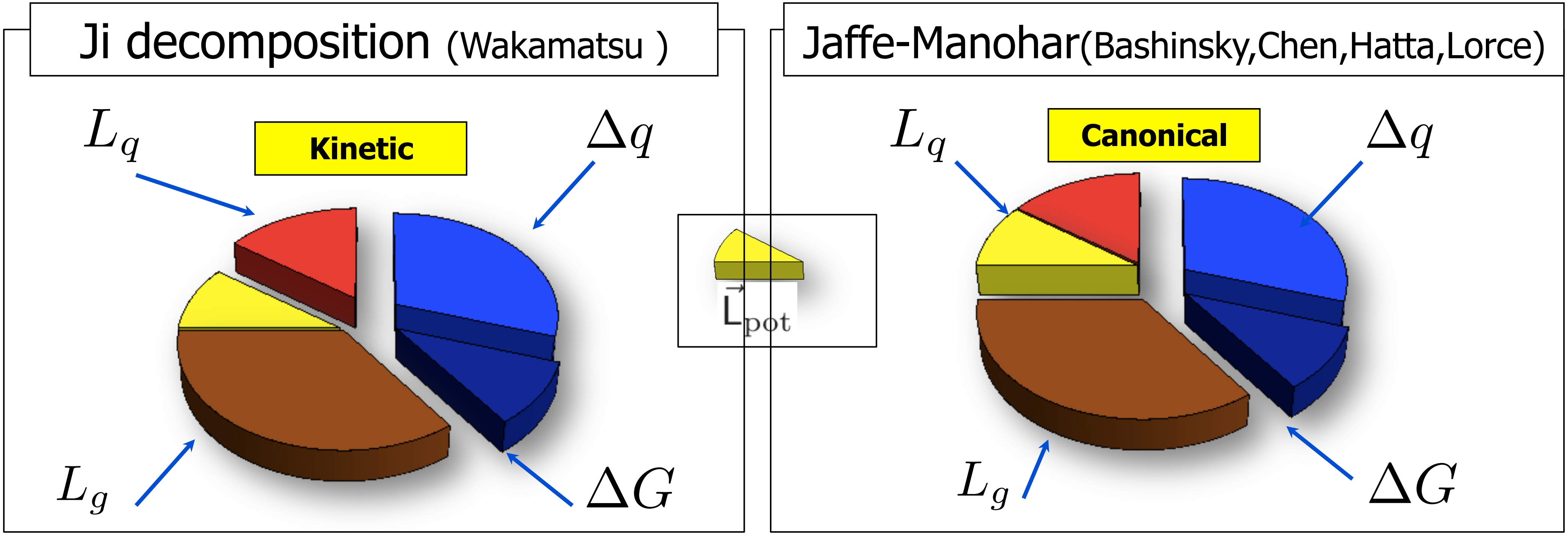

The quark spin and gluon spin contributions are common to both the Bashinsky-Jaffe decomposition (LF) and the improved Ji decomposition .

Polyakov et al, ,Ji,Xiong &Yuan, Hatta,Lorce,..

potential orbital momentum, can be interpreted as the orbital momentum generated due to the color force on quark

Need to go to twist-3 to compare kinetic and canonical quark OAM

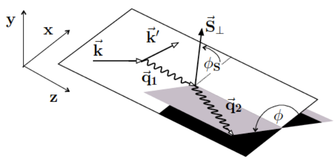

3D structure: GPDs

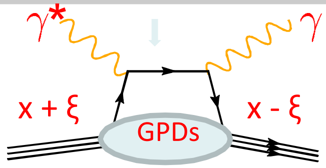

$\sigma_{LU}^{\sin\phi}$

$\sigma_{UL}^{\sin\phi}$

$\sigma_{UT}^{\cos\phi}$

	U	L	T
U	H		$\mathcal{E}_T$
L		$\tilde{H}$	
T	E		$H_T, \tilde{H}_T$

ep➔e’ pπ^0

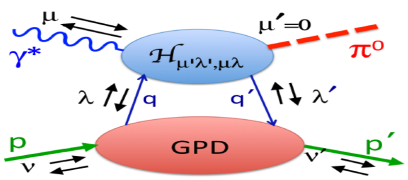

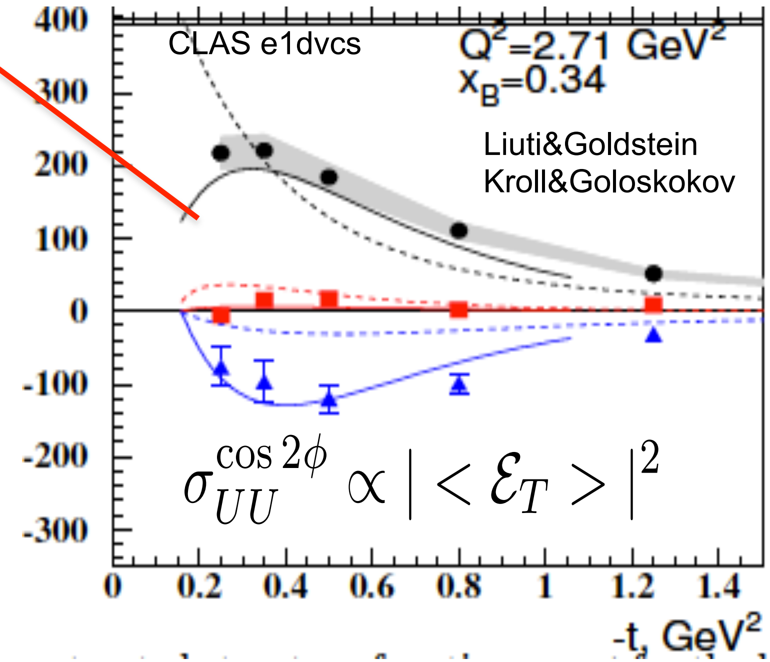

Asymmetries measured at HERMES & JLAB
More measurements at JLab, Compass, RHIC

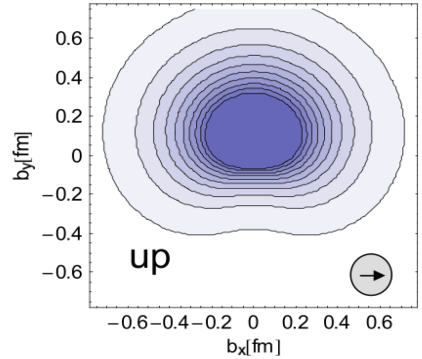

Lattice (QCDSF)

Michel Guidal
Francois-Xavier Girod

Transverse photon dominates the x-section for exclusive π^0 production

Spin-azimuthal asymmetries in hard exclusive production of photons and pions give access to underlying GPDs

Flavor-dependent multiplicities

A. Signori (Evolution-2013)

Using a set of Gaussian fits of the Multiplicities from HERMES and COMPASS

1. One-photon exchange
2. Small transverse momenta
3. Leading-twist (LT): not including powers of M/Q
4. Leading-order (LO): zero-order α^2_S

Introducing a flavor dependence

$$f_1^q(x,k_T) = f_1^q \frac{1}{\pi\mu_q^2} e^{-\frac{k_T^2}{\mu_q^2}}$$

$$D_1^{q\to h}(x,k_T) = D_1^{q\to h} \frac{1}{\pi\sigma_h^2} e^{-\frac{p_T^2}{\sigma_h^2}}$$

$$\boxed{\mu^2_{sea} > \mu^2_d > \mu^2_u}$$

$$\boxed{\sigma^2_{unfavored} > \sigma^2_{favored}}$$

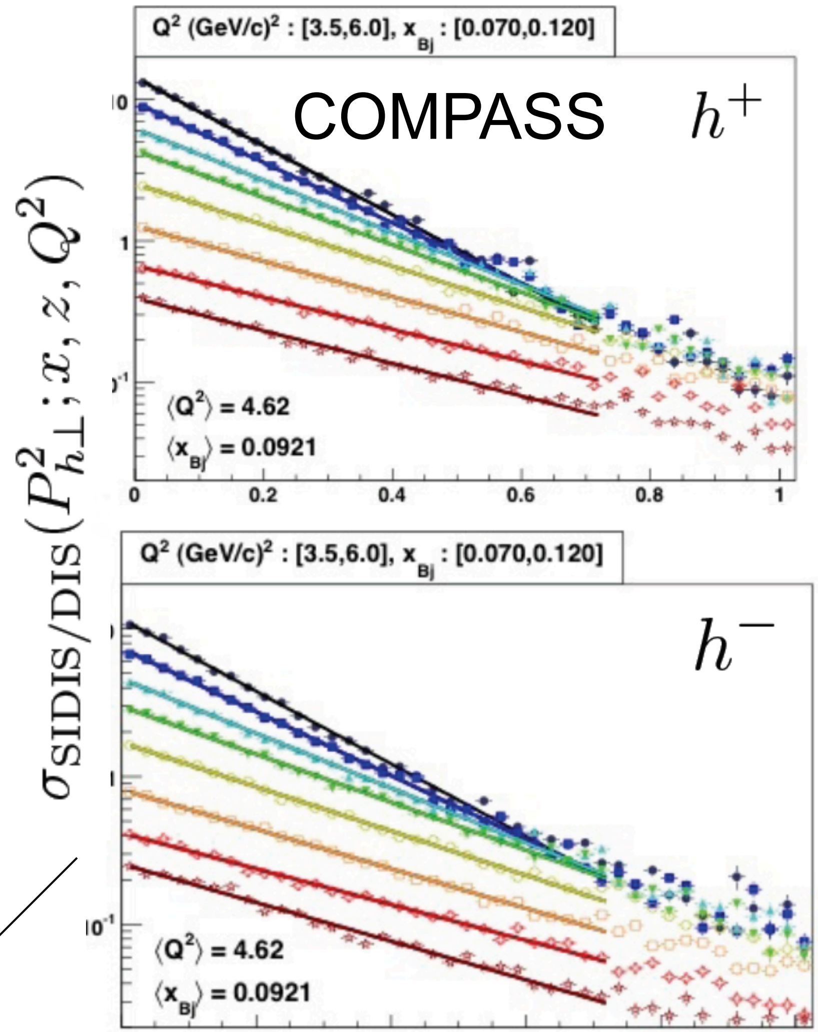

Large error bars
HERMES/COMPASS not consistent

Strong flavor dependence of transverse momenta in hadronization was predicted from model studies

Hrayr Matevosyan

COMPASS

SIDIS cross section: unpolarized part

$$\frac{d\sigma}{dx\,dy\,d\psi\,dz\,d\phi_h\,dP_{h\perp}^2} =$$

$$\frac{\alpha^2}{xyQ^2}\frac{y^2}{2(1-\varepsilon)}\left(1+\frac{\gamma^2}{2x}\right)\Big\{F_{UU,T}+\varepsilon F_{UU,L}+\sqrt{2\varepsilon(1+\varepsilon)}\cos\phi_h F_{UU}^{\cos\phi_h}$$

$$+\varepsilon\cos(2\phi_h)F_{UU}^{\cos 2\phi_h}+\lambda_e\sqrt{2\varepsilon(1-\varepsilon)}\sin\phi_h F_{LU}^{\sin\phi_h}$$

$$+S_\parallel\left[\sqrt{2\varepsilon(1+\varepsilon)}\sin\phi_h F_{UL}^{\sin\phi_h}+\varepsilon\sin(2\phi_h)F_{UL}^{\sin 2\phi_h}\right]$$

$$+S_\parallel\lambda_e\left[\sqrt{1-\varepsilon^2}F_{LL}+\sqrt{2\varepsilon(1-\varepsilon)}\cos\phi_h F_{LL}^{\cos\phi_h}\right]$$

$$+|\boldsymbol{S}_\perp|\left[\sin(\phi_h-\phi_S)\left(F_{UT,T}^{\sin(\phi_h-\phi_S)}+\varepsilon F_{UT,L}^{\sin(\phi_h-\phi_S)}\right)\right.$$

$$+\varepsilon\sin(\phi_h+\phi_S)F_{UT}^{\sin(\phi_h+\phi_S)}+\varepsilon\sin(3\phi_h-\phi_S)F_{UT}^{\sin(3\phi_h-\phi_S)}$$

$$\left.+\sqrt{2\varepsilon(1+\varepsilon)}\sin\phi_S F_{UT}^{\sin\phi_S}+\sqrt{2\varepsilon(1+\varepsilon)}\sin(2\phi_h-\phi_S)F_{UT}^{\sin(2\phi_h-\phi_S)}\right]$$

$$+|\boldsymbol{S}_\perp|\lambda_e\left[\sqrt{1-\varepsilon^2}\cos(\phi_h-\phi_S)F_{LT}^{\cos(\phi_h-\phi_S)}+\sqrt{2\varepsilon(1-\varepsilon)}\cos\phi_S F_{LT}^{\cos\phi_S}\right.$$

$$\left.\left.+\sqrt{2\varepsilon(1-\varepsilon)}\cos(2\phi_h-\phi_S)F_{LT}^{\cos(2\phi_h-\phi_S)}\right]\right\},$$

3 independent modulations in the hadron azimuthal distribution

Sivers

Collins

twist-2 contribution

Remaining four can be interpreted as twist-3 contributions

From A. Bacchetta et al., JHEP 0702:093,2007. e-Print: hep-ph/0611265

Unpolarized asymmetries, results on deuterium

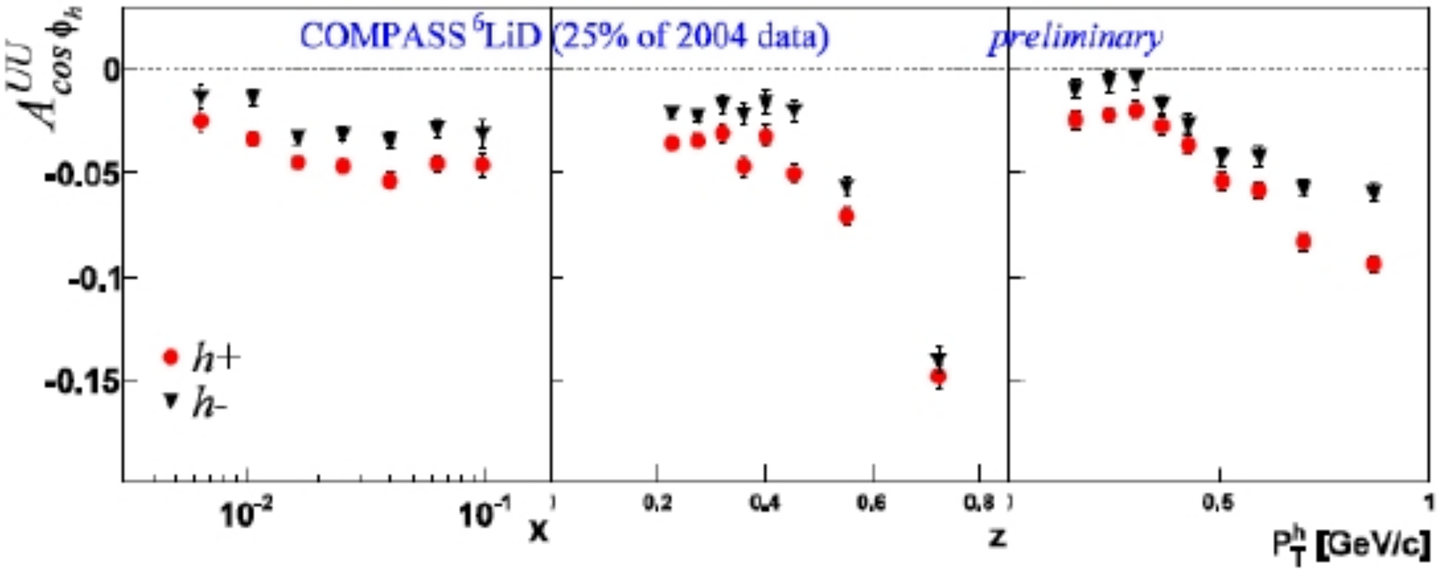

cos Φ

- Large signal over all the x range
- Strong z dependence, for z > 0.5

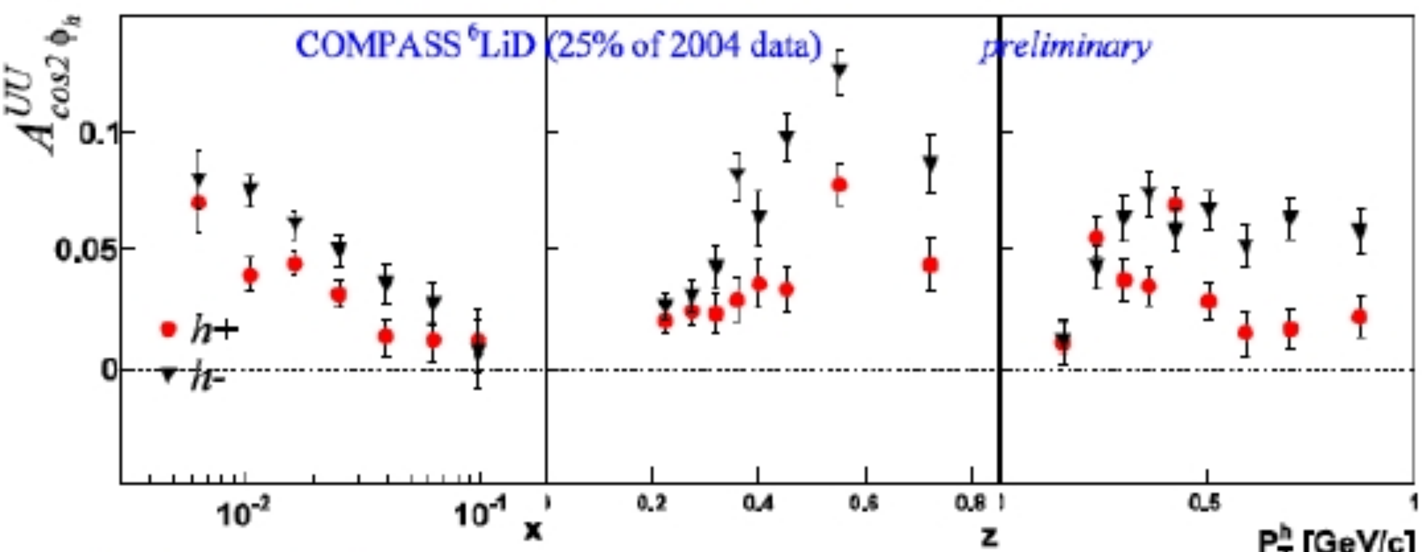

cos 2Φ

- Different for positive and negative hadrons
- Large signal at small x
- Strong dependence on x, z, and p_T, difficult to describe

$sys \approx 2 \cdot stat$

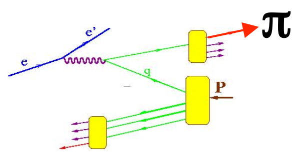

SIDIS at JLab12

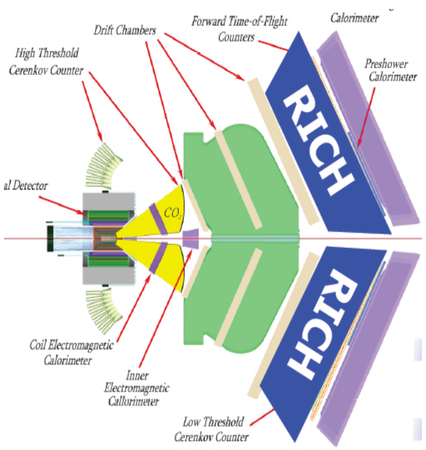

CLAS12

E12-06-112: π^+,π^-,π^0
E12-09-008: K^+, K^-, K^0

E12-07-107: π^+,π^-,π^0
E12-09-009: K^+,K^-,K^0

C12-11-111: π^+,π^-,π^0 K^+, K^-

H_2, NH_3, HD

Proton

Quark spin polarization / Nucleon polarization

N \ q	U	L	T
U	f_1		$h_1^\perp$
L		g_1	$h_{1L}^\perp$
T	$f_{1T}^\perp$	g_{1T}	h_1 $h_{1T}^\perp$

Hall C | Hall A

E12-09-017: π^+,π^-, K^+,K^-
C12-11-102: π^0

HMS SHMS

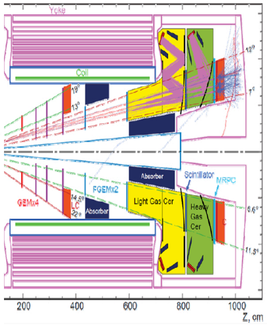

C12-11-108: π^+,π^-

Solid

H_2 | NH_3

CLAS12

E09-008: π^+,π^-,π^0 K^+, K^-,K^0

E07-107: π^+,π^-,π^0
E09-009: K^+,K^-,K^0

D_2, ND_3

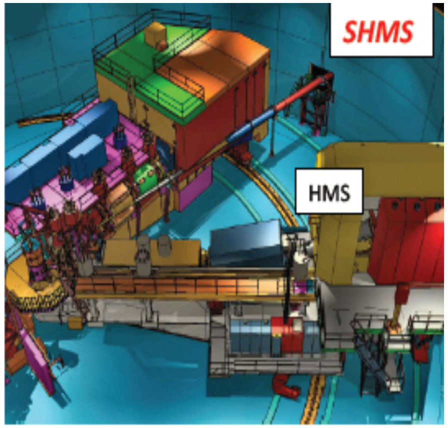

D_2

Quark spin polarization / Nucleon polarization

N \ q	U	L	T
U	f_1		$h_1^\perp$
L		g_1	$h_{1L}^\perp$
T	$f_{1T}^\perp$	g_{1T}	h_1 $h_{1T}^\perp$

Hall C

E12-09-017: π^+,π^-, K^+,K^-
C12-11-102: π^0

HMS SHMS

D_2

^3He

Quark spin polarization / Nucleon polarization

N \ q	U	L	T
U	f_1		$h_1^\perp$
L		g_1	$h_{1L}^\perp$
T	$f_{1T}^\perp$	g_{1T}	h_1 $h_{1T}^\perp$

Hall A

E12-07-007: π^+,π^- | Solid

E10-006: π^+,π^-
E12-09-018: π^+,π^-, K^+,K^-

Solid
SBS

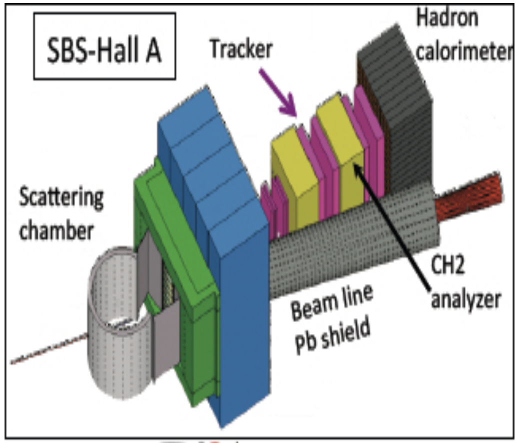

☞ Larry Cardman

M.Mirazita - LNF

Sivers Asymmetry in CLAS12 for π

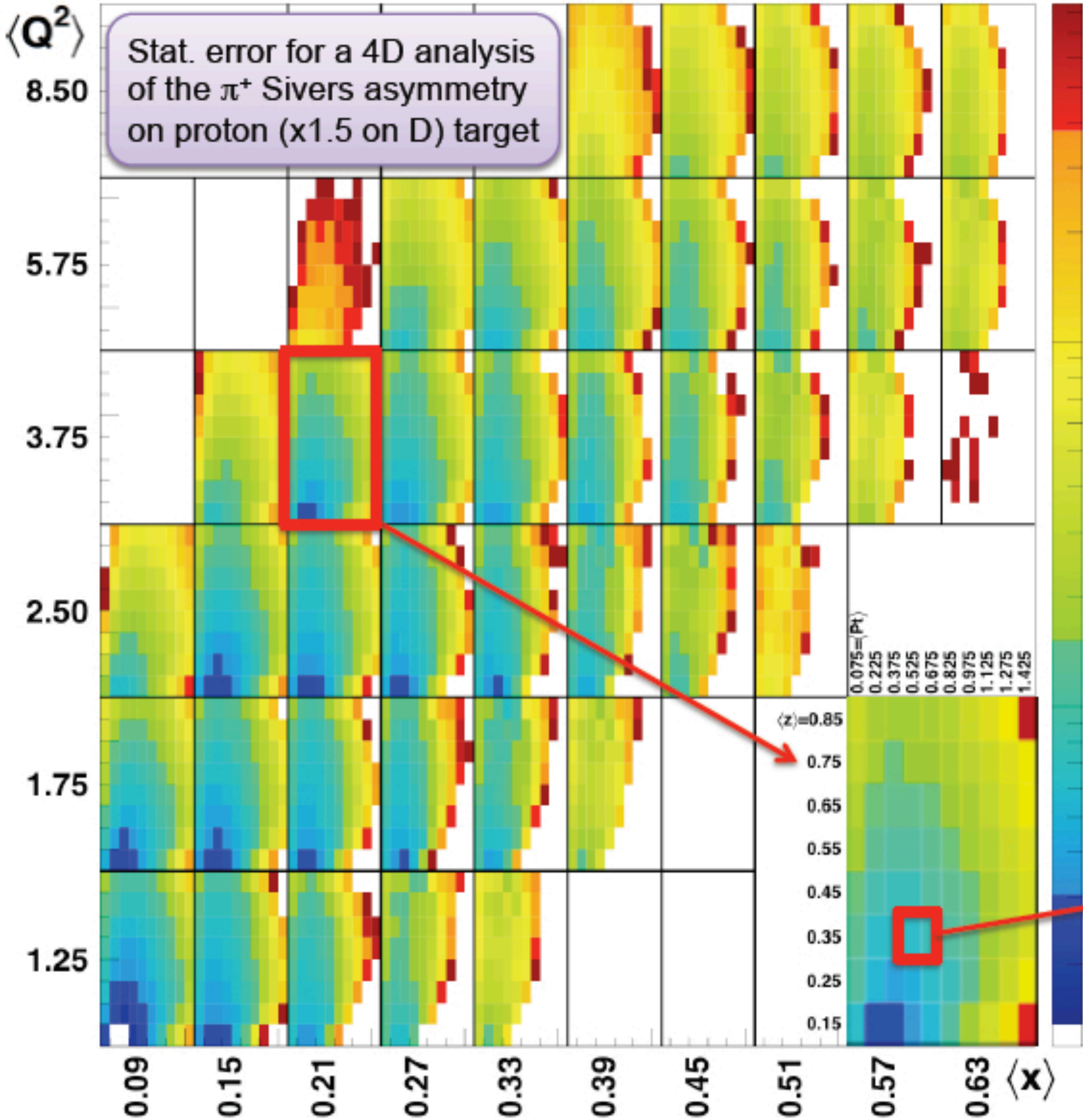

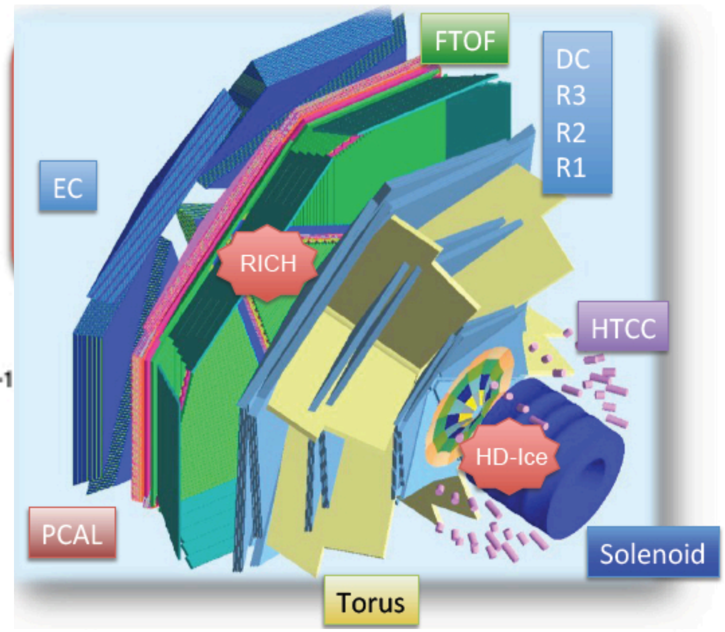

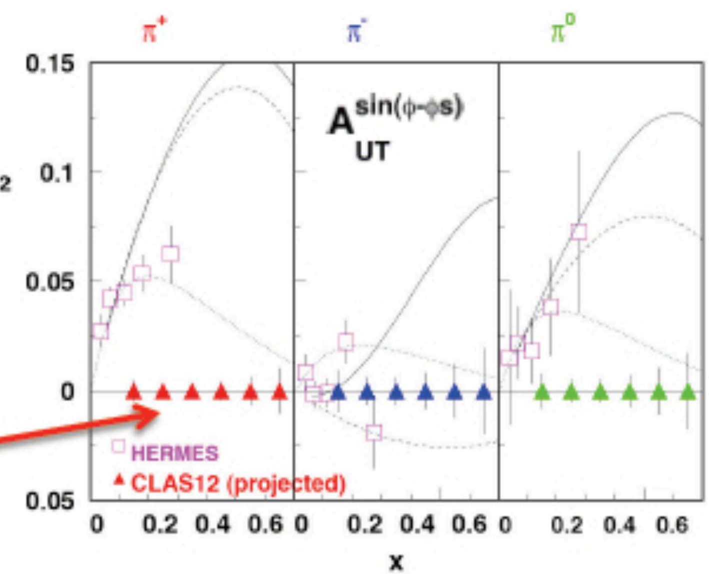

Curves from hep-ph/0507266 and hep-ph/0507181

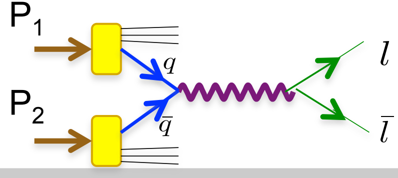

Drell-Yan

a test of QCD

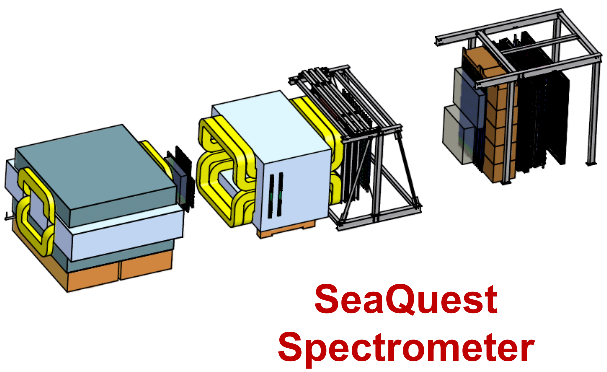

SIDIS Drell-Yan

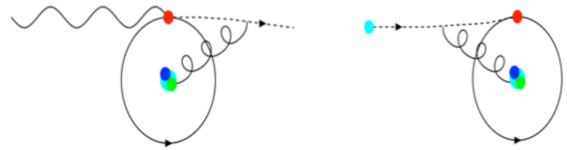

$$f_{1T}^{\perp q}(SIDIS) = -f_{1T}^{\perp q}(DY)$$

Low Drell-Yan cross section requires a high intensity beams

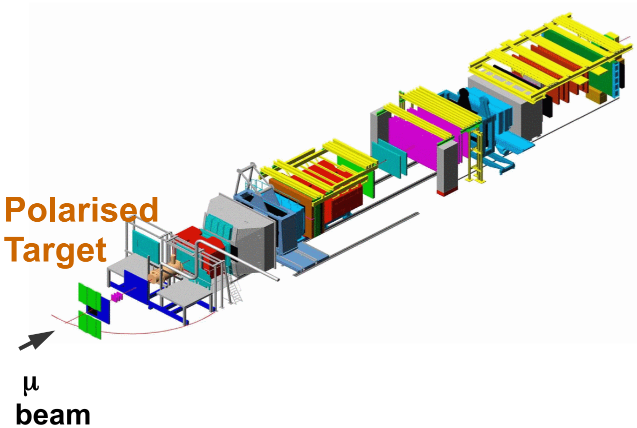

Nuclotron based Ion Collider fAcility

Proposed for consideration

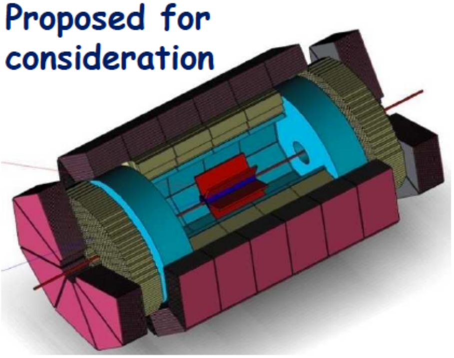

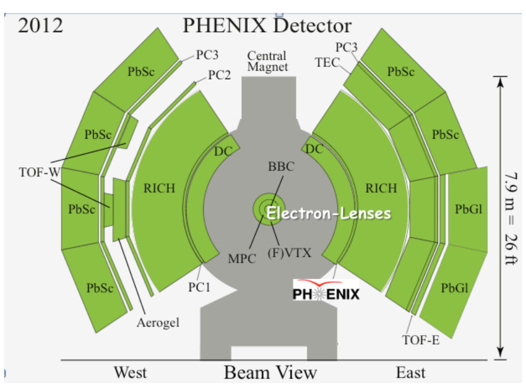

Clean probe to study hadron structure:

- convolution of parton distributions
- no QCD final state effects
- no fragmentation process

Feasibility studies

Several tests were already performed, showing the radiation conditions; the background reduction when using a hadron absorber; the concept of the dimuon trigger; detector occupancies and trigger rates.

2009: π^- beam 190 GeV/c on a 2-cells polyethylene target. Setup including hadron absorber and a beam plug. 3 days of data-taking.

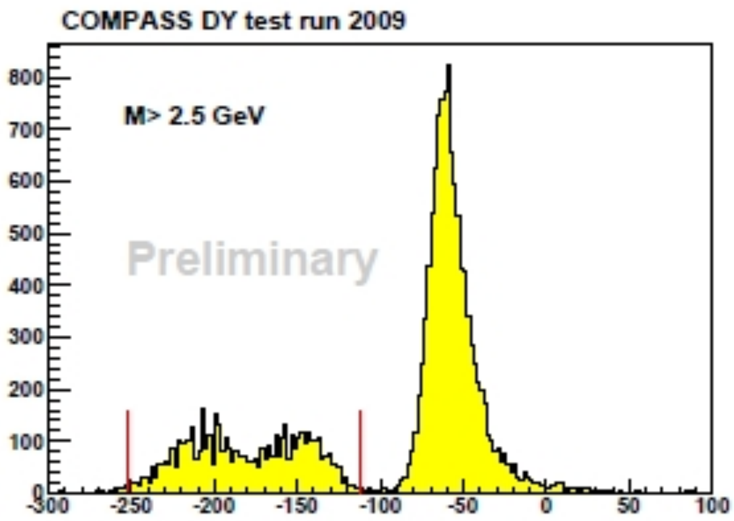

Reasonable Z_{vertex} separation, allowing to distinguish the 2 target cells and the absorber.

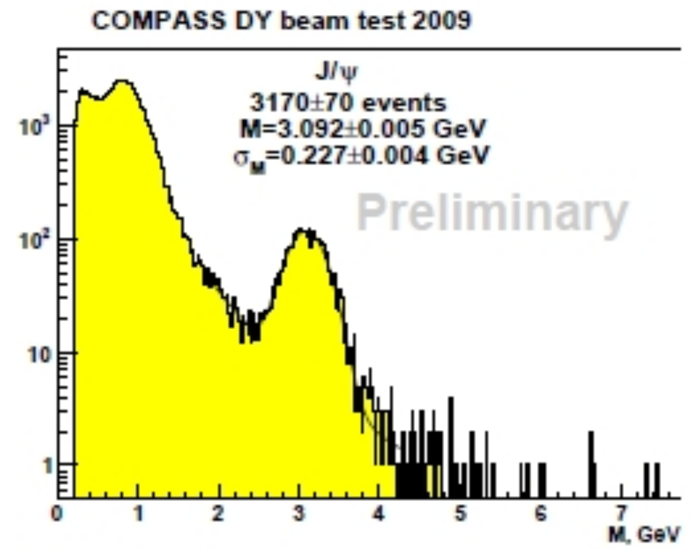

Mass resolution as expected.
J/ψ events match the expected yield.

SPECIAL RESEARCH CENTRE FOR THE SUBATOMIC STRUCTURE OF MATTER

INPC 2013

Firenze, Italia: June 2-7, 2013.

MONTE CARLO APPROACH TO FRAGMENTATION FUNCTIONS USING THE *NJL-JET MODEL*

Hrayr Matevosyan

Collaborators:
A.W. Thomas & W. Bentz

CoEPP ARC Centre of Excellence for Particle Physics at the Terascale

THE UNIVERSITY of ADELAIDE

OUTLOOK

- **Introduction.**
- **Monte Carlo Approach within the *quark-jet formalism*.**
- ***Developments:***
  - ***Transverse Momentum: Access to TMD PDFs.***
  - ***Polarization: Collins Effect.***
  - ***Two-hadron correlations: Dihadron Fragmentations.***
- **Conclusions.**

MOTIVATION

- Providing guidance based on a sophisticated model for applications to problems where phenomenology is difficult/ inadequate.
- A *robust* and *expandable* Monte Carlo framework for describing both *Favored and Unfavored* fragmentation functions in multi-hadron emission process using microscopic quark models as input.
- NO model parameters fitted to fragmentation data!
- Momentum and quark flavor conservation is imposed.
- Extensions to TMD, Polarized Quark Fragmentation, Dihadron Fragmentations.
- Allows to investigate various aspects: convergence with the number of emitted hadrons, effects of various cuts, etc.

COLLINS FRAGMENTATION FUNCTION FROM NJL-JET

H.M.,Bentz, Thomas, PRD.86:034025, 2012.

- **Extend the NJL-jet Model to Include the Quark's Spins.**

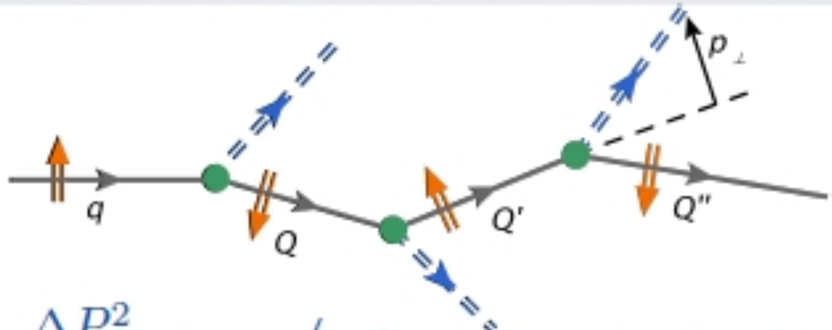

$$D_{h/q^\uparrow}(z, P_\perp^2, \varphi)\, \Delta z\, \frac{\Delta P_\perp^2}{2}\, \Delta\varphi = \left\langle N_{q^\uparrow}^h(z, z+\Delta z; P_\perp^2, P_\perp^2 + \Delta P^2; \varphi, \varphi + \Delta\varphi) \right\rangle$$

- **Model Calculated Elementary Collins Function as Input**

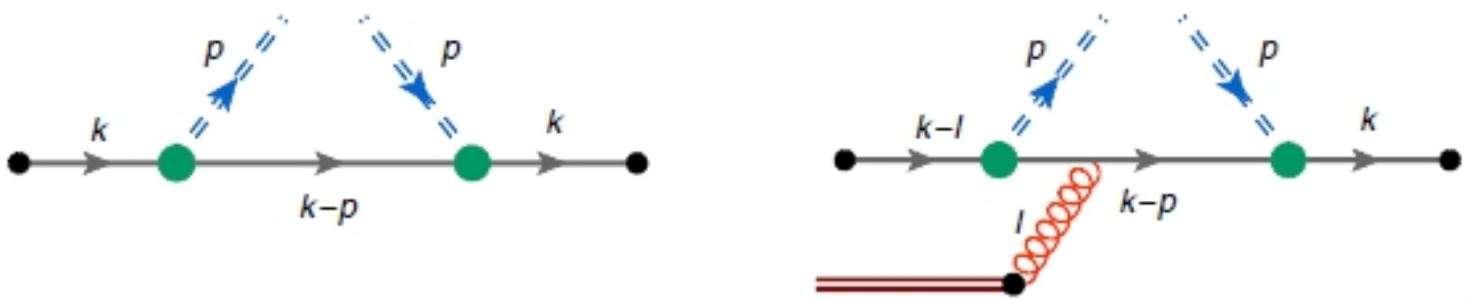

- ***Spin non-flip and flip probabilities:***

$$\boxed{|a_1|^2 \sim l_x^2,\ |a_{-1}|^2 \sim l_y^2 + (M_2 - (1-z)M_1)^2}$$

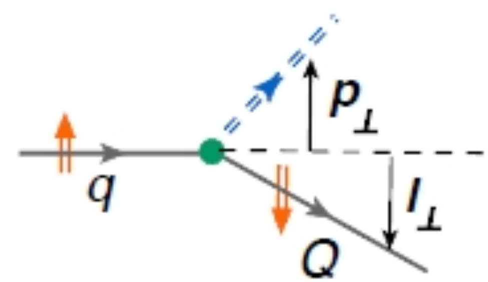

1/2 MOMENT OF COLLINS FUNC.

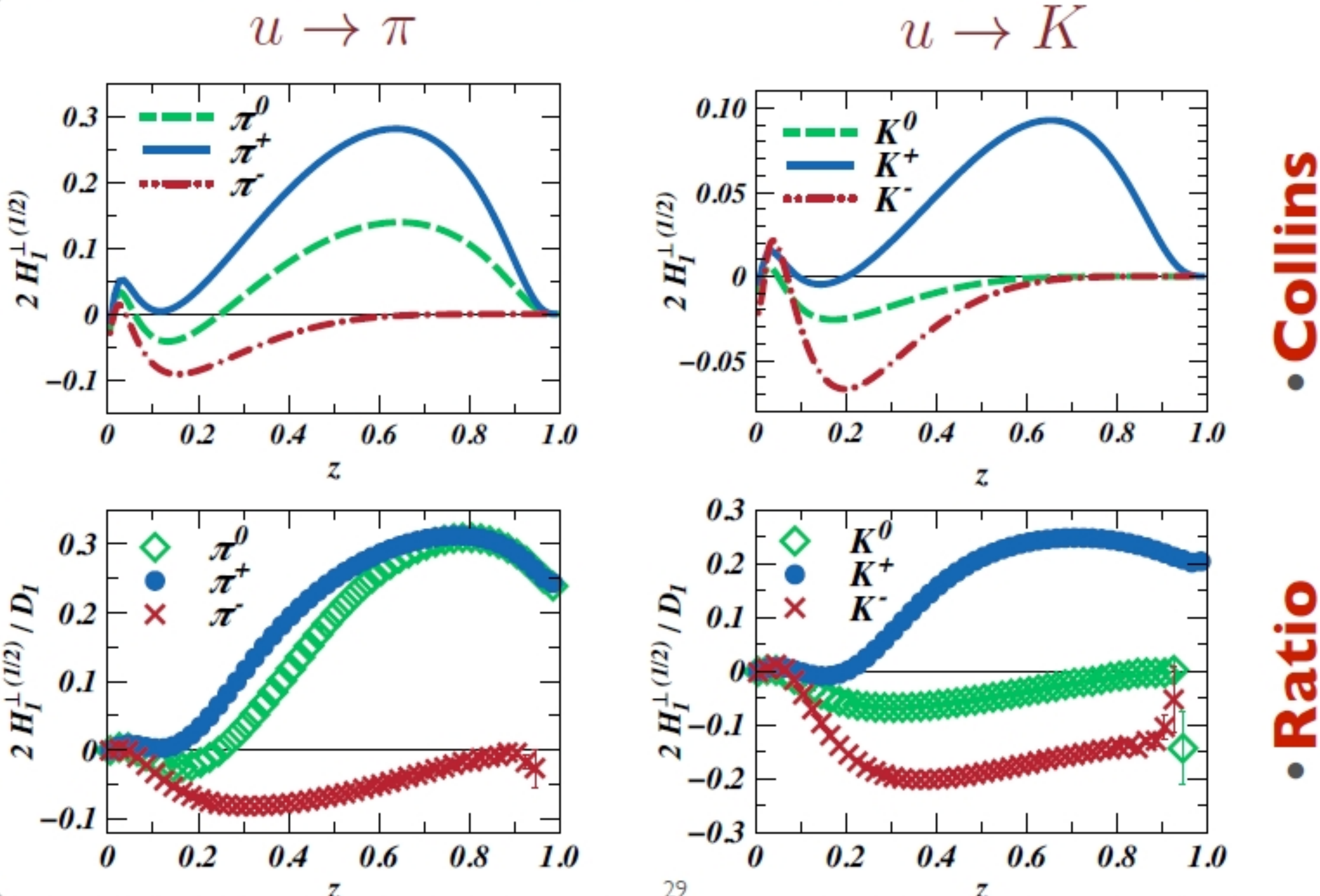

Polarized pp collisions at RHIC

$$A_{LL} = \frac{\sigma^{++} - \sigma^{+-}}{\sigma^{++} + \sigma^{+-}} \propto \frac{\Delta f_a \Delta f_b}{f_a f_b} \hat{a}_{LL}$$

Δf: polarized parton distribution functions

$\frac{\Delta G}{G} \frac{\Delta G}{G}$ $\frac{\Delta q}{q} \frac{\Delta G}{G}$ $\frac{\Delta q}{q} \frac{\Delta q}{q}$

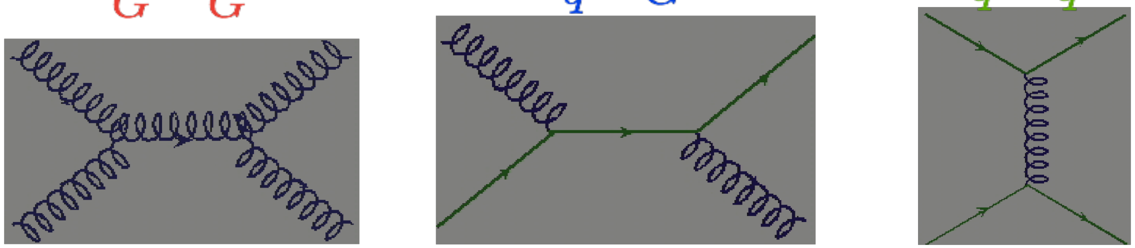

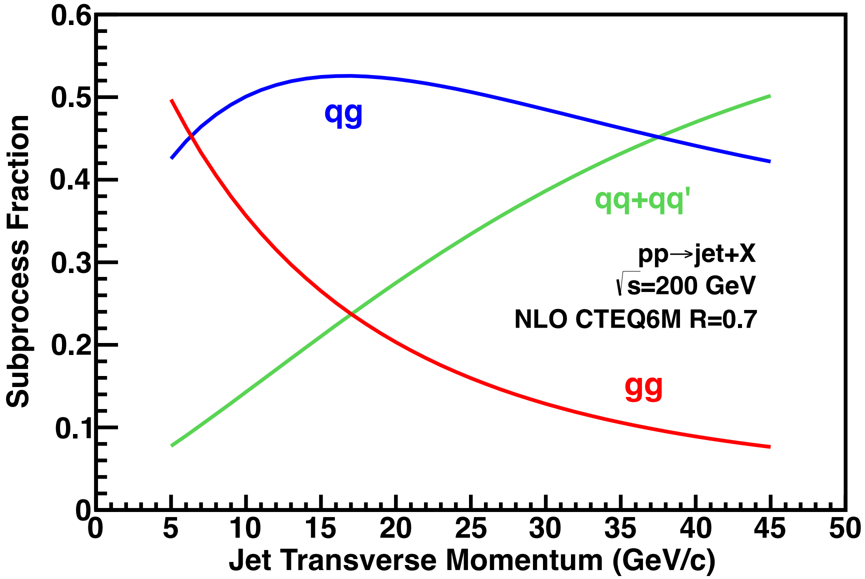

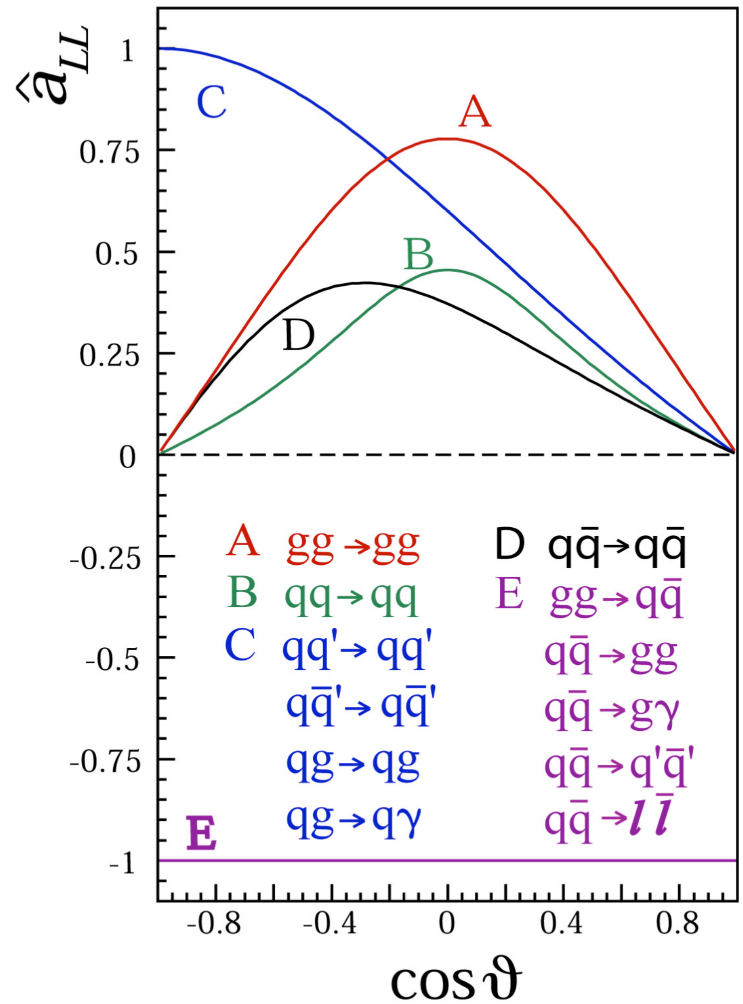

For most RHIC kinematics, ***gg*** and ***qg*** ***dominate***, making A_{LL} for jets sensitive to ***gluon polarization***.

From 2006 to 2009

arXiv:1106.5769

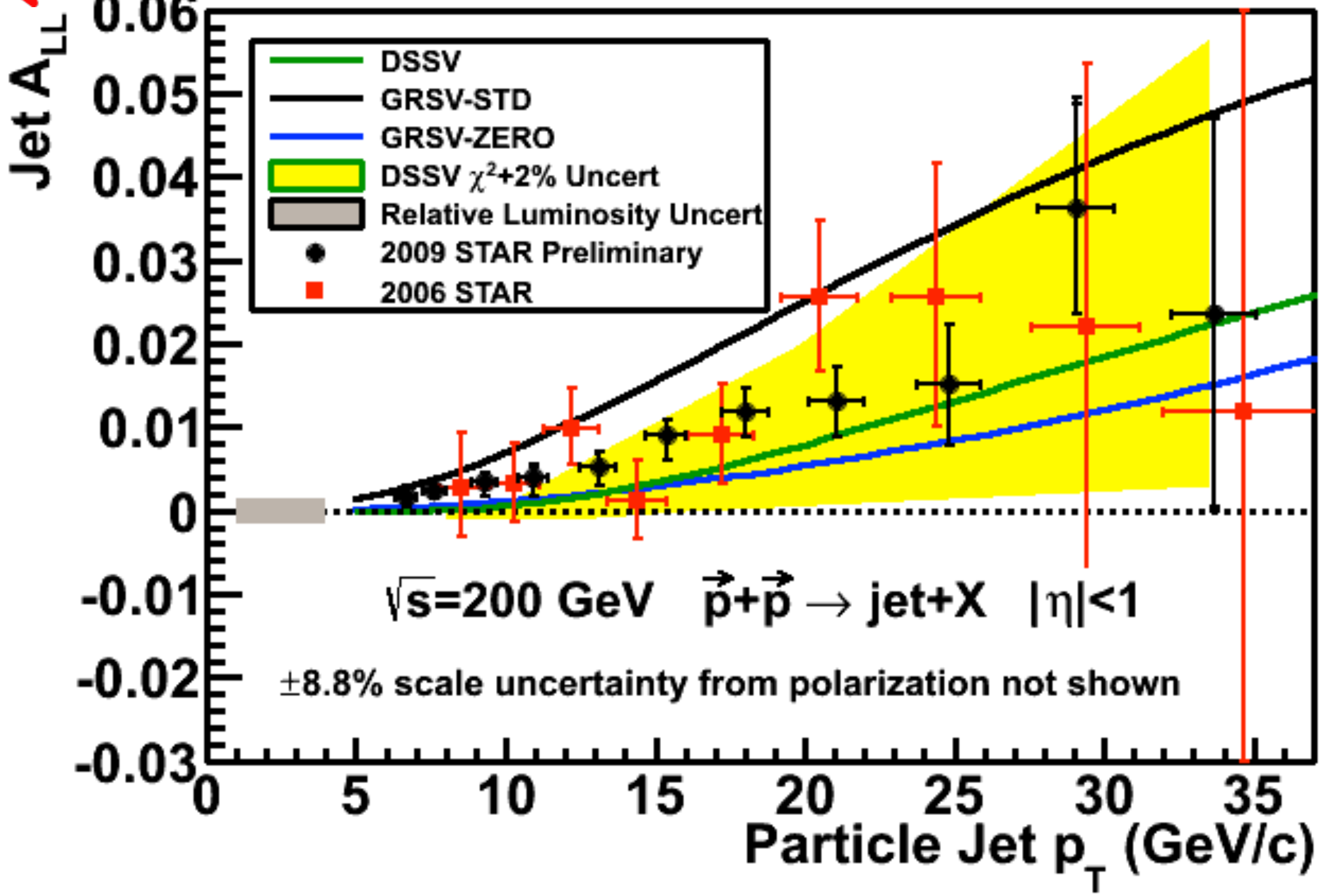

- 2009 STAR data is a factor of 3 (high-p_T) to >4 (low-p_T) more precise than 2006 STAR data
- Results fall between predictions from **DSSV** and **GRSV-STD**
- Precision sufficient to merit finer binning in pseudorapidity

New global analysis with 2009 RHIC data

arXiv:1304.0079

Special thanks to the DSSV group!

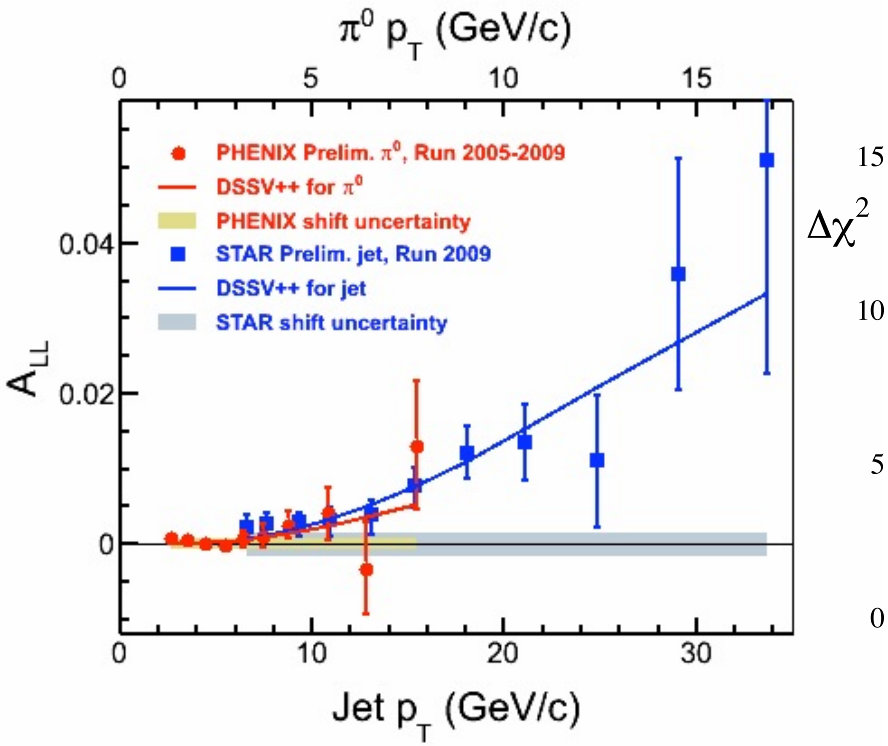

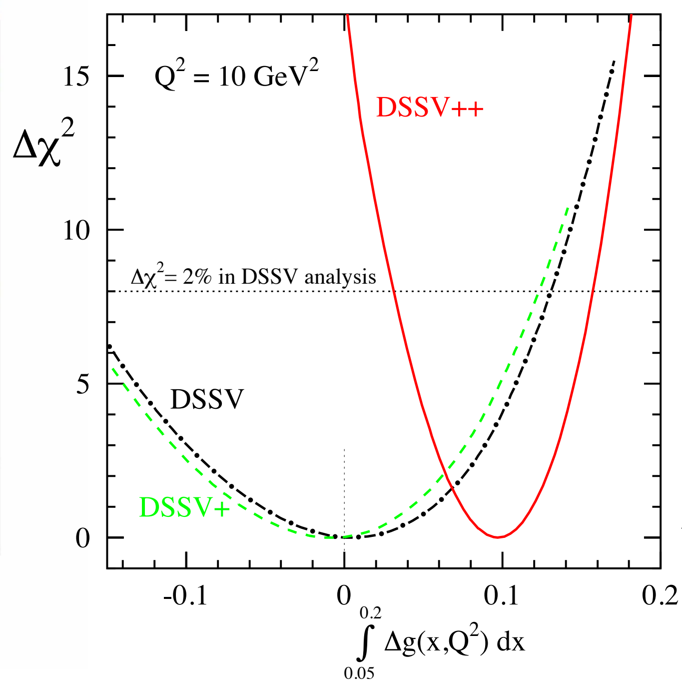

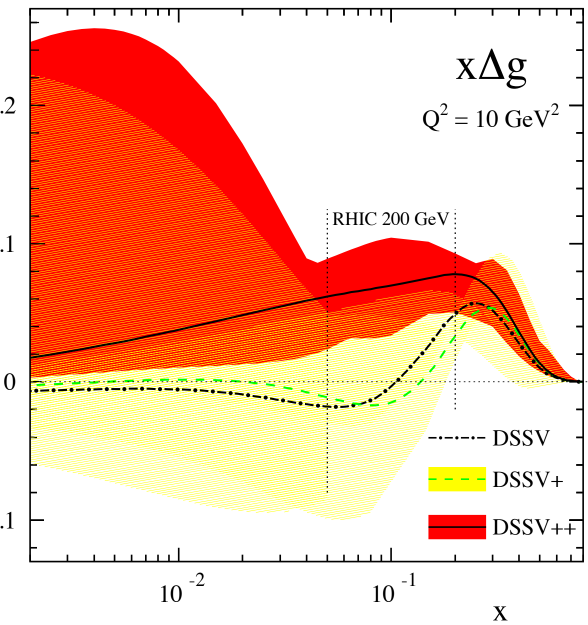

- **DSSV++** is a new, preliminary global analysis from the DSSV group that includes the 2009 RHIC A_{LL} data (STAR inclusive jets and PHENIX π^0's)

$$\int_{0.05}^{0.20} \Delta g(x, Q^2 = 10\ \text{GeV}^2)\, dx = 0.10^{+0.06}_{-0.07}$$

- First experimental evidence of **non-zero Δg(x)** in RHIC range ($0.05 \leq x \leq 0.2$)

Hadrons in Nuclei

Kaon and Anti-Kaon in Nuclear Matter

Laura Fabbietti
Technische Universität München and
Excellence Cluster Universe

AntiKaon Flow

FOPI, submitted to PLB

Ni+Ni 1.9 AGeV

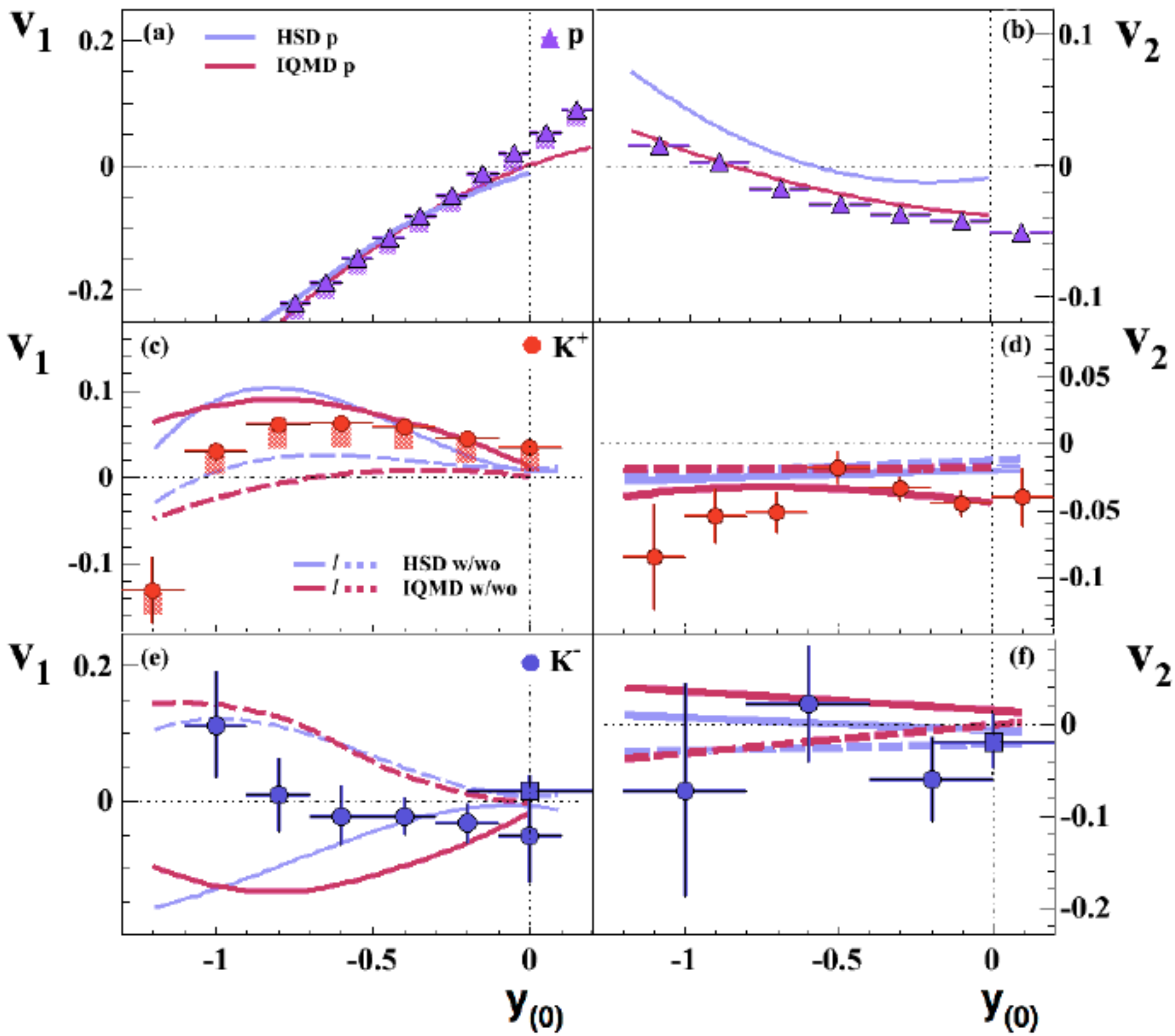

- Models predict the highest sensitivity to a potential for v_1 at backwards rapidities
- $\langle U_K \rangle \sim$-50 MeV
- Not conclusive
- Other ways?
- HADES measured Au+Au @ 1.25 AGeV

->~3500 K^-

Kaonic Hydrogen and scattering Data

SIDDHARTA experiment @LNF : Kaonic Hydrogen, most precise measurement of the **K-p scattering length** at the threshold

SIDDHARTA, Phys. Lett. B 697 (2011) 199.
SIDDHARTA, Phys. Lett. B 681 (2009) 310.

$$\mathrm{Re}\ a(K^-p) = -0.65 \pm 0.10\ \ \mathrm{fm} \qquad \mathrm{Im}\ a(K^-p) = 0.81 \pm 0.15\ \ \mathrm{fm}$$

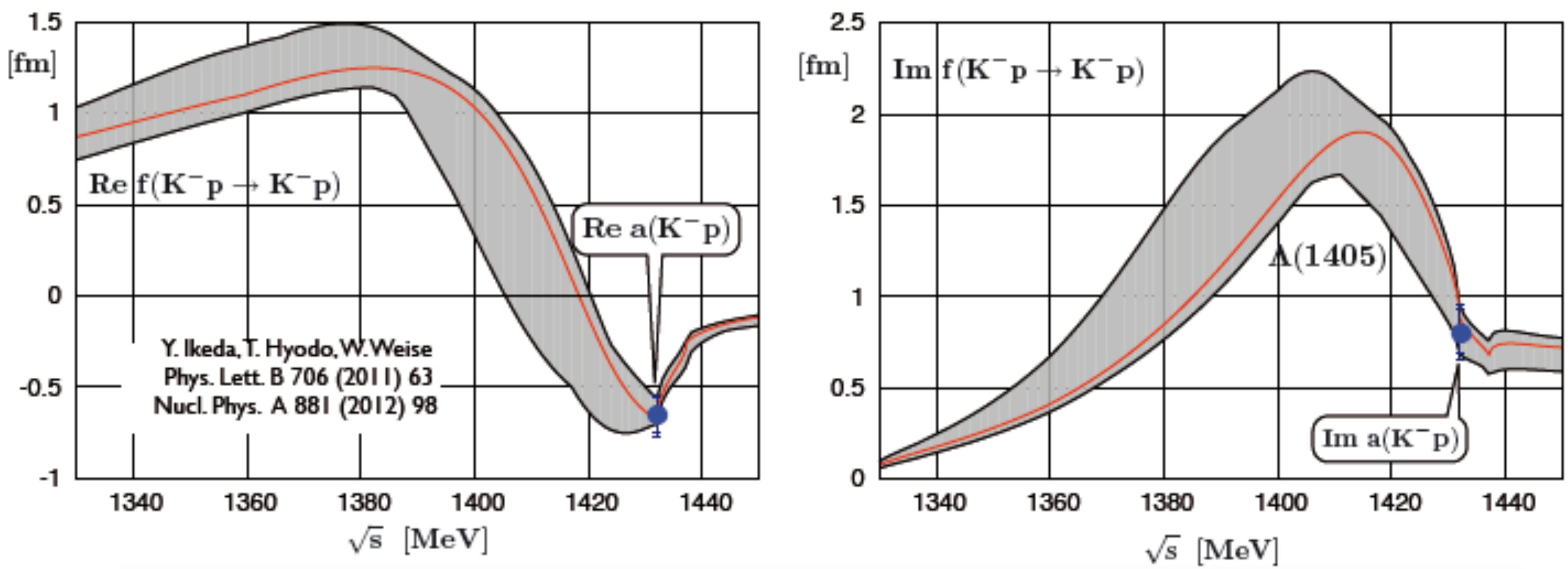

Only Nucleons in Neutron Stars

$$P = P(\varepsilon, \rho, T)$$

EOS gets softer

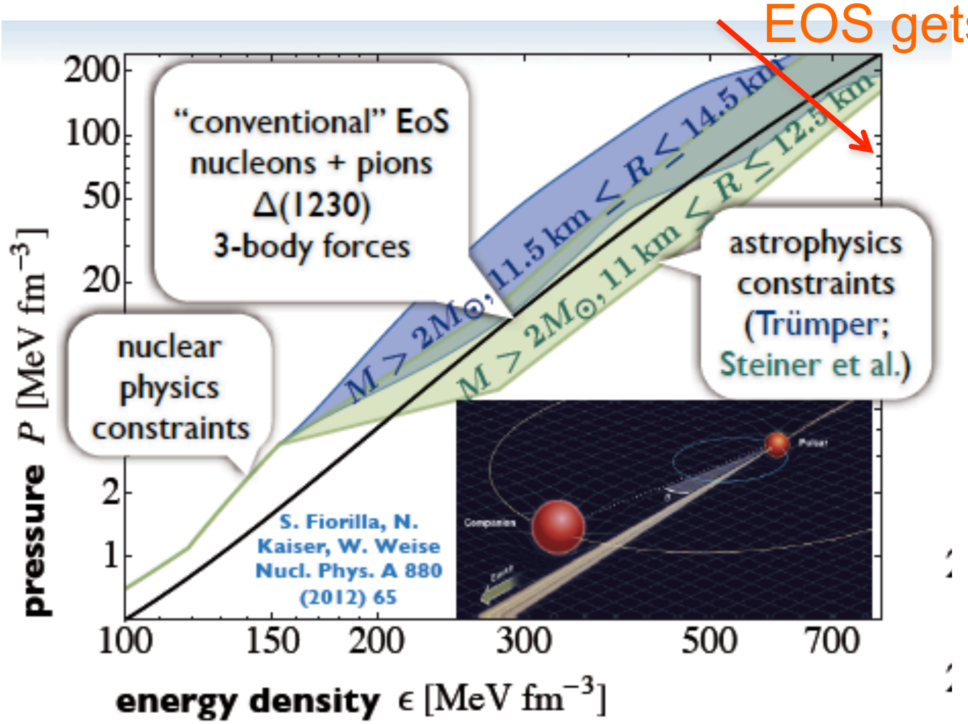

Private communication W. Weise

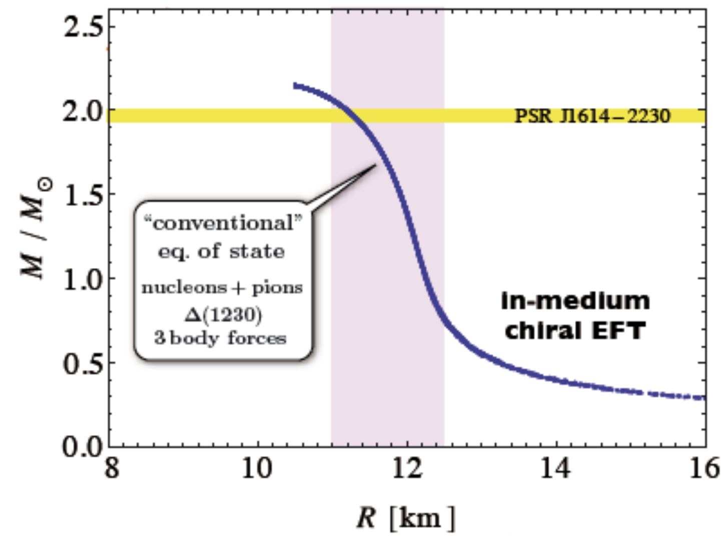

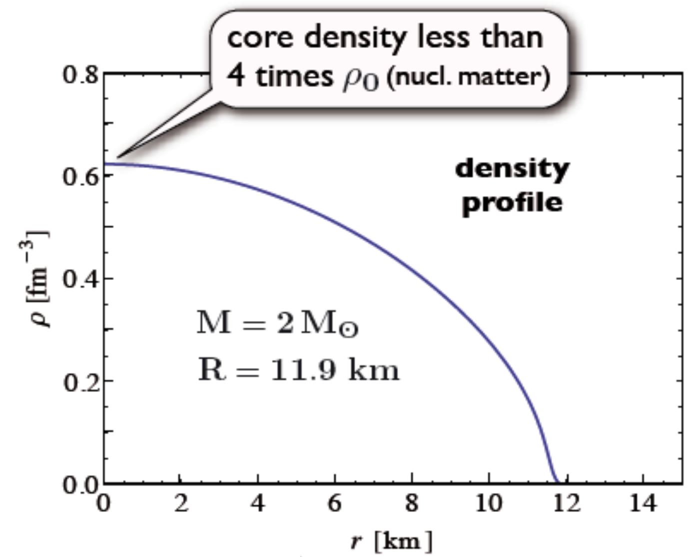

From the EOS to the Mass-Radius relationship through the TOV equations:

$$\frac{dP(r)}{dr} = -\frac{G}{c^2}\frac{\left[\varepsilon(r)+P(r)\right]\left[M(r)+4\pi r^3 P(r)/c^2\right]}{r\left[r-2GM(r)/c^2\right]}$$

$$\frac{dM(r)}{dr} = 4\pi\varepsilon(r)r^2$$

Small Neutron Stars and Hyperon Appereance

The heavy-ion results constrain nuclear matter at densities relevant to light neutron stars

Sagert, Tolos, Chaterjee, Schaffner-Bielich /PhysRevC.86.045802

Measure the radius of Stars with M< 1.4 M⊙

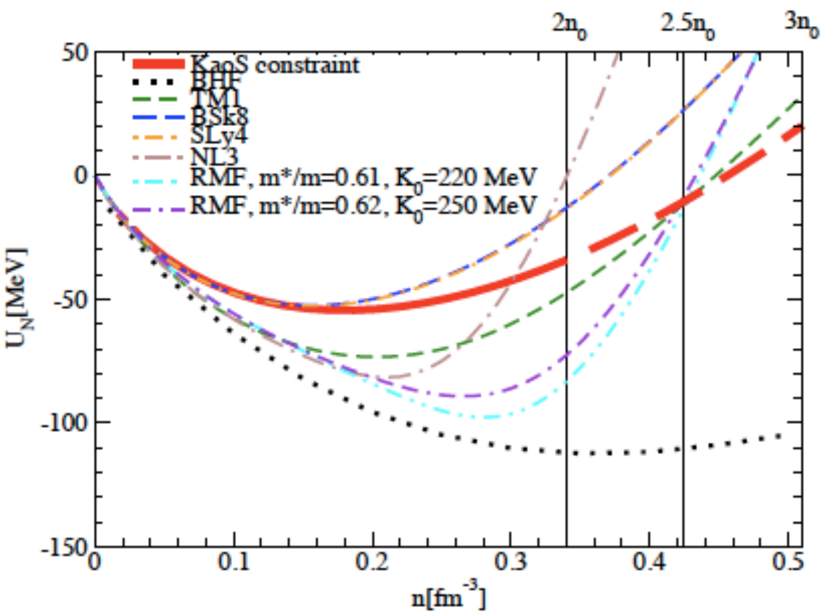

On the other hand..

J. Schaffner-Bielich, **NPA 804** (2008)

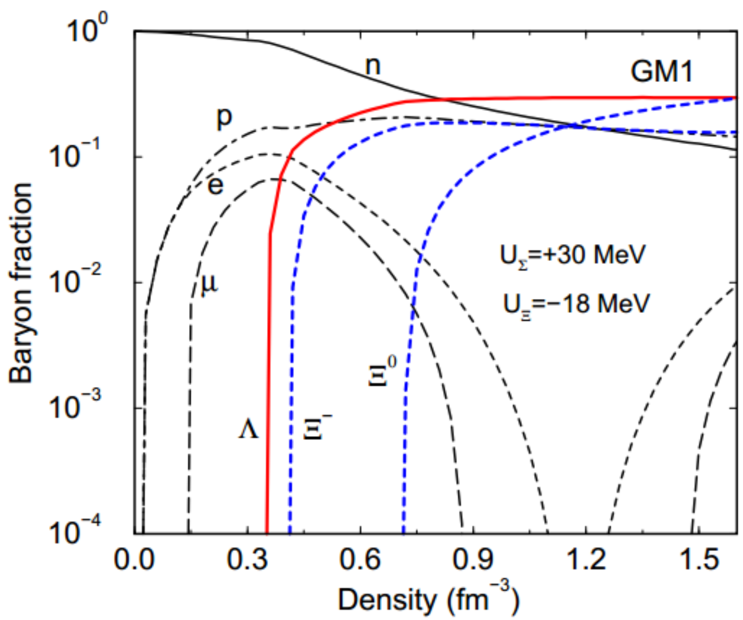

What about Hyperons?
Pt /Y, PWA, Resonances and..
Λp correlations in cold nuclear matter

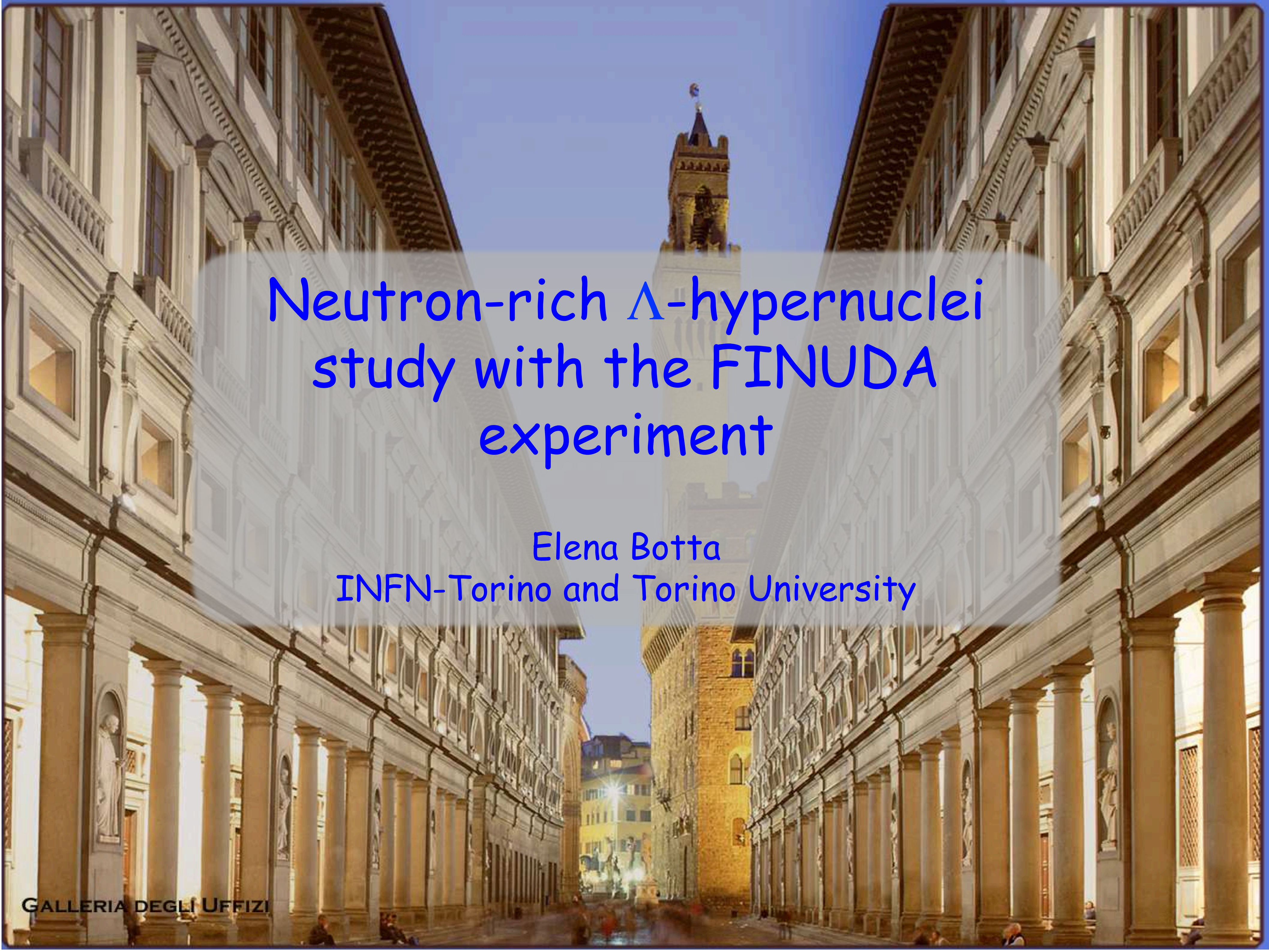

Neutron-rich Λ-hypernuclei study with the FINUDA experiment

Elena Botta
INFN-Torino and Torino University

Search for light n-rich hypernuclei in FINUDA

Production reaction

(K^-_{stop}, π^+)

$K^- + p \rightarrow \Lambda + \pi^0$ $\quad \pi^0 + p \rightarrow n + \pi^+$ (2-step) S-EX + C-EX

$K^- + p \rightarrow \overline{K^0} + n$ $\quad \overline{K^0} + p \rightarrow \Lambda + \pi^+$ (2-step) C-EX + S-EX

$K^- + p \rightarrow \Sigma^- + \pi^+$ $\quad \Sigma^- + p \leftrightarrow n + \Lambda$ (1-step) S-EX

K.Kubota et al, NPA 602 (1996) 327.

${}^{9}_{\Lambda}$He (^{9}Be) U.L.=2.3 $10^{-4}/K^-_{stop}$; ${}^{12}_{\Lambda}$Be(^{12}C) U.L.=6.1 $10^{-5}/K^-_{stop}$;

${}^{16}_{\Lambda}$C(^{16}O) U.L.=6.2 $10^{-5}/K^-_{stop}$

PLB 640 (2006) 145: upper limits ${}^{6}_{\Lambda}$H, ${}^{7}_{\Lambda}$H and ${}^{12}_{\Lambda}$Be

oct 2003 - jan 04: ~220 pb^{-1}

${}^{6}_{\Lambda}$H (^{6}Li) U.L.= (2.5 ± 1.4) $10^{-5}/K^-_{stop}$; ${}^{7}_{\Lambda}$H(^{7}Li) U.L.= (4.5± 1.4) $10^{-5}/K^-_{s}$;

${}^{12}_{\Lambda}$Be(^{12}C) U.L.= (2.0 ± 0.4) $10^{-5}/K^-_{stop}$ (inclusive π+ spectra analysis)

PRL 108 (2012) 042501, NPA 881 (2012) 269: ${}^{6}_{\Lambda}$H observation

PRC 86 (2012) 057301: upper limits ${}^{9}_{\Lambda}$He

${}^{6}_{\Lambda}H/K^{-}_{stop}$ production rate

Background sources:

• fake coincidences: $T(\pi^{+})+T(\pi^{-})$(202÷204 MeV) & π+(250÷255 MeV/c) & π^{-}(130÷137 MeV/c) 0.27±0.27 ev.

• $K^{-}_{stop} + {}^{6}Li \rightarrow \Sigma^{+} + \pi^{-} + {}^{4}He + n$ (end point ~190 MeV/c)
$\quad \hookrightarrow n + \pi^{+}$ (end point ~282 MeV/c) 0.16±0.07 ev.

• $K^{-}_{stop} + {}^{6}Li \rightarrow {}^{4}_{\Lambda}H + n + n + \pi^{+}$ (end point ~252MeV/c) negligible
$\quad \hookrightarrow {}^{4}He + \pi^{-}$ ($p(\pi^{-})$ = 132.8 MeV/c) $T(\pi^{+})+T(\pi^{-})$ cut

${}^{6}_{\Lambda}H/K^{-}_{stop}$ production rate

Total background: BGD1 + BGD2 = 0.43 ± 0.28 events on ${}^{6}Li$

Poisson statistics: 3 events DO NOT belong to pure background: C.L.= 99%

$$R * BR(\pi-) = (3 - BGD1 - BGD2) / [\varepsilon(\pi-)\, \varepsilon(\pi+)\, (n.\ K^{-}_{stop} \text{ on } {}^{6}Li)]$$

$$\mathbf{R * BR(\pi-) = (2.9 \pm 2.0)\ 10^{-6}/K^{-}_{stop}}$$

$$\mathbf{R = (5.9 \pm 4.0)\ 10^{-6}/K^{-}_{stop}}$$

H. Tamura, et al.,
PRC 40 (1989) R479
$BR(\pi-)\ {}^{4}_{\Lambda}H = 0.49$

$(2.5 \pm 0.4^{+0.4}_{-0.1})\ 10^{-5}/K^{-}_{stop}$
Agnello et al., *PLB 64(2006) 145*

FINUDA Coll. and A. Gal, PRL 108 (2012) 042501, NPA 881 (2012) 269

Conclusions

(K^-_{stop}, π^+) production rate vs A

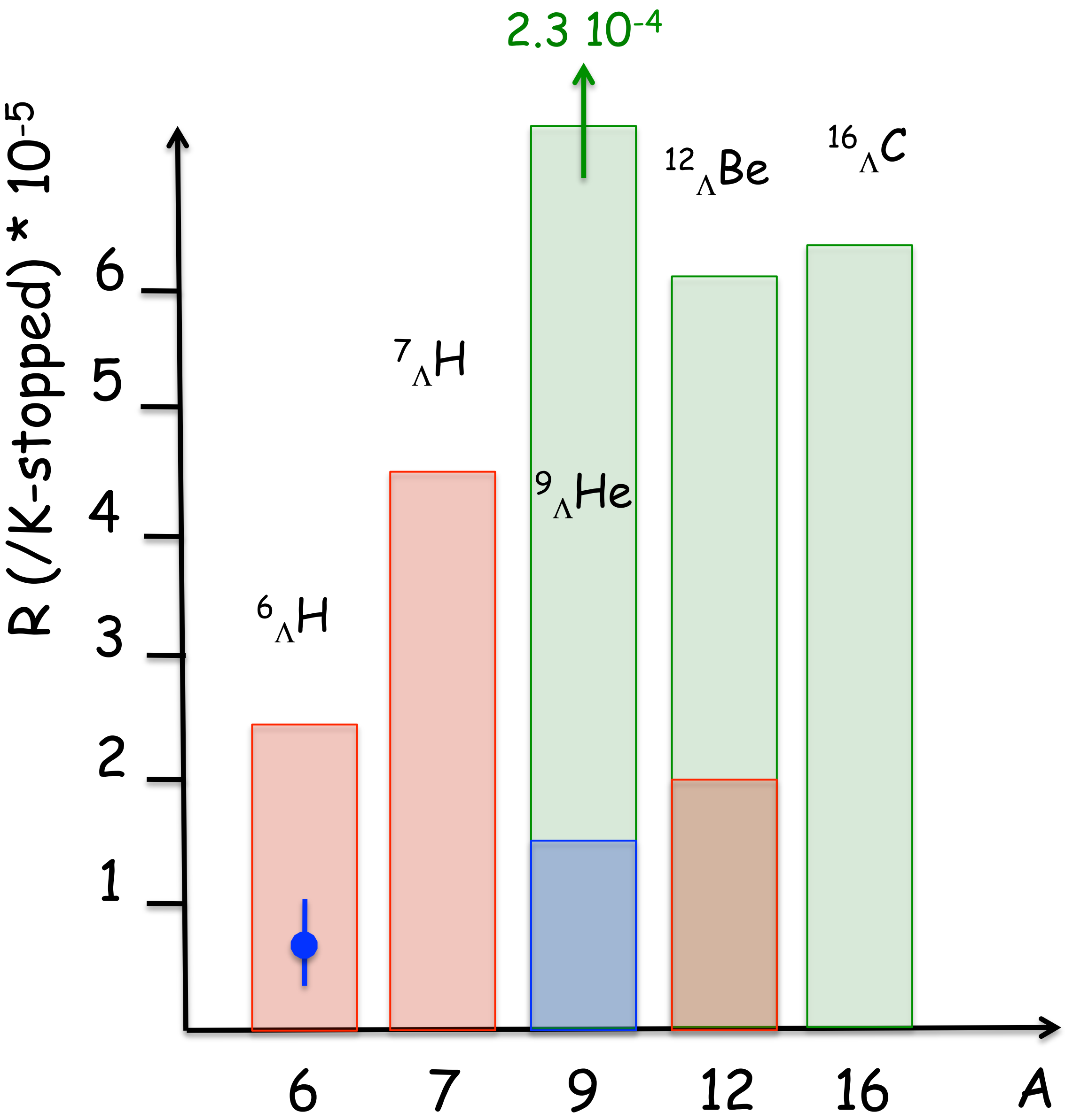

FINUDA: inclusive spectra

FINUDA: coincidence

KEK

full bars: U.L., 90% C.L.

experimental and theoretical efforts needed (H. Sugimura and A. Gal talks)

Hadronic interactions of K^- in KLOE

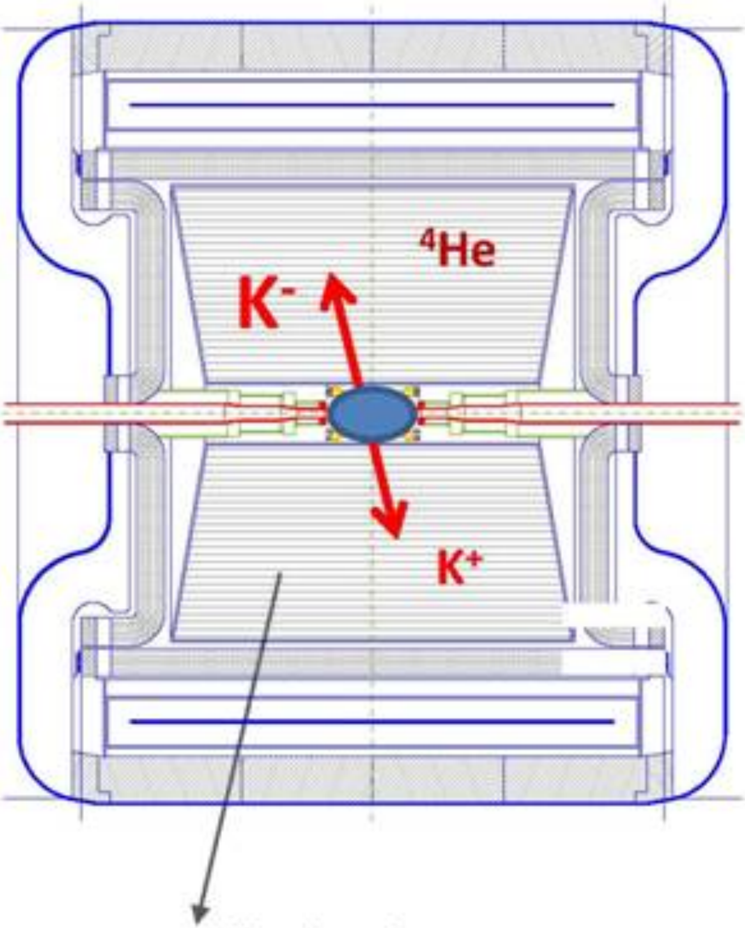

KLOE Drift Chamber

- The Drift Chambers of KLOE contain mailny **^{4}He**
- From analysis of KLOE data and Monte Carlo:
  0.1 % of K^- from daΦne should **stop in the DC volume**
- This would lead to hundreds of possible kaonic clusters produced in the 2 fb^{-1} of KLOE data.

Λ(1405) scientific case

$(M\,,\,\Gamma) = (1405.1^{+1.3}_{-1.0}\,,\,50 \pm 2)$ MeV, $I = 0$, $S = -1$, $J^p = 1/2^-$, Status: ****, strong decay into $\Sigma\pi$

Its **nature** is being a **puzzle now for decades**:

1) ***three quark state***: expected mass ~ 1700 MeV

2) ***penta quark***: more unobserved excited baryons

3) ***unstable* KN *bound state***

4) ***two poles***: ($z_1 = 1424^{+7}_{-23}$, $z_1 = 1381^{+18}_{-6}$) MeV (Nucl. Phys. A881, 98 (2012))

Higher mass pole mainly coupled to KN

mainly coupled to $\Sigma\pi$ -> **line-shape depends on production mechanism**

Line-shape also depends on the decay channel : $\Sigma^0\pi^0$ $\Sigma^+\pi^-$ $\Sigma^-\pi^+$

BEST CHOICE:

production in KN reactions (only chance to observe the high mass pole) **decaying in $\Sigma^0\pi^0$** (free from $\Sigma(1385)$ background)

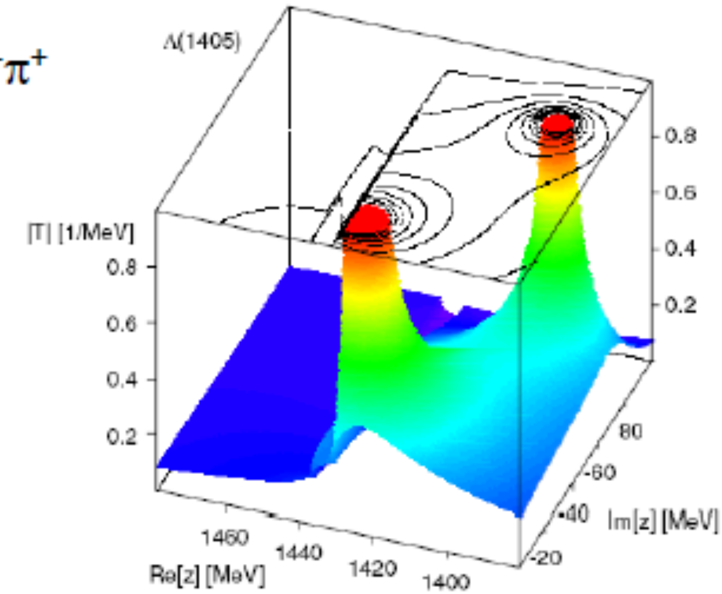

Λ(1405) charged channel: $\Sigma^+\pi^-$

Λ(1405) signal searched in $\mathbf{K^- p} \rightarrow \Sigma^+\pi^-$ detected via: $(\mathbf{p}\pi^0)\pi^-$

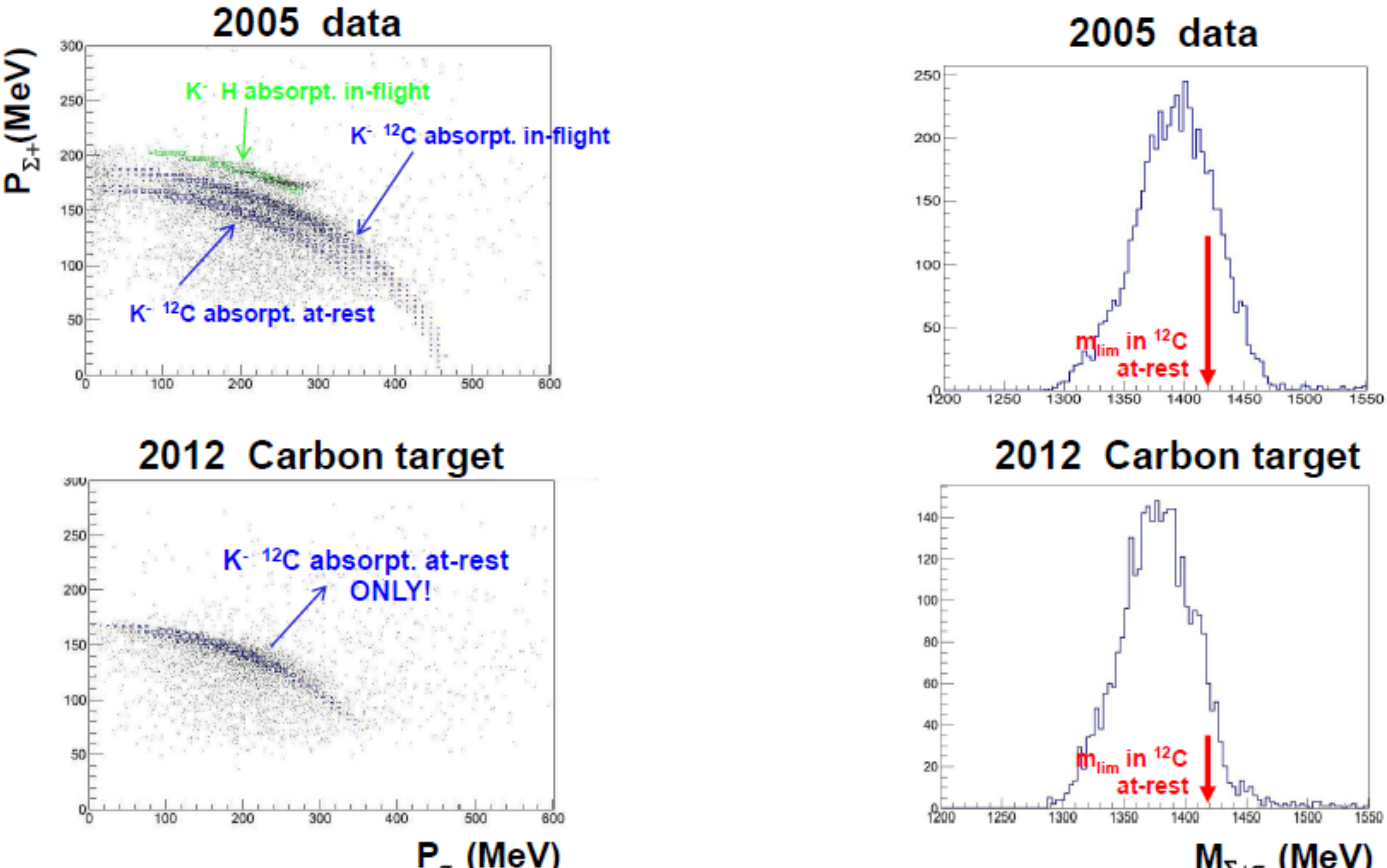

Antimatter α TOF PID

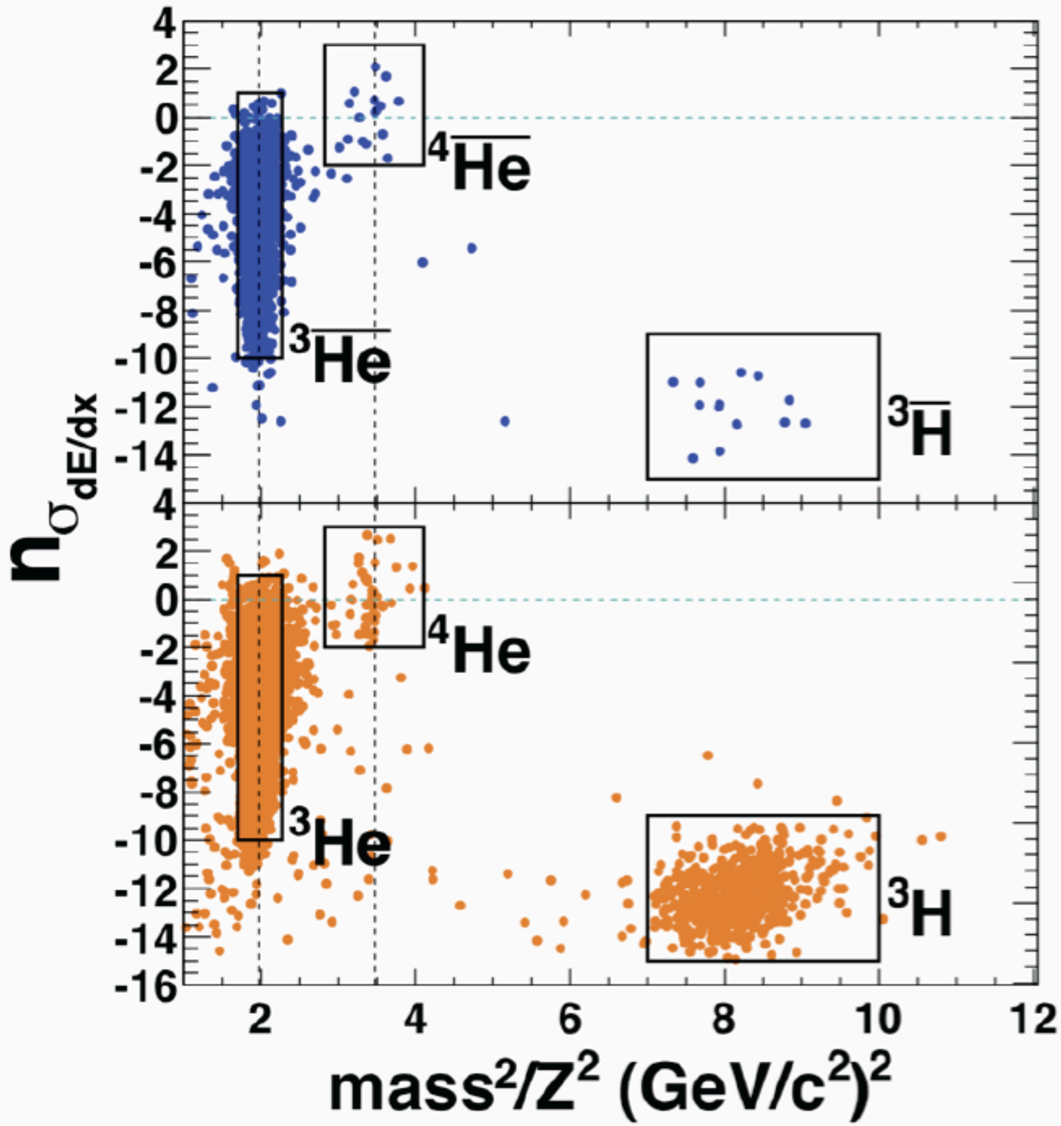

1) Mass value is calculated via formula : $m^2/Z^2 = p^2/Z^2(\frac{1}{\beta^2} - 1)$ where velocity $\beta = L/\Delta t$, and Δt is measured by upVpd and TOF, *L* is the traveling path length provided by TPC. *p* is momentum measured by TPC, and *Z* is the charge number of tracks.

2) Two clusters of $^{4}\overline{He}$ and ^{4}He nucleus are found to be located at $n\sigma_{dE/dx} = 0$, $m^2/Z^2 = 3.48\ (GeV/c^2)^2$.

Yu-Gang Ma
Shanghai Institute of Applied Physics (SINAP),
Chinese Academy of Sciences

Antimatter α TOF PID

中国科学院上海应用物理研究所
SINAP
Shanghai Institute of Applied Physics, Chinese Academy of Sciences

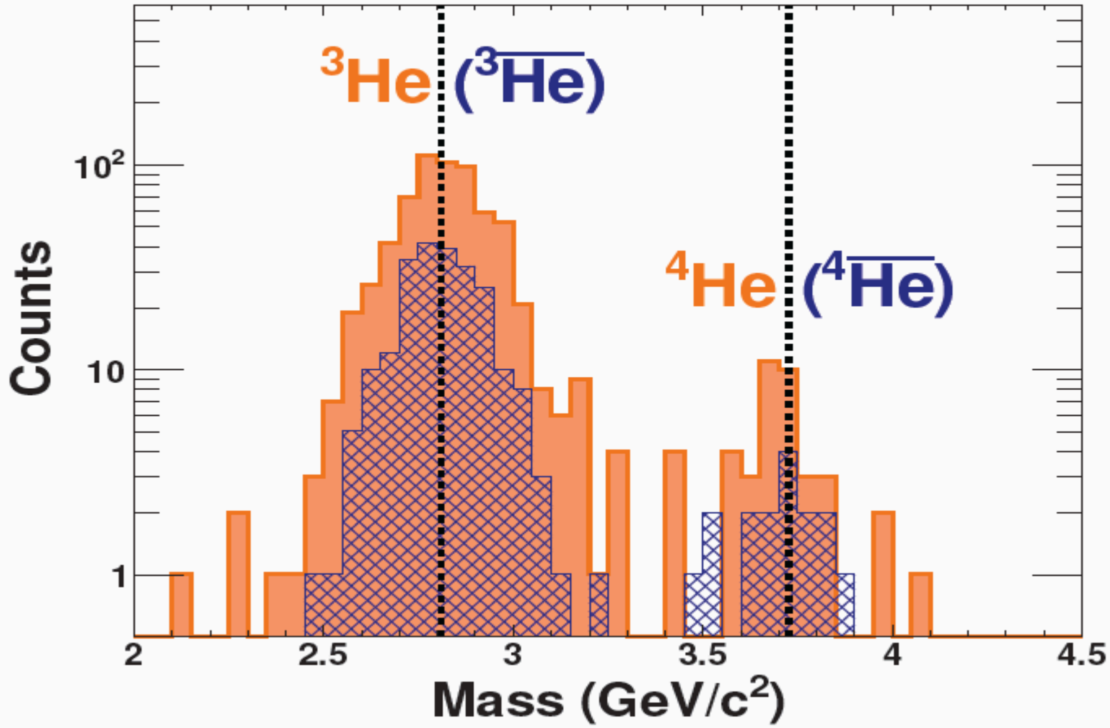

LETTER
nature
doi:10.1038/nature10079

Observation of the antimatter helium-4 nucleus

The STAR Collaboration*

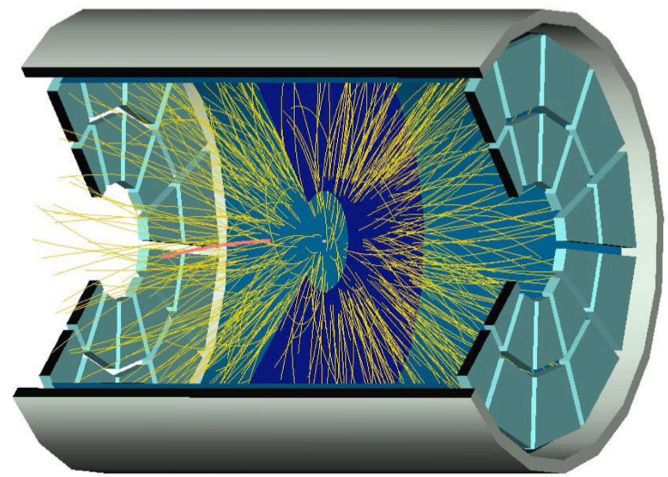

1) An clean separation for ^{3}He ($^3\overline{\text{He}}$) and ^{4}He ($^4\overline{\text{He}}$) can be seen by projecting to mass axis. $^4\overline{\text{He}}$ candidates are counted within the cuts window: -2. <$n\sigma_{dE/dx}$< 3., and, 3.35GeV/c^2 <mass< 4.04GeV/c^2.

2) 16+2 $^4\overline{\text{He}}$ candidates were identified by STAR experiment, with 15 (1) of them from Au+Au 200 (62) GeV data sampled by HLT in 2010, 2 of them from Au+Au 200 GeV data recorded by TPC alone in 2007.

just because something is impossible today
doesn't mean it will be impossible in the future.

anti-Helium 4

Anti-Alpha

For the full statistics of 2011 we identified 10 Anti-Alphas using TPC and TOF

Corresponds to 23×10^6 events of a trigger mix (central, semi-central and min. bias)

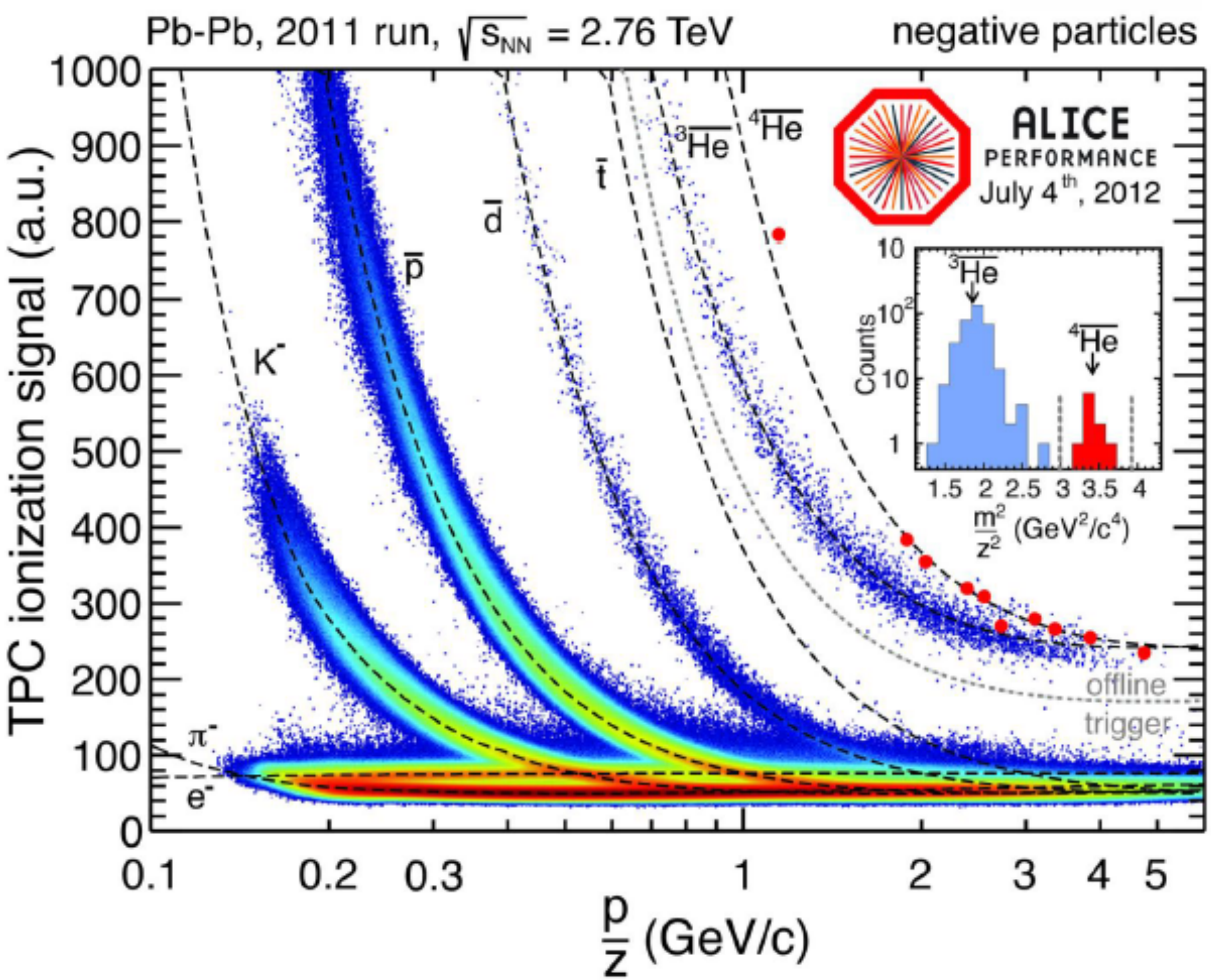

Lifetime puzzle: So short?

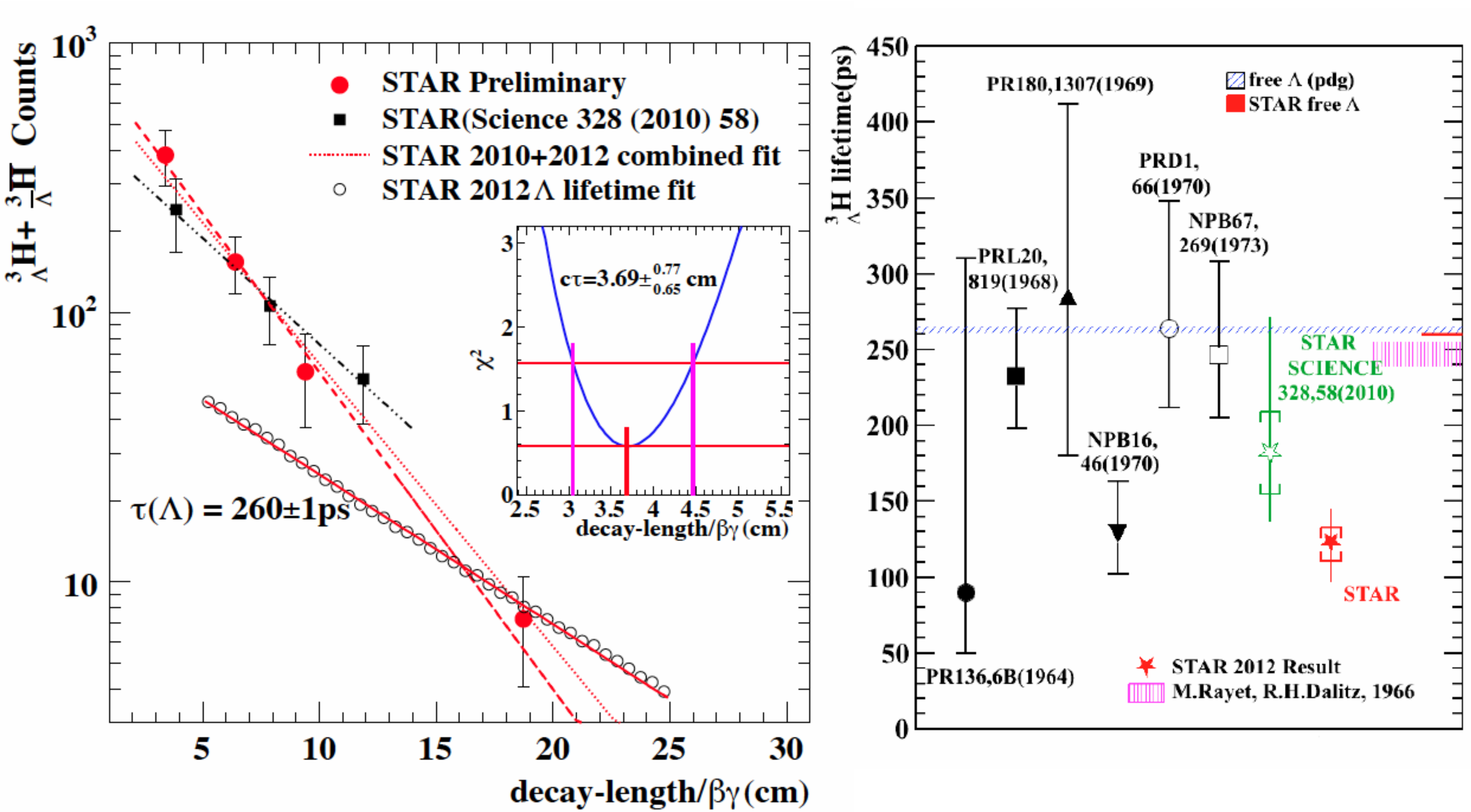

STAR 2012 result: $\tau = 123 \pm^{26}_{22} \pm 10\, ps$

STAR 2010+2012 combined fit: $\tau = 138 \pm^{23}_{20}\, ps$

Zhu Yuhui（SINAP）, PhD thesis, 2013

Nuclear Astrophysics

Laboratory for Underground Nuclear Astrophysics

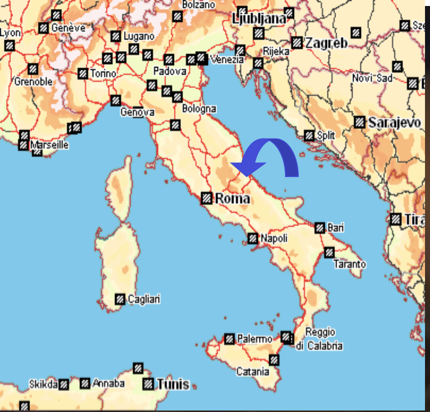

Radiation	LNGS/surface
Muons	10^{-6}
Neutrons	10^{-3}

Alessandra Guglielmetti
Universita' degli Studi di Milano and
INFN, Milano, ITALY

Element abundances in the solar system

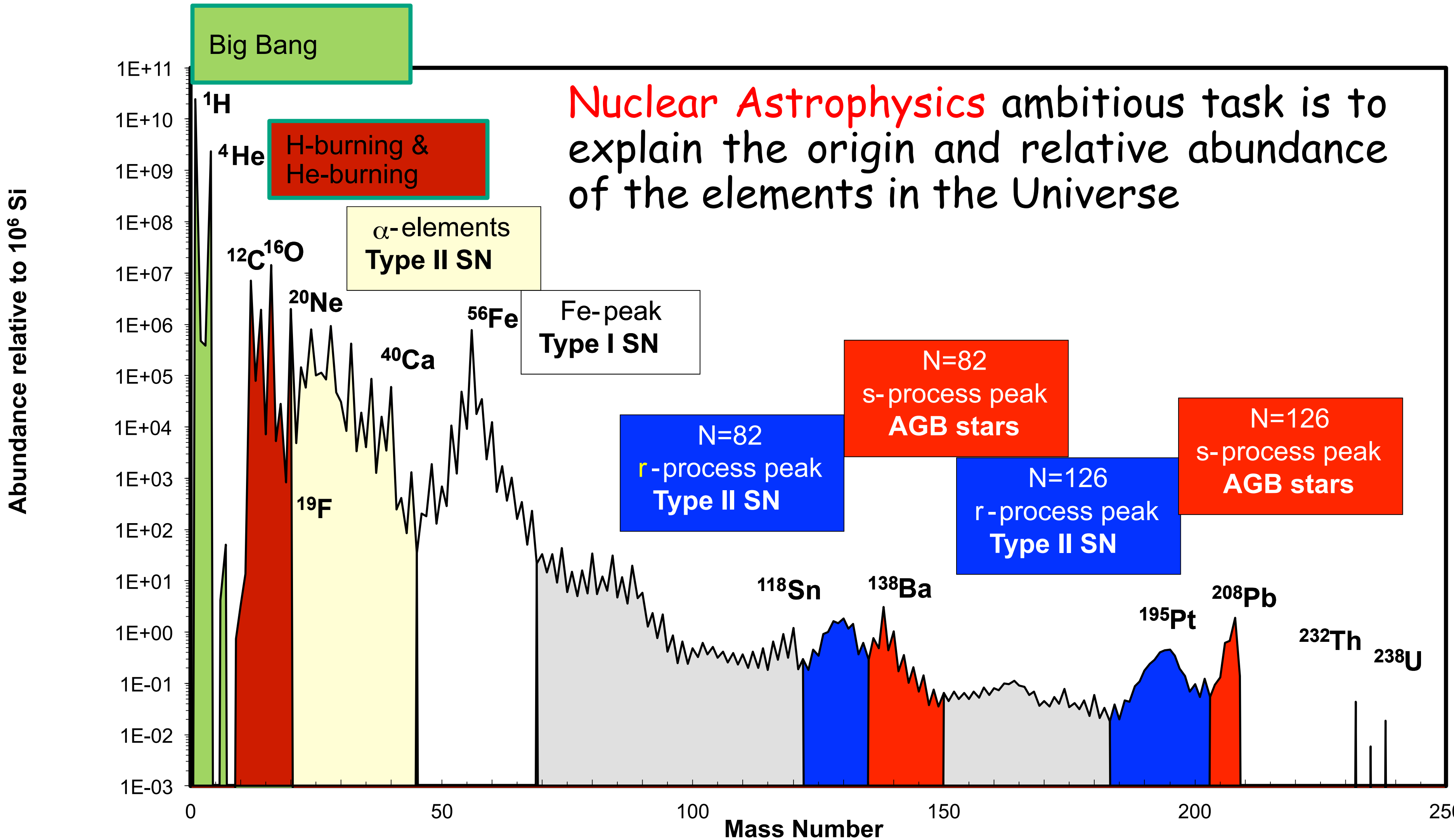

Neutrino production in stars

$p + p \rightarrow {}^2H + e^+ + \nu$
$p + e^- + p \rightarrow {}^2H + e^+ + \nu$
$^3He + p \rightarrow {}^4He + e^+ + \nu$
$^7Be + e^- \rightarrow {}^7Li + \nu$
$^8B \rightarrow {}^8Be + e^+ + \nu$

p-p chain

$^{13}N \rightarrow {}^{13}C + e^+ + \nu$
$^{15}O \rightarrow {}^{15}N + e^+ + \nu$
$^{17}F \rightarrow {}^{17}O + e^+ + \nu$

CNO cycle

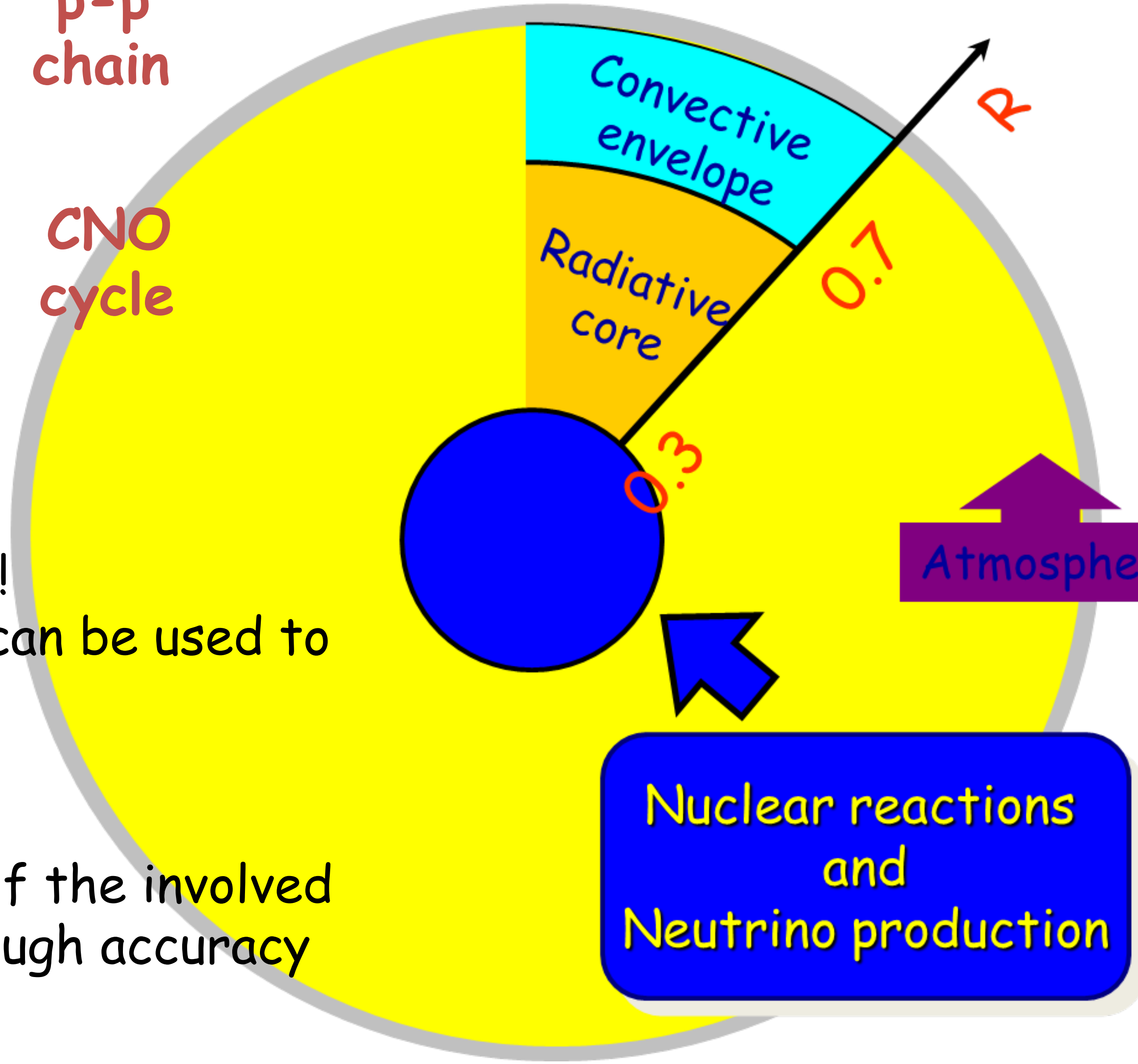

Solar neutrino puzzle: solved!
Neutrino flux from the Sun can be used to study:

- Solar interior composition
- Neutrino properties

<u>ONLY</u> if the cross sections of the involved reactions are known with enough accuracy

LUNA 400 kV program

	reaction	Q-value (MeV)
completed	$^{17}O(p,\gamma)^{18}F$	5.6
just started	$^{17}O(p,\alpha)^{14}N$	1.2
	$^{18}O(p,\gamma)^{19}F$	8.0
	$^{18}O(p,\alpha)^{15}N$	4.0
	$^{23}Na(p,\gamma)^{24}Mg$	11.7
just started	$^{22}Ne(p,\gamma)^{23}Na$	8.8
completed	$D(\alpha,\gamma)^{6}Li$	1.47

Still three reactions to be measured→ to be completed by 2015

Higher energy machine→ 3.5 MV single ended positive ion accelerator

$^{12}C(\alpha,\gamma)^{16}O$ – Holy Grail of Nuclear Astrophysics

Stellar Helium burning in Red Giant Stars

the He burning is ignited on the ^{4}He and ^{14}N ashes of the preceding hydrogen burning phase (pp and CNO)

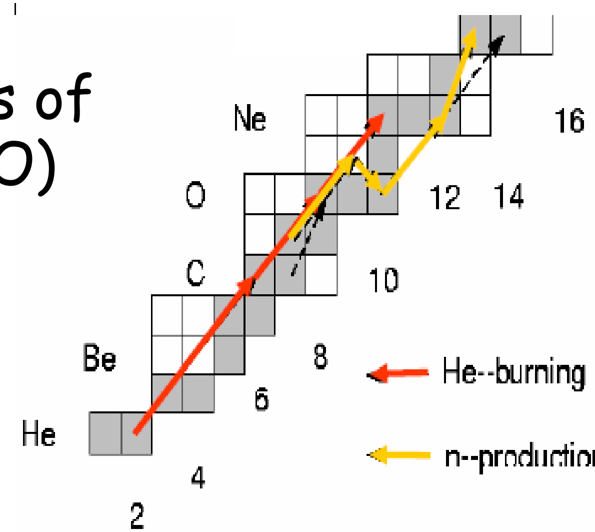

relevant questions:

Energy production and time scale of Helium burning:

$^4He(2\alpha,\gamma)^{12}C(\alpha,\gamma)^{16}O(\alpha,\gamma)^{20}Ne$

Neutron sources for s process:

$^{14}N(\alpha,\gamma)^{18}F(\beta+\nu)^{18}O(\alpha,\gamma)^{22}Ne(\alpha,n)$

$^{22}Ne(\alpha,\gamma)$

Consequences

- late stellar evolution
- composition of C/O White dwarfs
- Supernova type I explosion
- Supernova type II nucleosynthesis

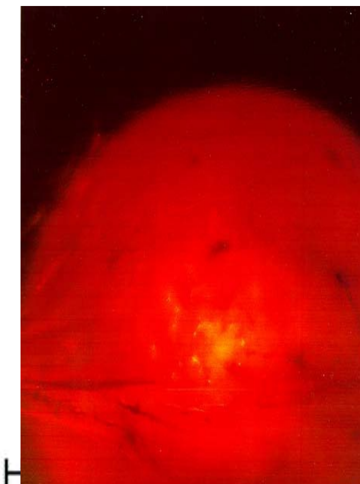

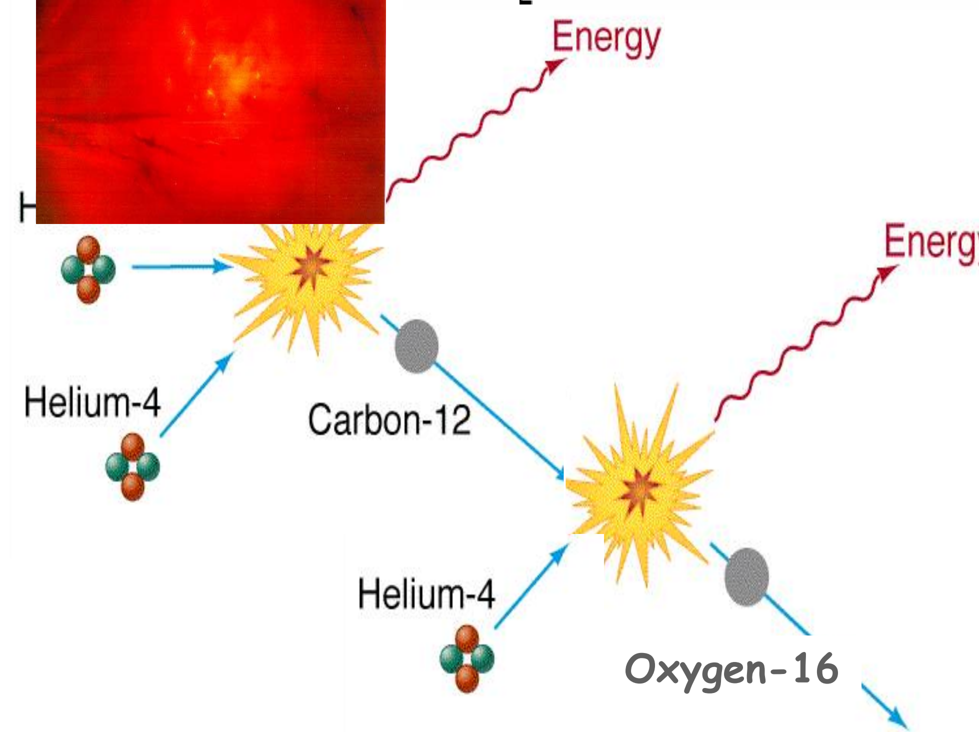

Neutrinos and Nuclei

Experimental Method of θ_{13} Measurement

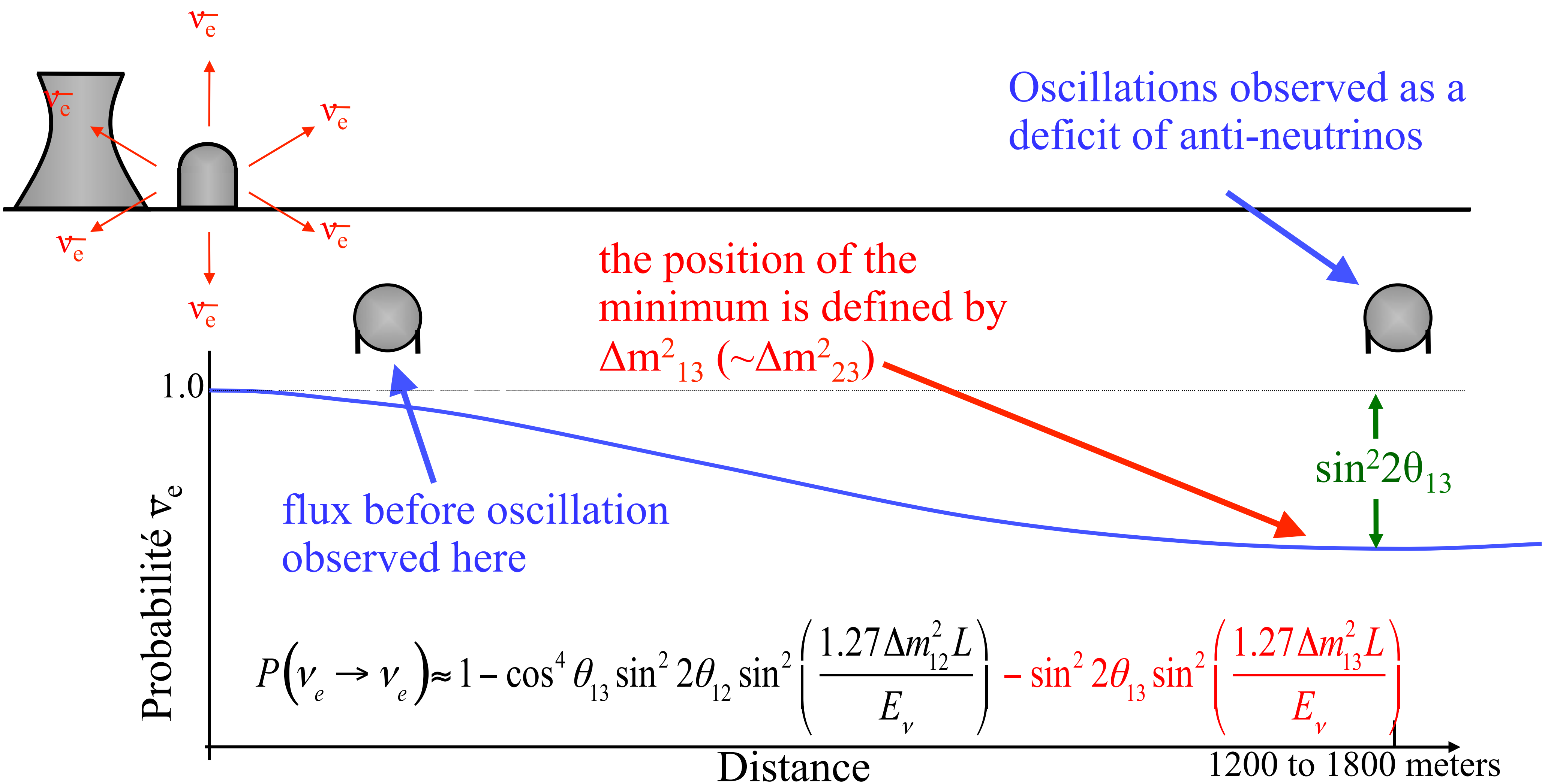

❑ Find disappearance of $\overline{\nu_e}$ fluxes due to neutrino oscillation as a function of energy using multiple, identical detectors to reduce the systematic errors in 1% level.

Soo-Bong Kim (KNRC, Seoul National University)

Reactor Antineutrino Oscillations

RENO

Daya Bay

DOUBLE CHOOZ

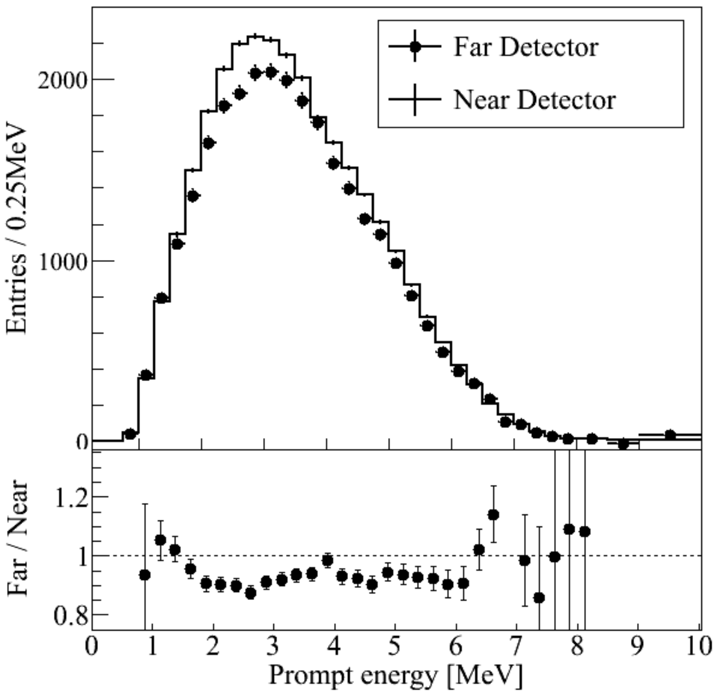

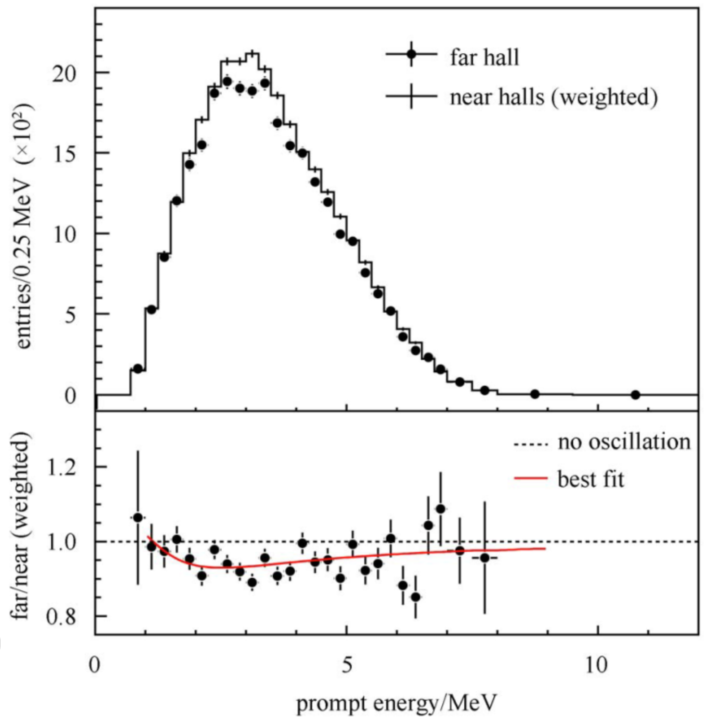

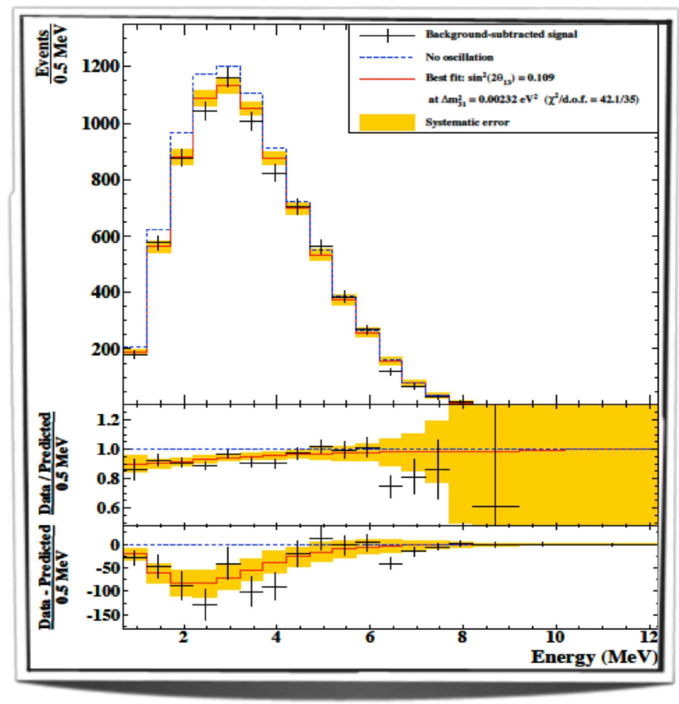

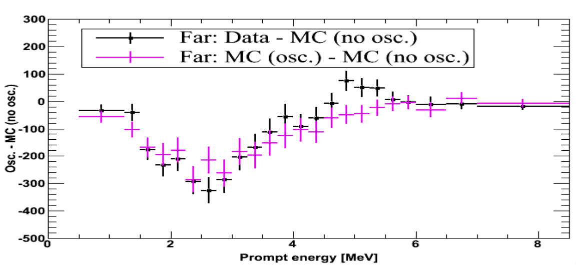

- A clear disappearance of reactor antineutrinos is observed. The smallest mixing angle θ_{13} that was the most elusive puzzle of neutrino oscillations, is firmly measured by the reactor experiments.

$$\sin^2 2\theta_{13} = 0.100 \pm 0.010(stat) \pm 0.015(syst)$$ (RENO)

$$\sin^2 2\theta_{13} = 0.089 \pm 0.010(stat) \pm 0.005(syst)$$ (Daya Bay
)

$$\sin^2 2\theta_{13} = 0.109 \pm 0.030(stat) \pm 0.025(syst)$$ (Double Chooz)

- A surprisingly large value of θ_{13} will strongly promote the next round of neutrino experiments to find the CP phase and determine the mass hierarchy.

- Precise measurement of θ_{13} by the reactor experiments will provide the first glimpse of $\delta_{CP.}$ If accelerator results are combined.

Hot and Dense Nuclear Matter

The Relativistic Heavy Ion Collider
Recent Results

Enrique Diaz

Steve Zimic

Thomas Ullrich
BNL and Yale University

INPC 2013, Florence, June 7, 2013

Office of Science
U.S. Department of Energy

BROOKHAVEN NATIONAL LABORATORY

RHIC: Huge Performance Improvements

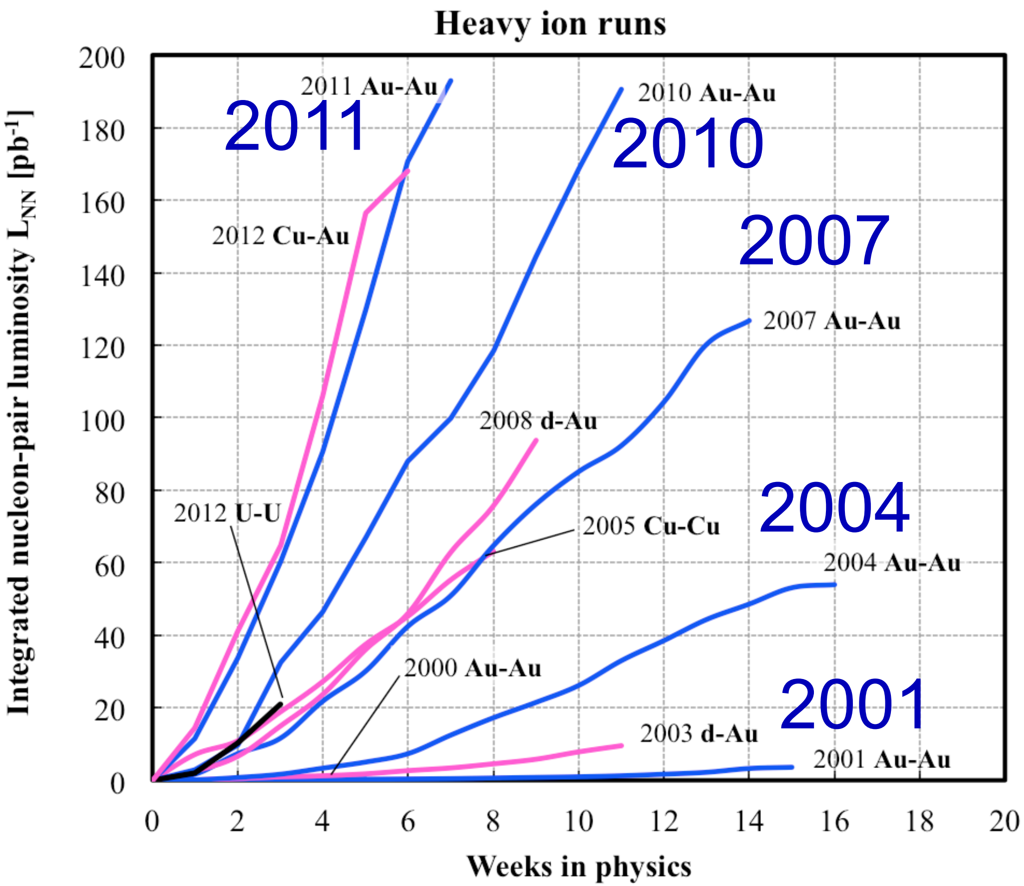

Collisions System	Beam Energy (GeV/n)
Used to date	
Au+Au	3.85, 4.6, 5.75, 9.8, 13.5, 19.5, 31, 65, 100
d+Au	100
Cu+Cu	11, 31, 100
p↑+p↑	11, 31, 100, 205, 250, 255
Cu+Au	100
U+U	96
Considered for future	
Au+Au	2.5, 7.5
p↑+Au	100
p↑+^{3}He↑	166

2 new colliding beam species/combinations in 2012

RHIC: Charting the Phase Diagram

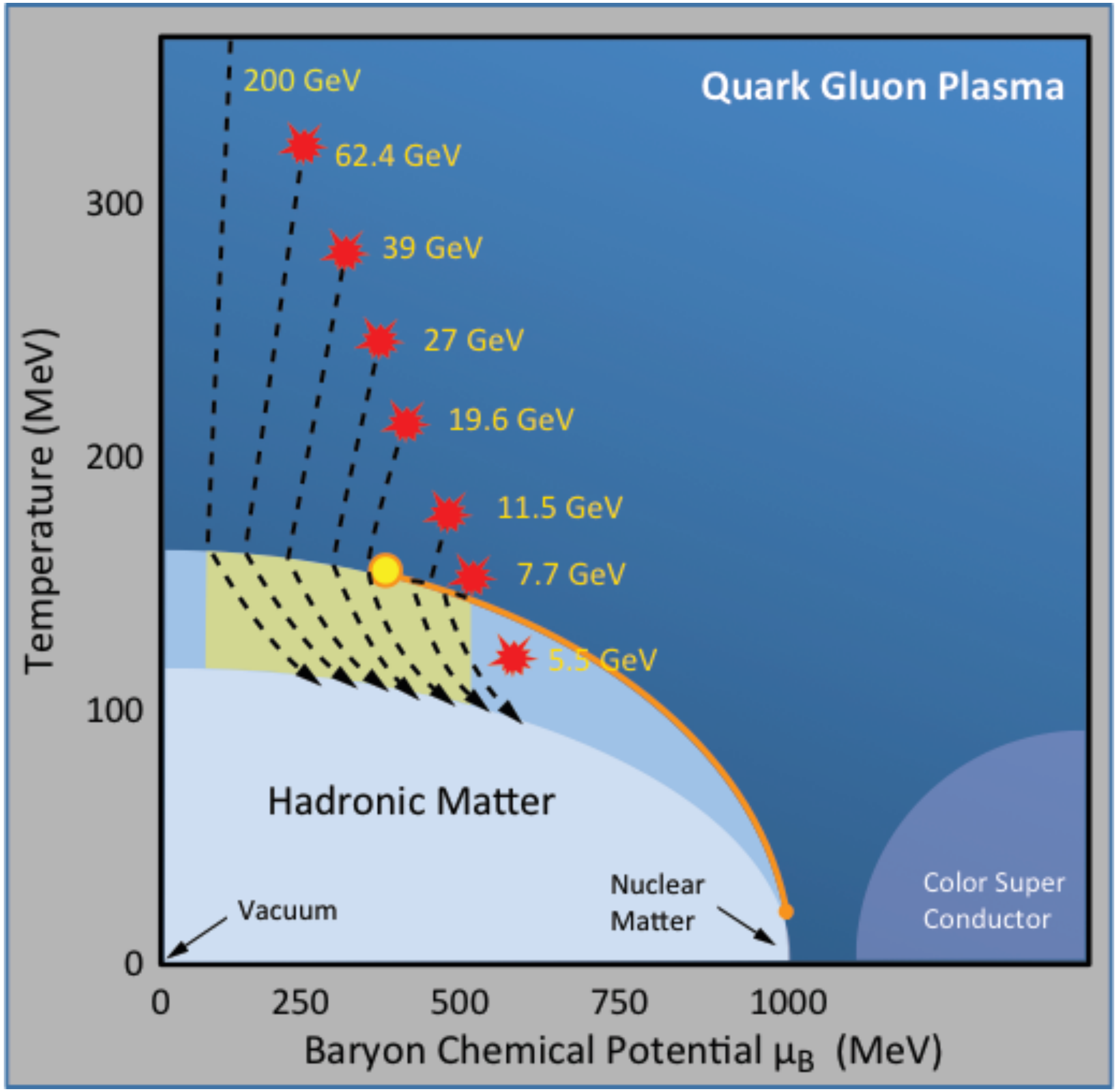

Beam energy range in area of relevance is unique to RHIC

Mapping the features of the QCD matter phase diagram is key to our understanding dense matter

Three Goals:

- Turn-off of QGP signatures
- Critical Point
- First order phase transition

RHIC Beam-Energy-Scan: $\sqrt{s}$ as control parameter to vary initial temperature and chemical potential

Beam Energy Scan: Charged Hadron R_{CP}

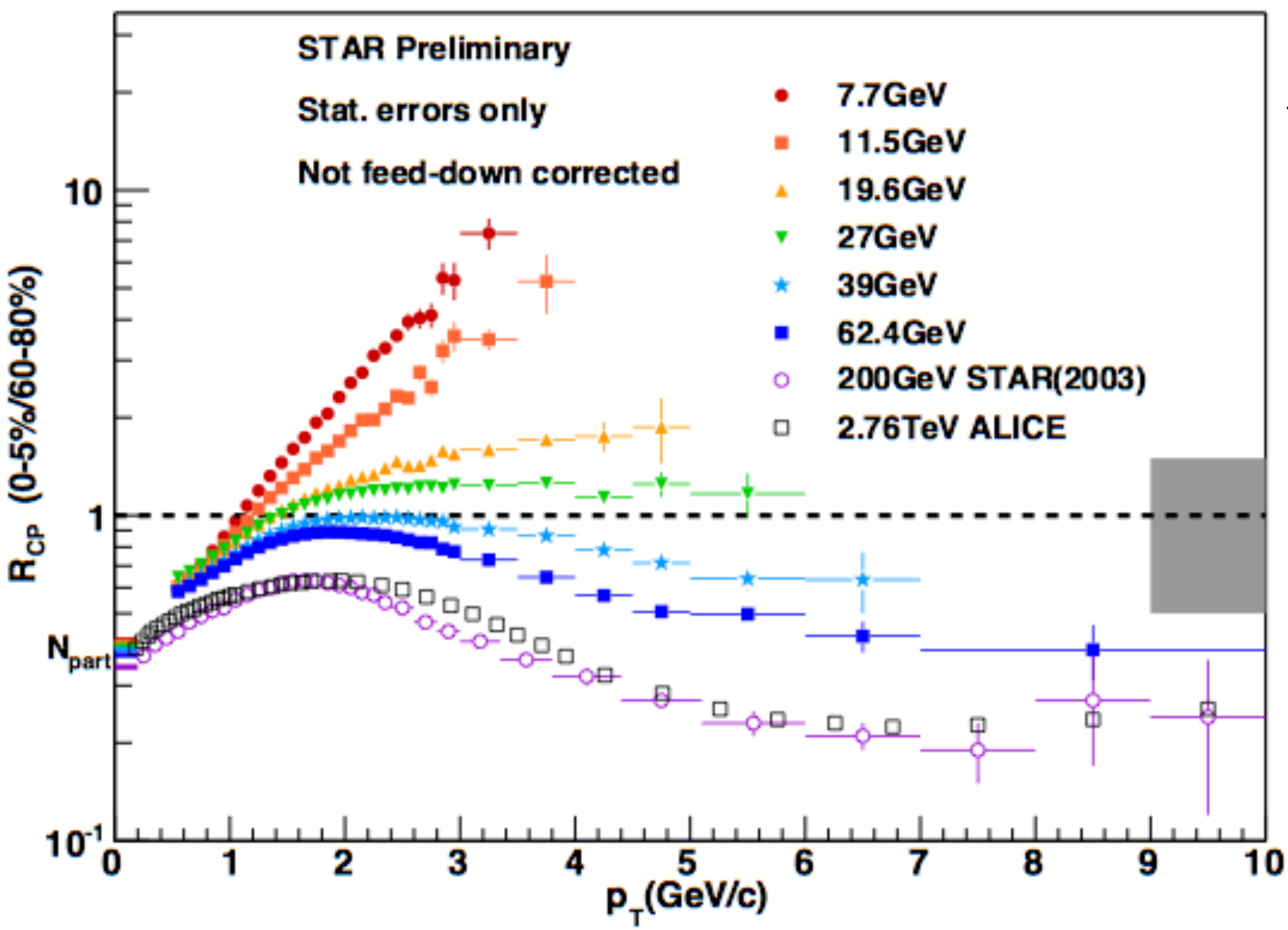

Drops below unity for $\sqrt{s_{NN}} \geq 39$ GeV

At low energies strongly enhanced Cronin effect

Note: R_{CP} < 1 does not imply the absence of suppression (jet quenching)

Need to disentangle Cronin effect and Parton Energy Loss

Higher Flow Harmonics

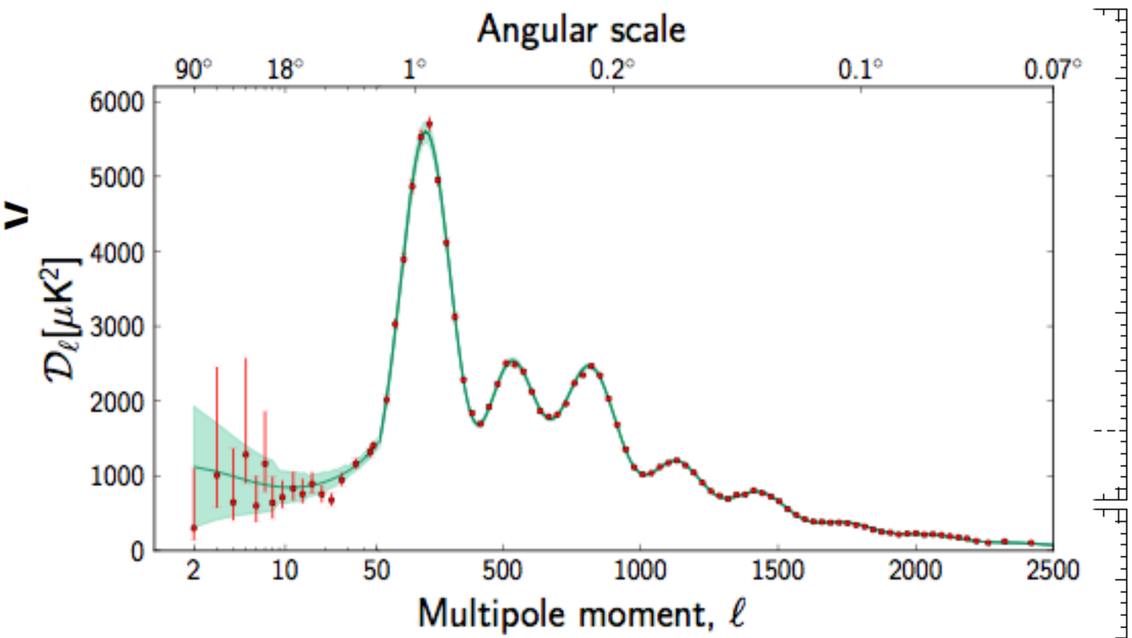

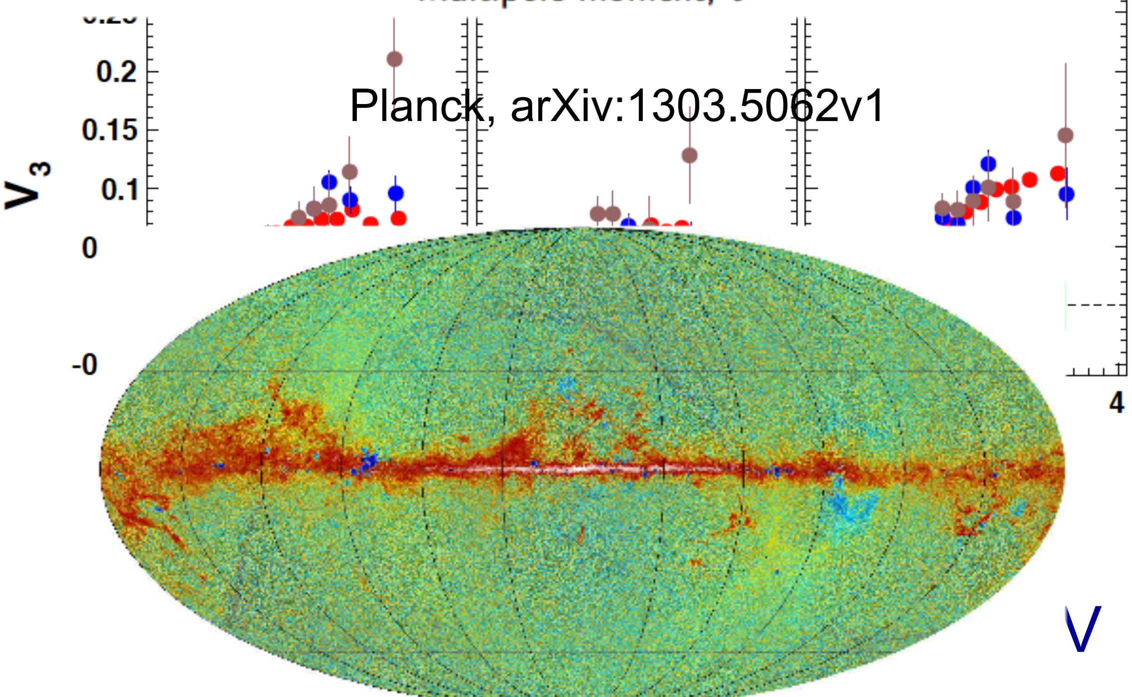

Planck, arXiv:1303.5062v1

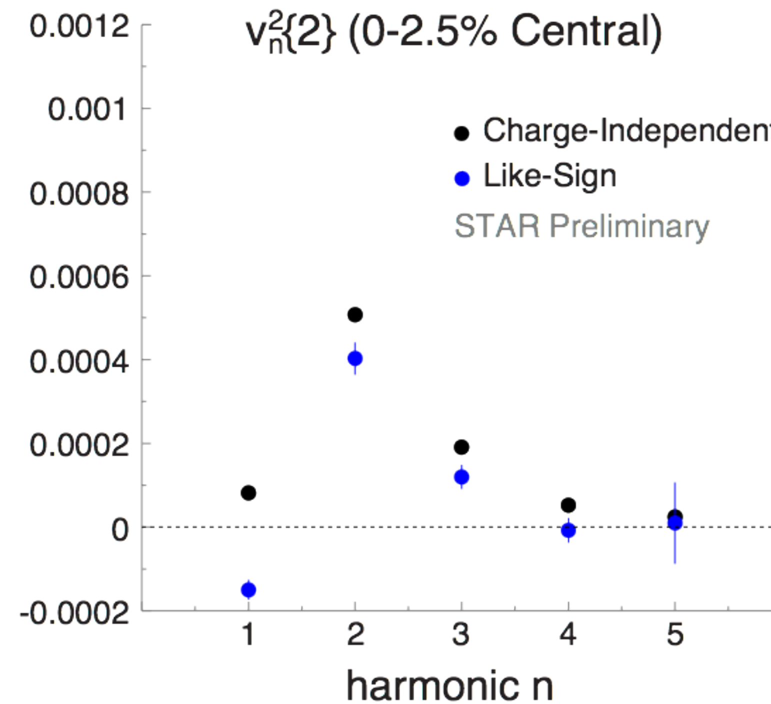

Numerous effects cancel out?

Analog to measurements of early universe sound harmonics…

Heavy Ion harmonics give key constraints on viscous damping and initial spatial correlations

Beam Energy Scan: Energy Density

Bjorken Energy Density: $$\varepsilon_{BJ} = \frac{1}{A_\perp \tau} \frac{dE_T}{dy}$$

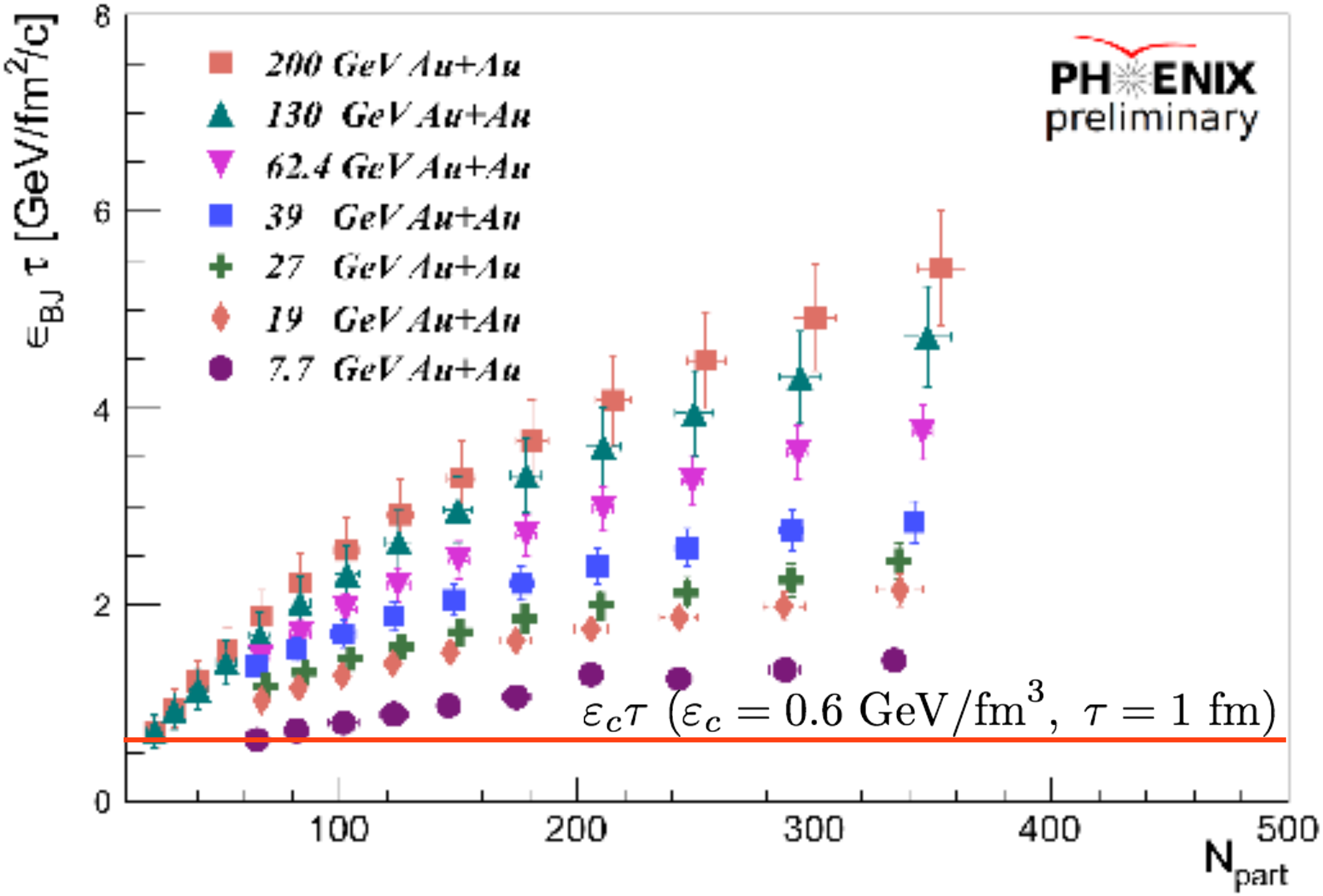

Critical Energy from Lattice:
$\varepsilon_\chi \sim 0.6$ GeV/fm^3

$\varepsilon_{B\vartheta}$ above critical density for all collision energies and centralities

NB.: means QGP at lower energies cannot be excluded from $\varepsilon_{B\vartheta}$

Recent results from heavy-ions collisions at CERN

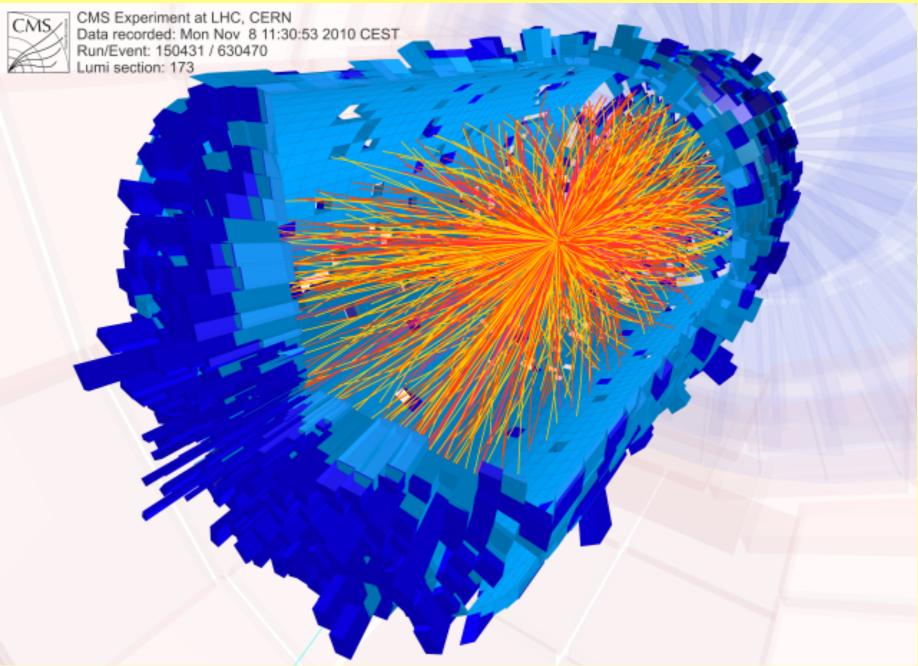

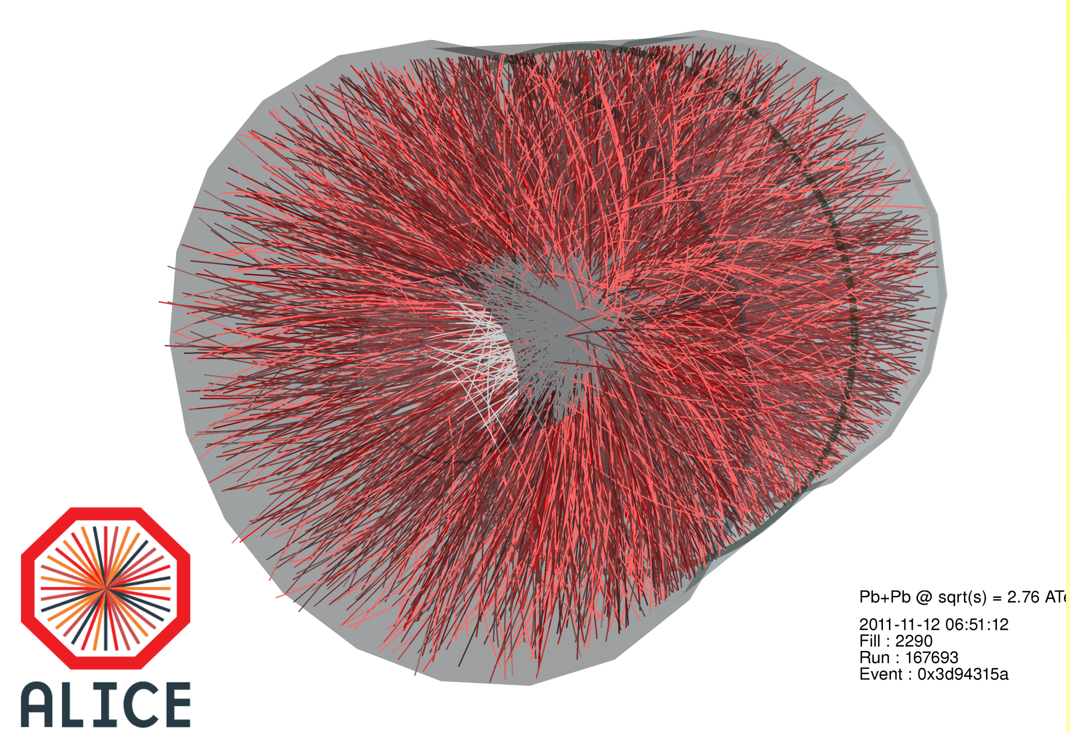

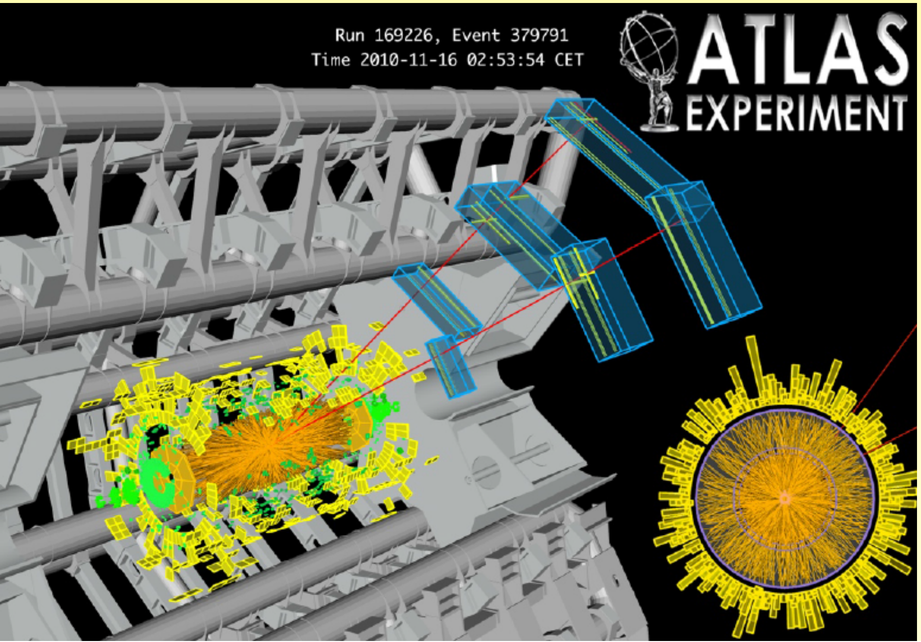

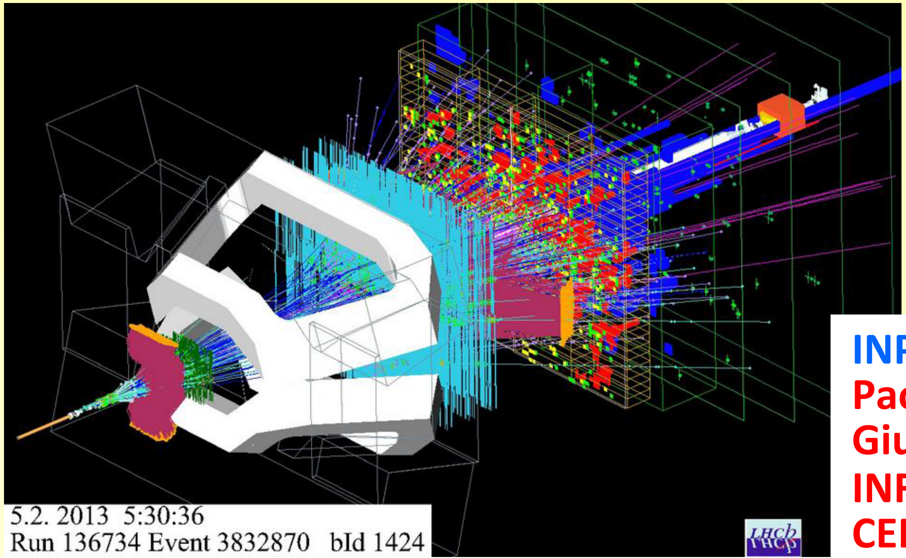

INPC 2013
Paolo Giubellino
INFN Torino & CERN

Azimuthal Asymmetry

SCIENCE Vol: 298 2179 (2002) ^{7}Li

- Fourier expansion of azimuthal distribution:

$$\frac{dN}{p_T dp_T dy d\varphi} = \frac{1}{2\pi}\frac{dN}{p_T dp_T dy}\left(1 + 2v_1\cos(\varphi) + 2v_2\cos(2\varphi) + \ldots\right)$$

$$v_1 = \langle \cos\varphi \rangle \quad \text{"directed flow"}$$

$$v_2 = \langle \cos 2\varphi \rangle \quad \text{"elliptic flow"}$$

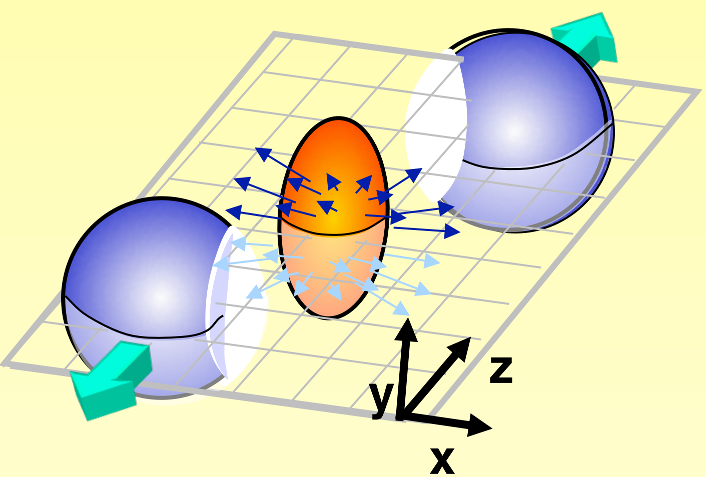

Flow: Correlation between coordinate and momentum space => azimuthal asymmetry of interaction region transported to the final state

→ measure the strength of collective phenomena

Large mean free path

particles stream out isotropically, no memory of the asymmetry

extreme: ideal gas (infinite mean free path)

Small mean free path

larger density gradient -> larger pressure gradient -> larger momentum

extreme: ideal liquid (zero mean free path, hydrodynamic limit)

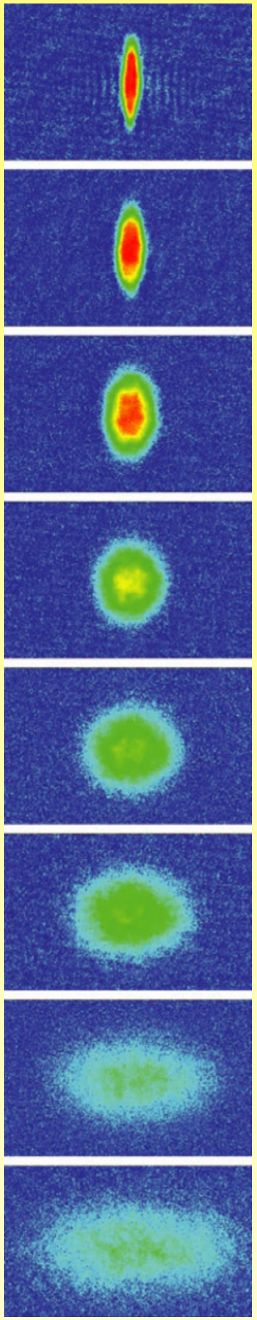

Ultra-cold ^{7}Li 10^{-12} eV , 2 ms of expansion

The shape of an individual event!

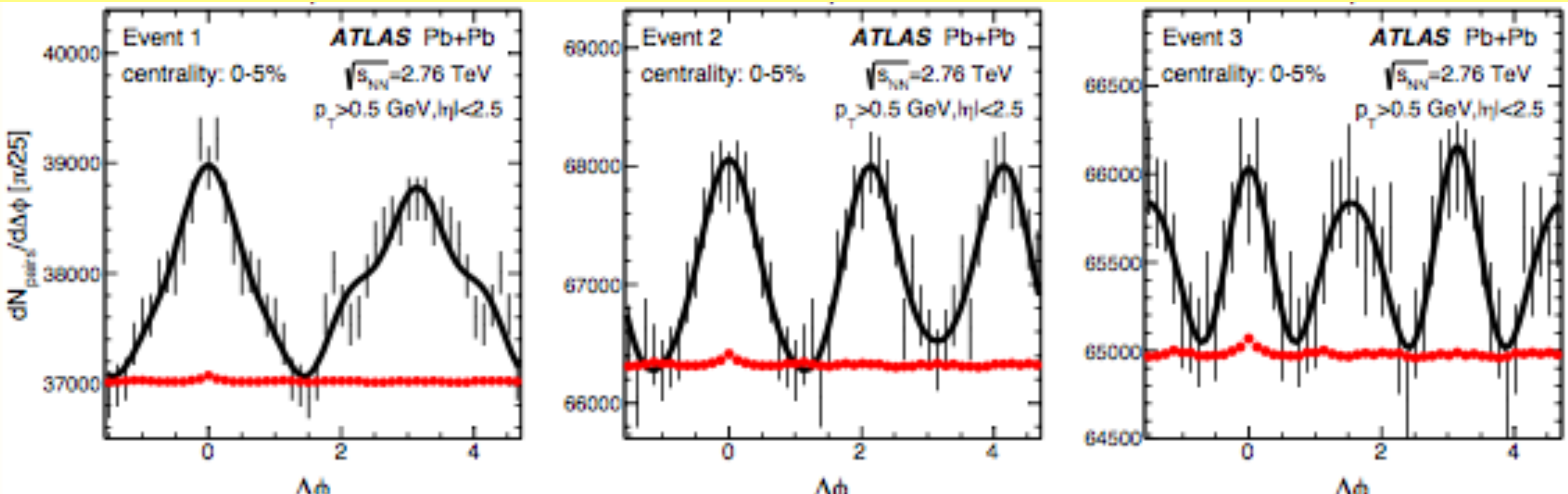

http://arxiv.org/abs/1305.2942

→ study of fluctuations and of event features vs. flow patterns

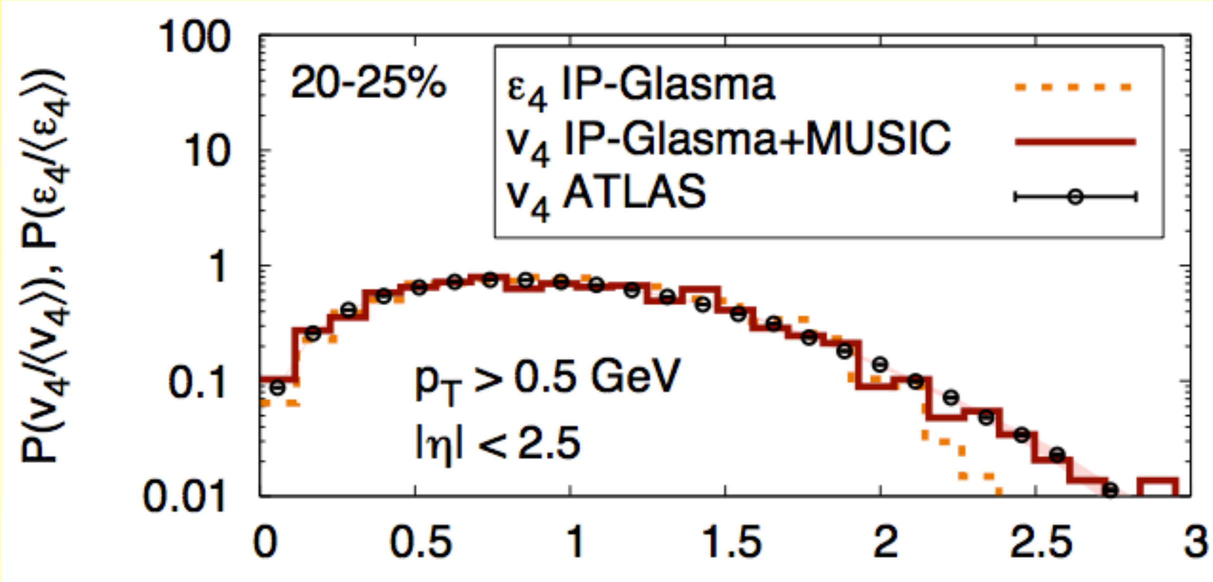

ATLAS, arXiv:1209.6330

Precision measurements: Ultra Central Collisions

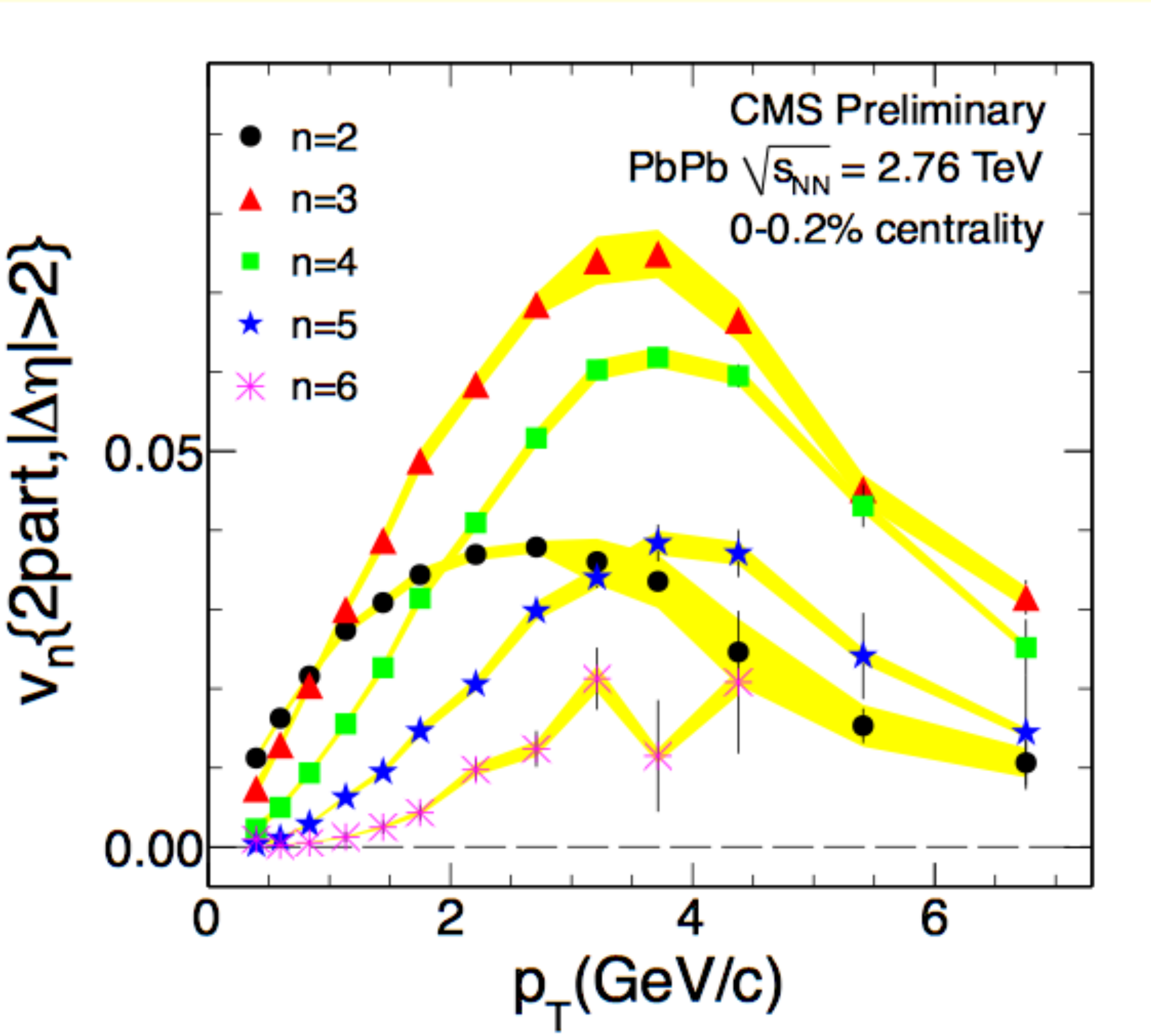

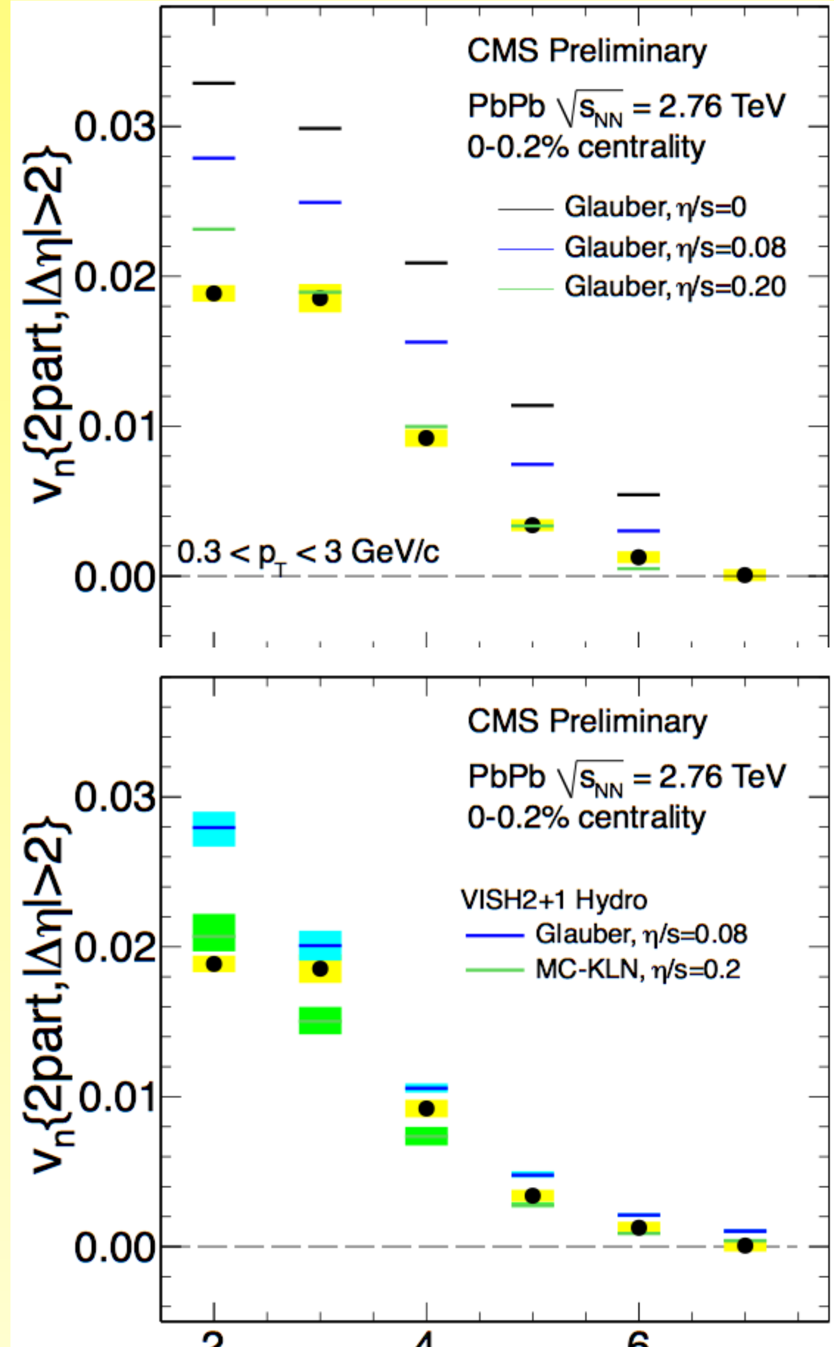

CMS-HIN-12-011

Ultra-central collisions: less uncertainty on initial conditions
Strong constraints on transport coefficients

Detailed studies: Jet peak shape deformation

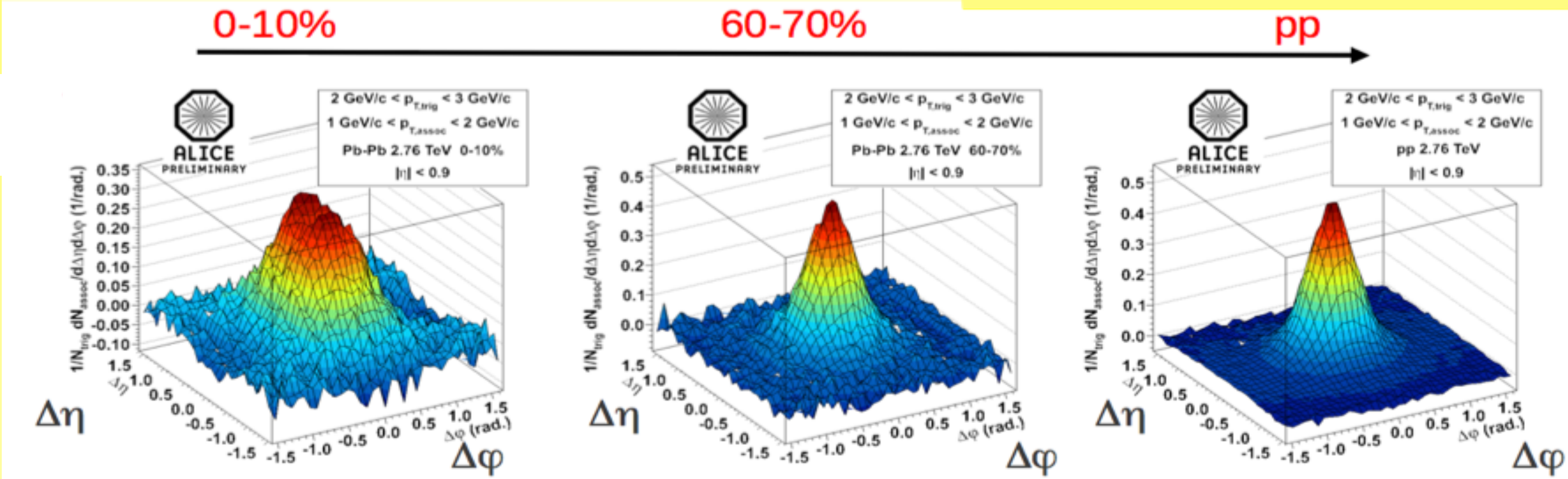

Long-range Δη correlations subtracted Near-side "jet" peak

conical jet shape deformed by longitudinal flow ?

N. Armesto et al., PRL 93,242301 (2004)

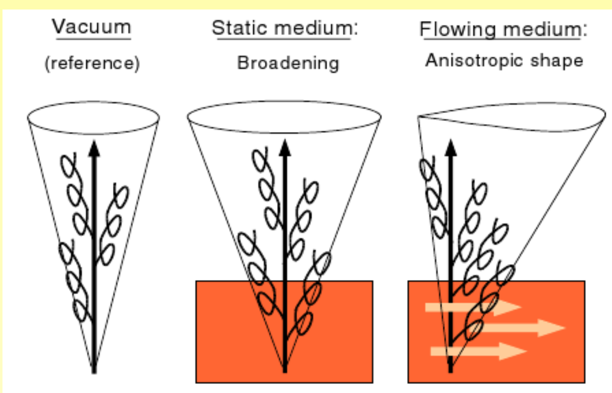

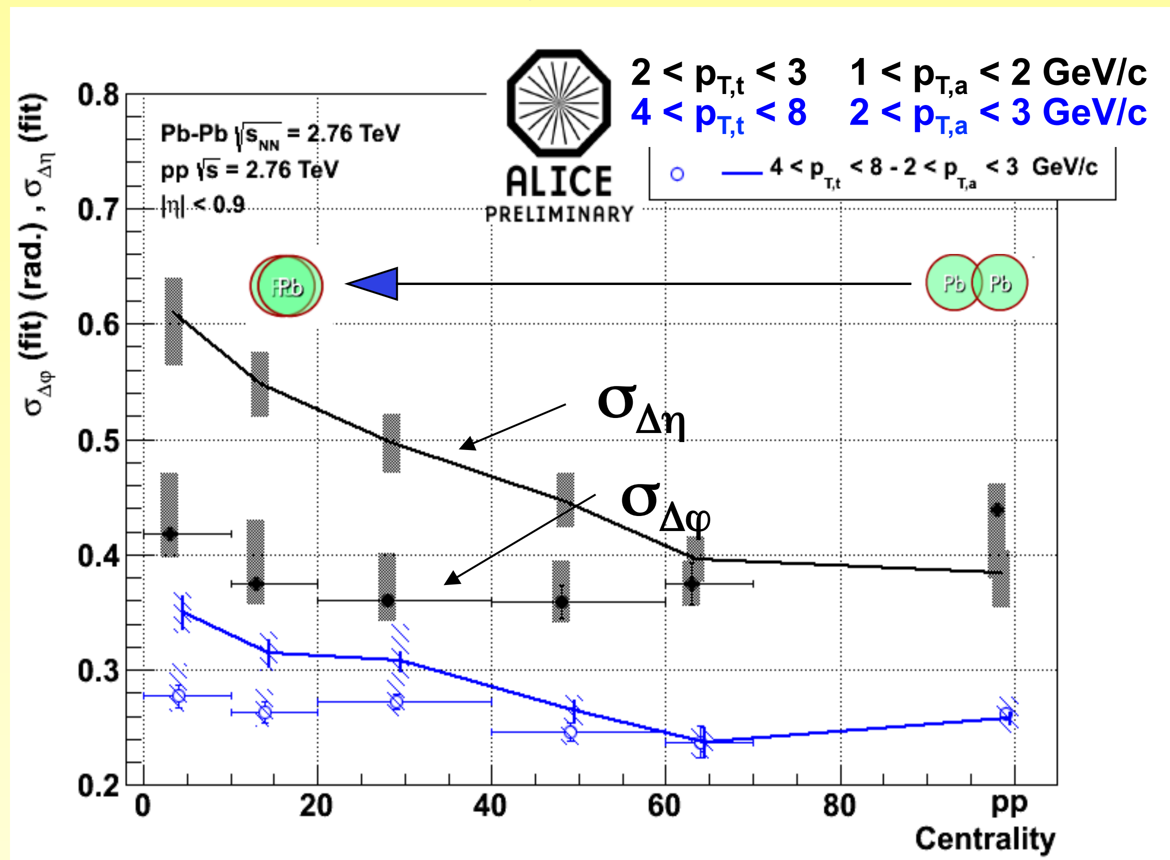

$\sigma_{\Delta\varphi}$ constant whereas $\sigma_{\Delta\eta}$ increases with centrality.

$\sigma_{\Delta\eta} > \sigma_{\Delta\varphi}$ predicted by models including longitudinal flow.

Jets in heavy ion collisions: full jet spectrum

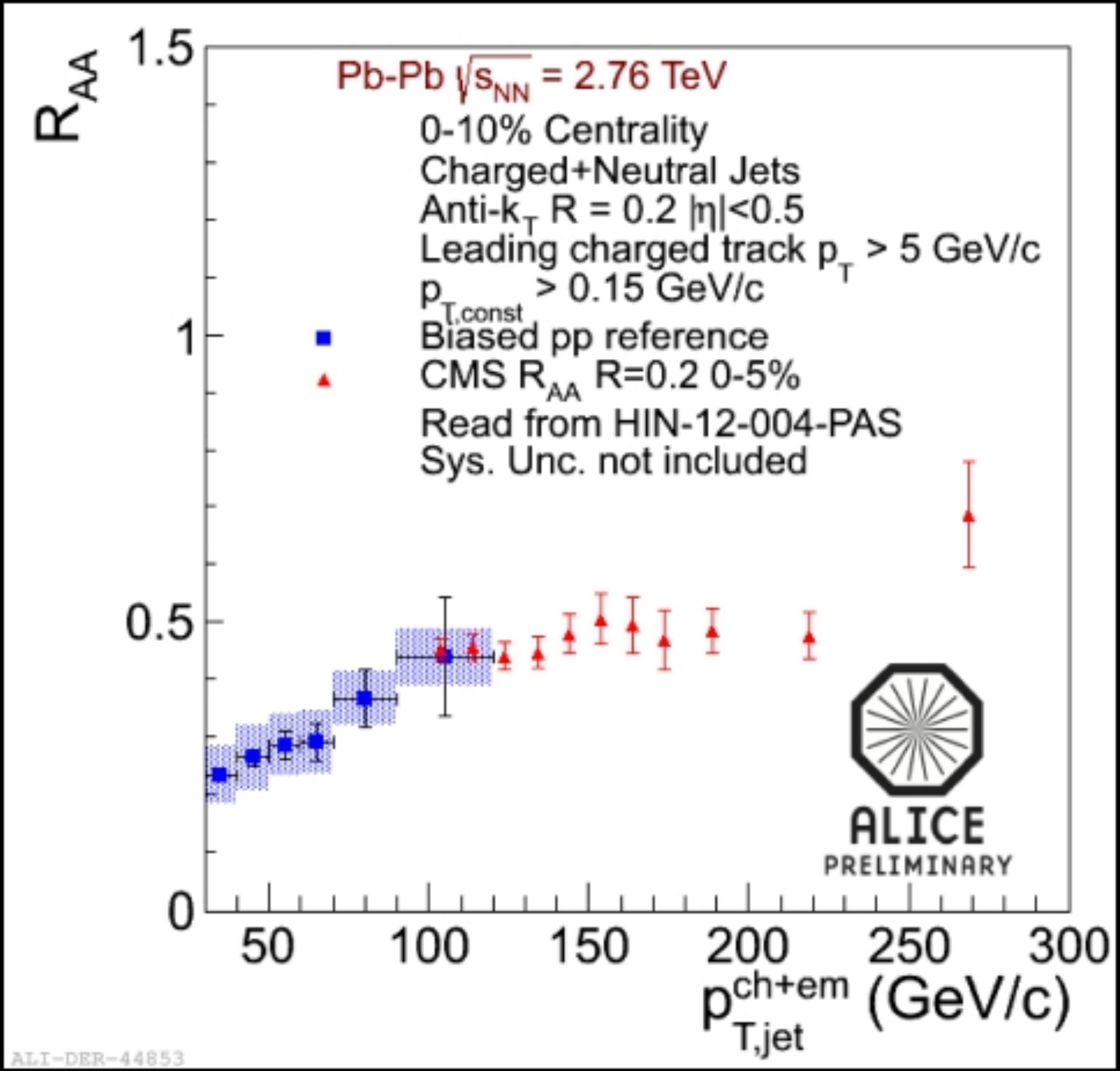

ALICE and CMS measurements complimentary

***R_{AA}* increases with *p_T* at *p_T*<100 GeV**

R_{AA}* approx. constant at high *p_T

Jets in heavy ion collisions: recoil jet suppression

R=0.2 p_T^{const}>0.15 GeV **R=0.4 p_T^{const}>2 GeV**

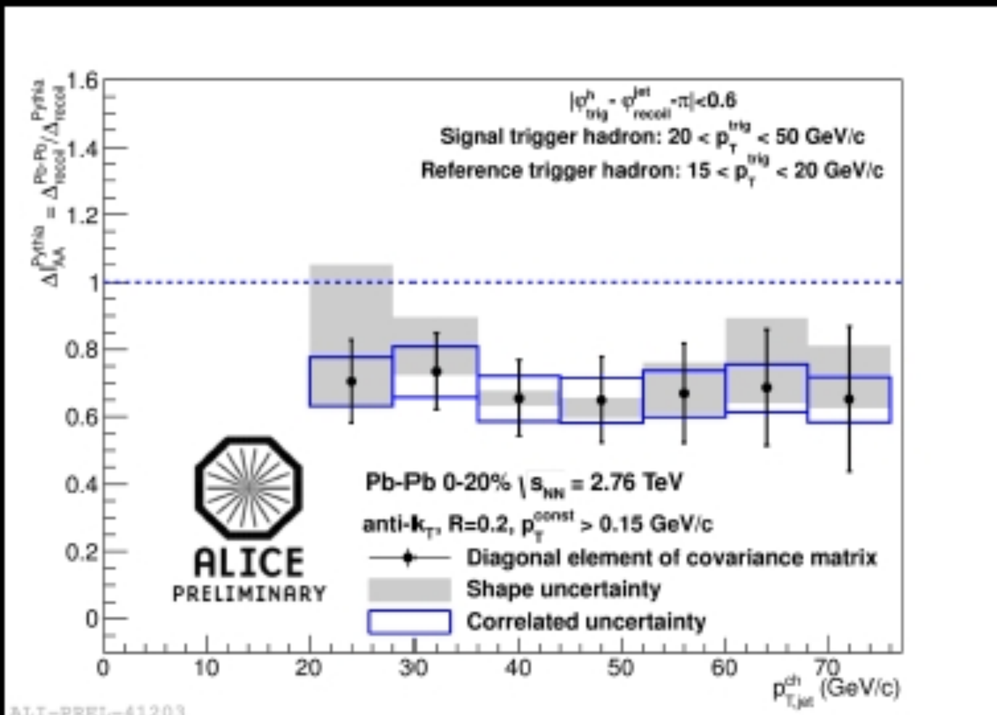

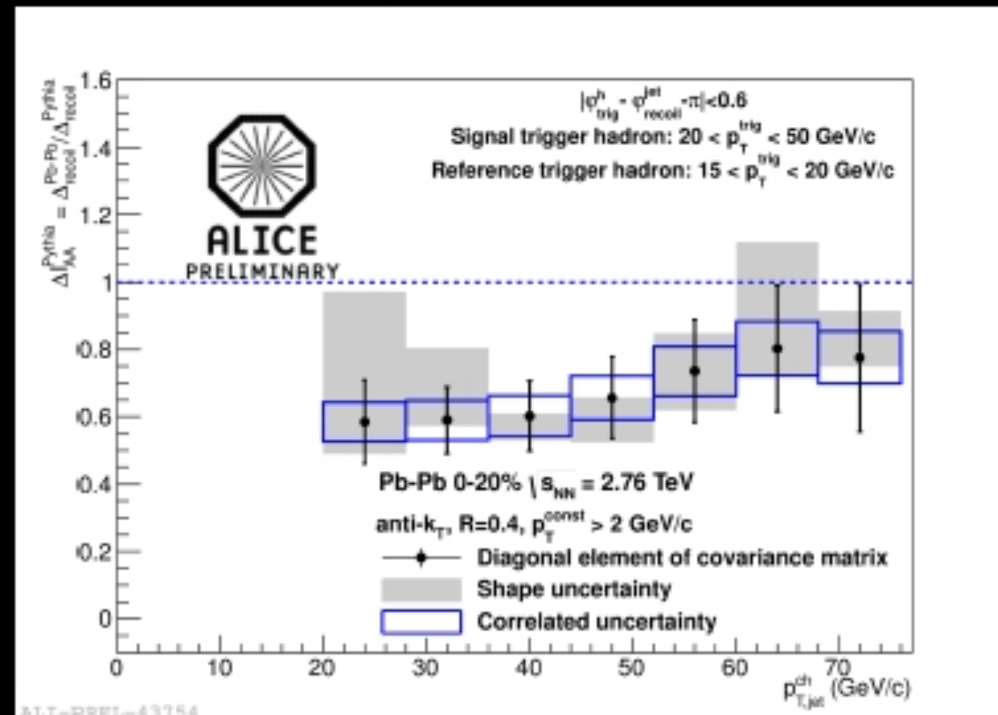

Modifications of the jet structure are explored by varying the jet resolution R and the minimum constituent p_T cut.

No hints for energy redistribution below R=0.4 within large systematic errors

Working on the reduction of the systematics to constrain quenching effects

J/ψ ~~suppression~~ ?

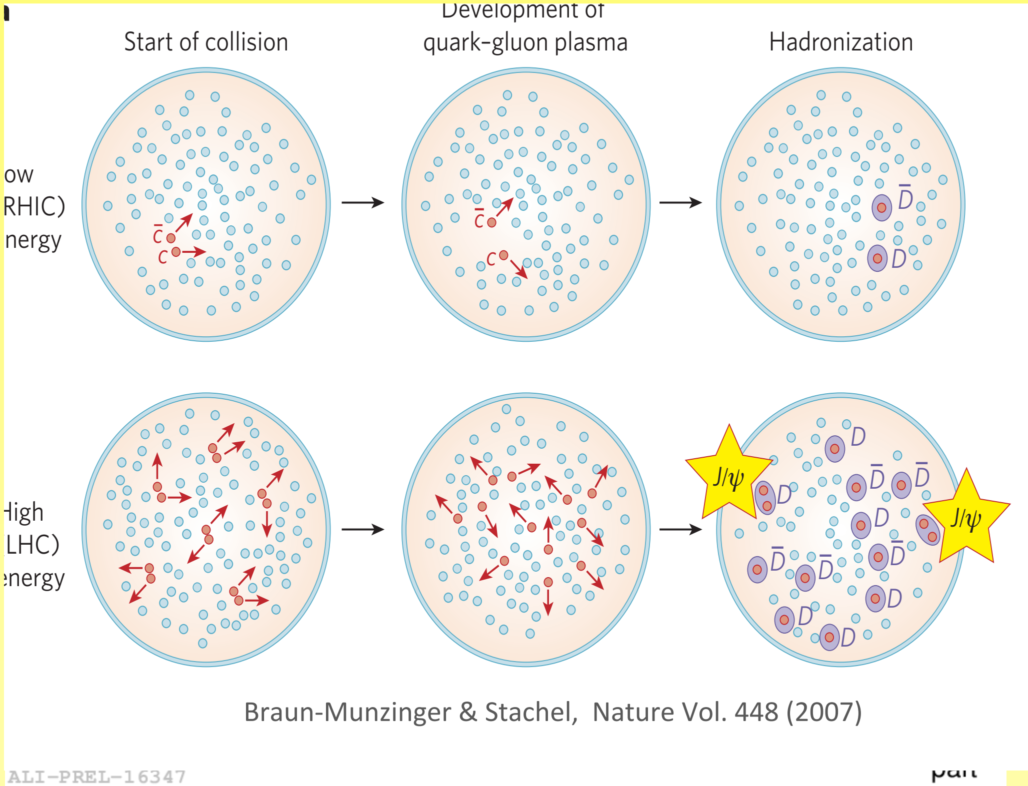

less suppression than RHIC

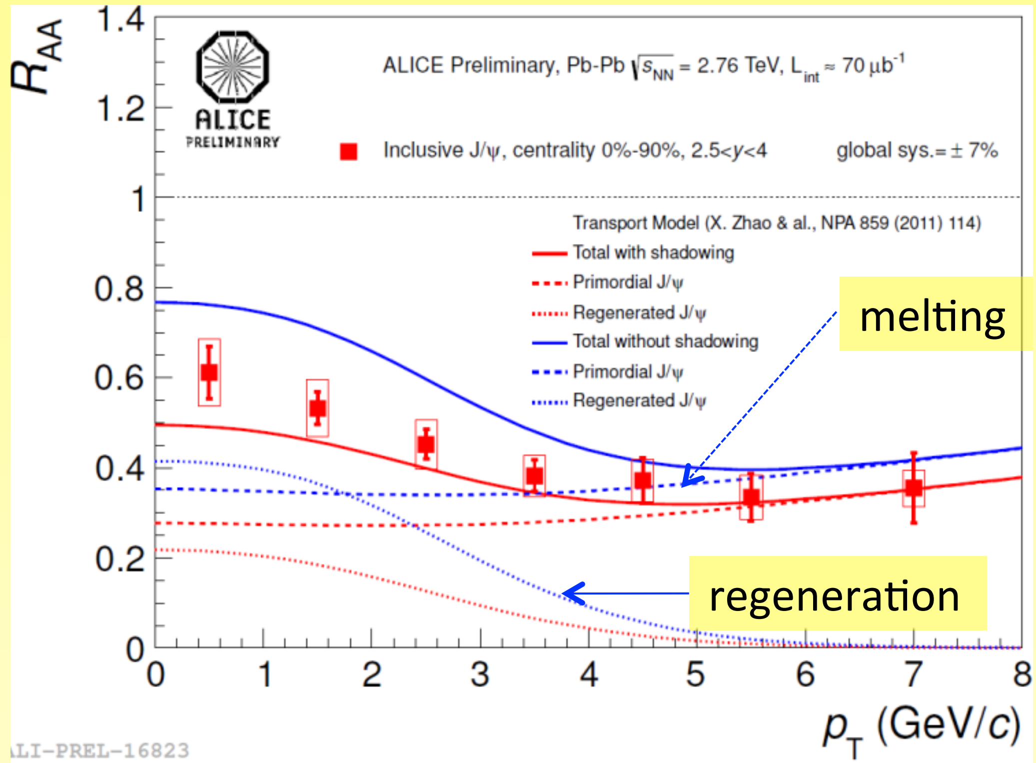

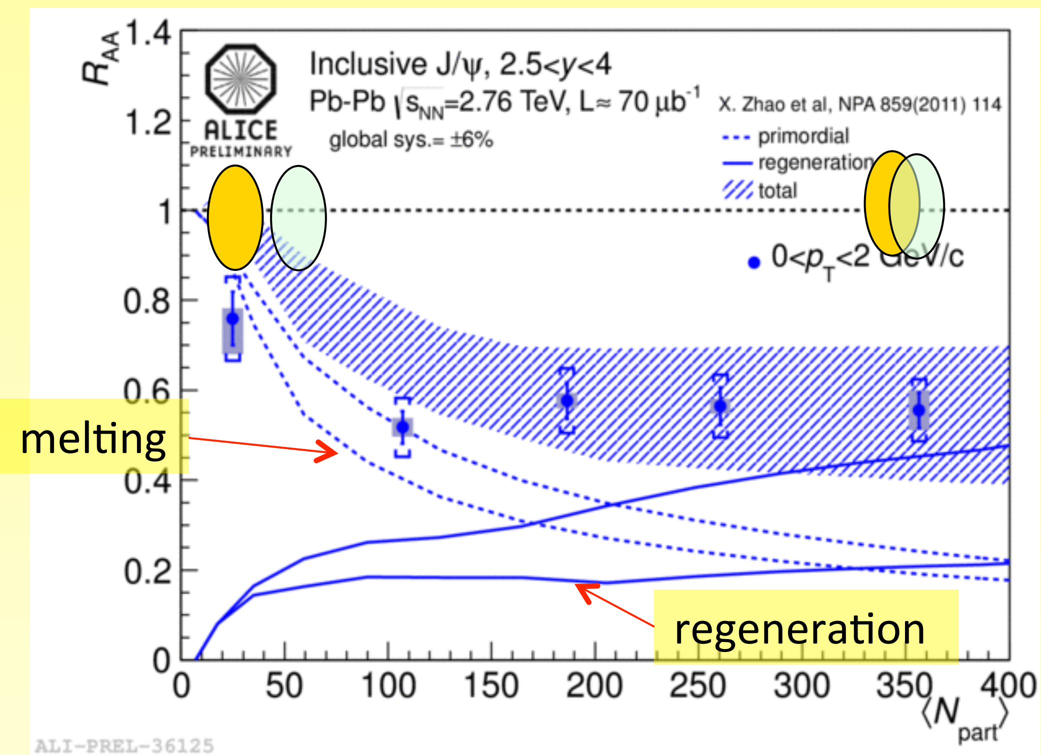

p_T dependence in agreement with models including regeneration.

Nuclear modification factor pPb vs PbPb

$$R_{AB} = \frac{\mathrm{d}N_{AB}/\mathrm{d}p_{\mathrm{T}}}{\langle N_{\mathrm{coll}}\rangle \mathrm{d}N_{\mathrm{pp}}/\mathrm{d}p_{\mathrm{T}}}$$

- R_{pPb} (at mid-rapidity) consistent with unity for p_T > 2 GeV/c
- High-p_T charged particles exhibit binary scaling
- Unlike in PbPb, no suppression at high p_T is observed
- Suppression at high p_T in PbPb is not an initial state effect

ALICE, PRL 110 (2013) 082302

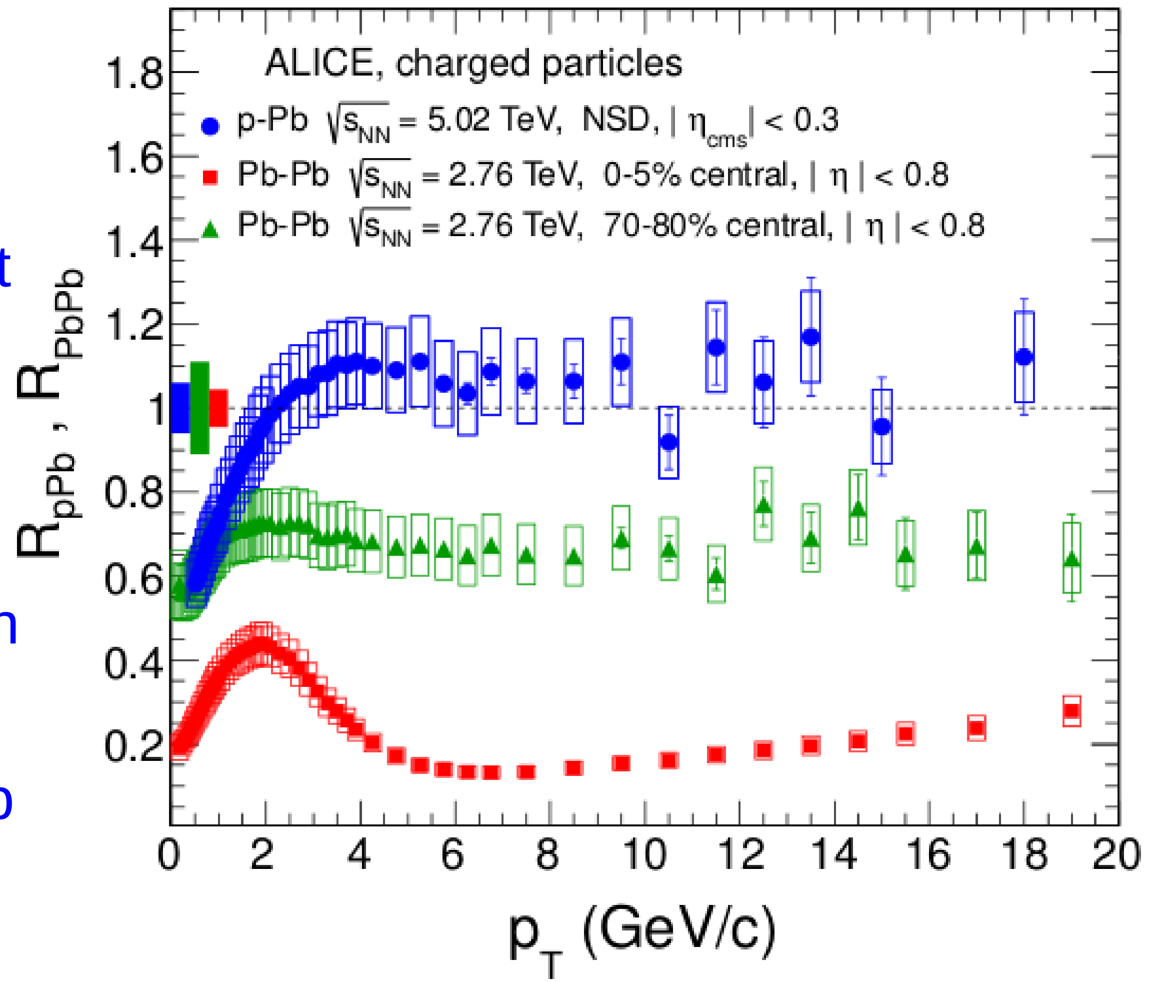

Constantin Loizides
(LBNL/EMMI)

Charged particle pseudorapidity density

ALICE, PRL 110 (2013) 032301

- Tracklet based analysis
  - Dominant systematic uncertainty from NSD normalization of 3.1%
- Reach of SPD extended to |η|<2 by extending the z-vertex range
- Results in ALICE laboratory system
  - $y_{cms} = -0.465$
- Comparison with models
  - Most models within 20%
  - Saturation models have too steep rise between p and Pb region
  - See for further comparisons Albacete et al., arXiv:1301.3395

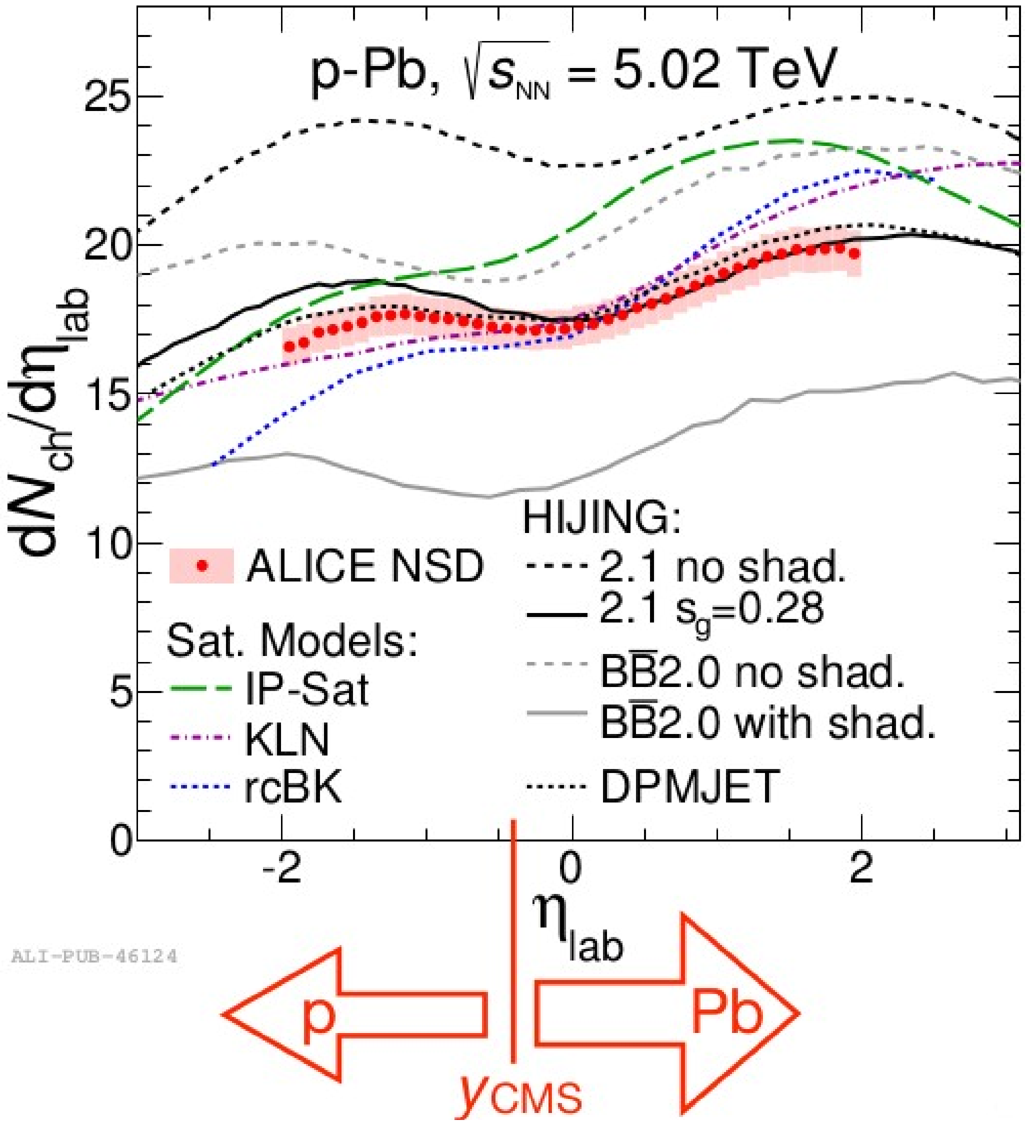

NB: HIJING calculations are expected to increase by ~4% from INEL to NSD

Constantin Loizides
(LBNL/EMMI)

Two-particle angular correlations

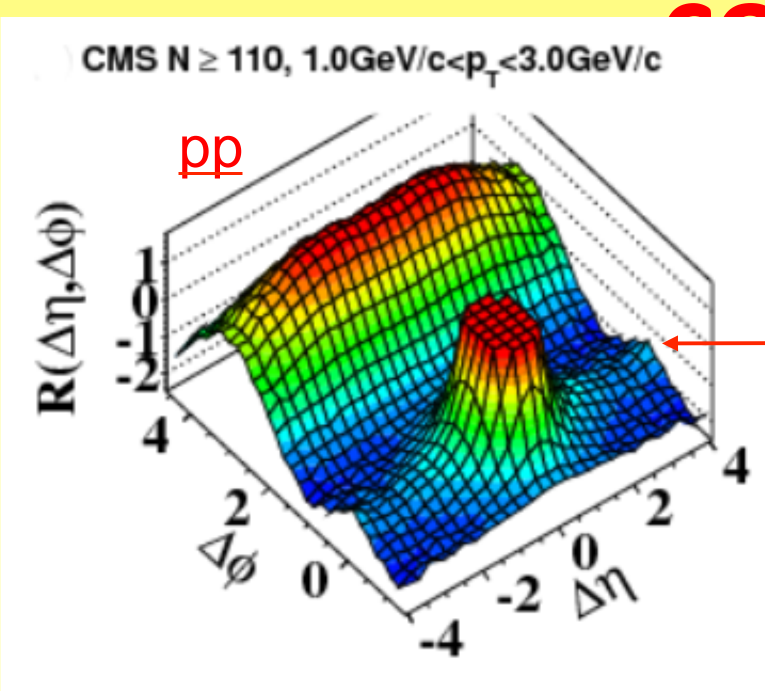

CMS, JHEP 1009 (2010) 91

Near-side ridges apparent in high multiplicity events at LHC energies

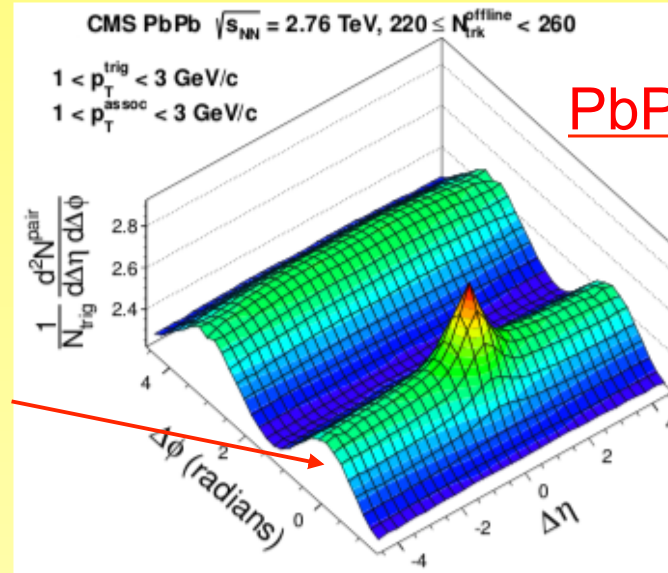

CMS, arXiv:1305.0609

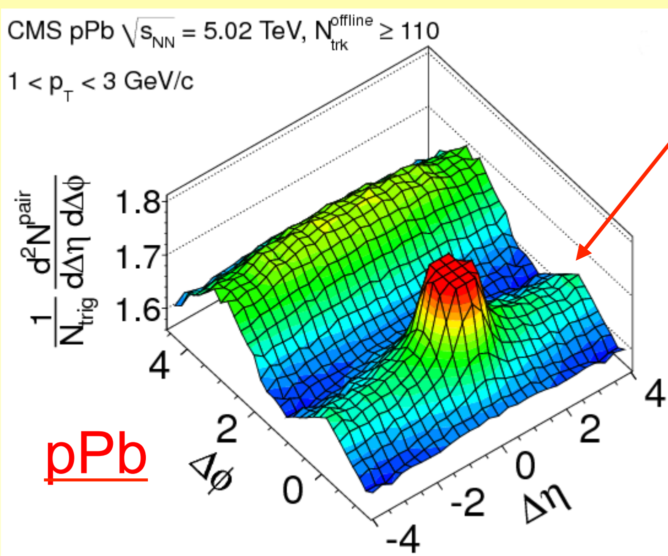

CMS, PLB 718 (2012) 795

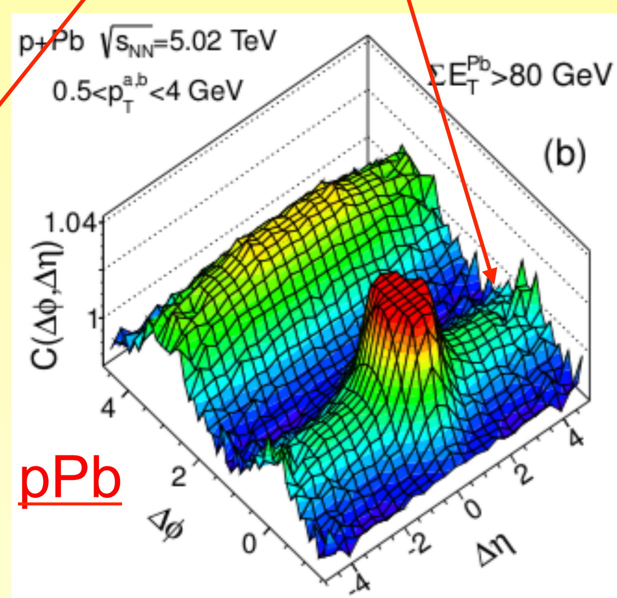

ATLAS, arXiv:1212.5198

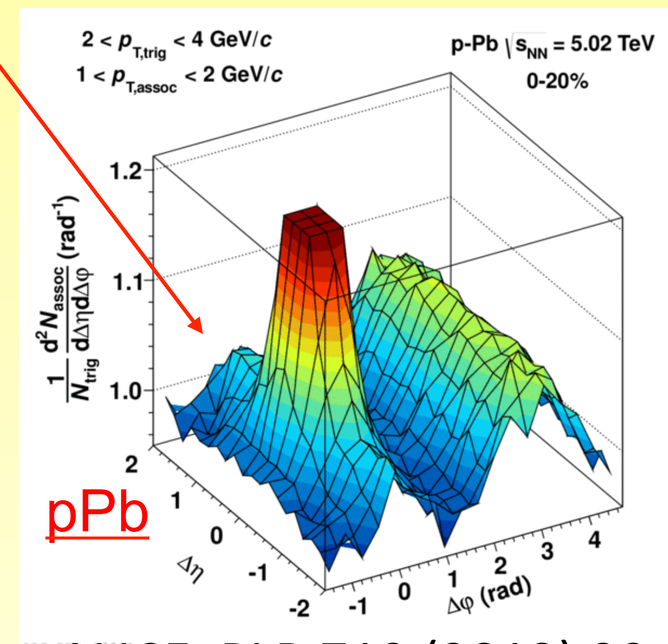

ALICE, PLB 719 (2013) 29

Correlations in 7 TeV pp collisions

JHEP 1009, 091

Results based on $1 fb^{-1}$,
i.e. sampling 50 billion pp events
with high multiplicity trigger

Intermediate p_T: 1-3 GeV/c

(b) MinBias, $1.0 GeV/c < p_T < 3.0 GeV/c$

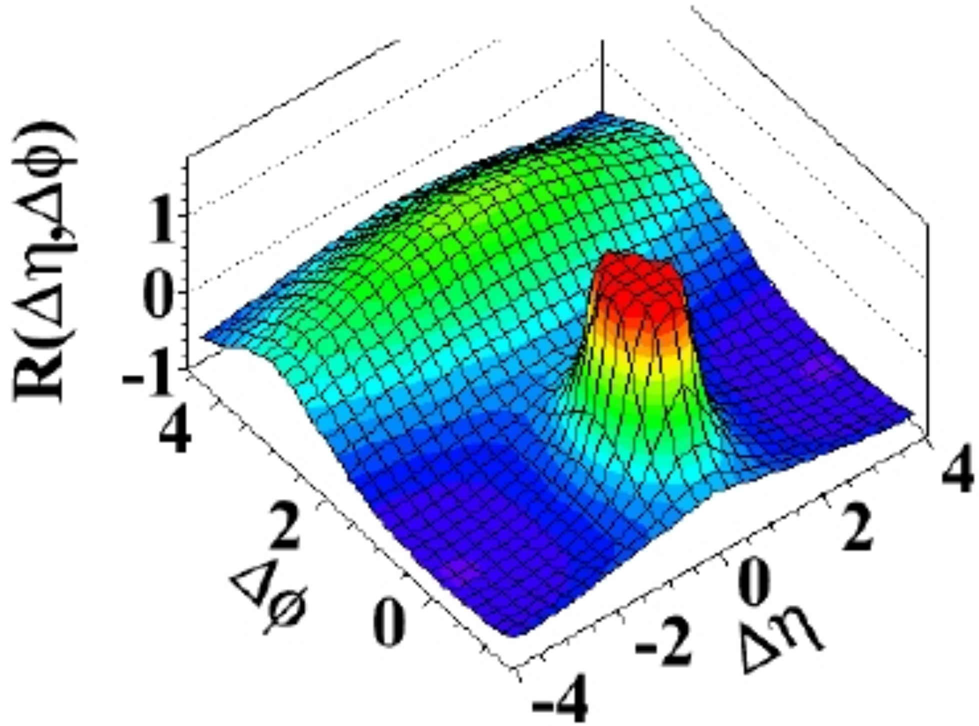

(d) N>110, $1.0 GeV/c < p_T < 3.0 GeV/c$

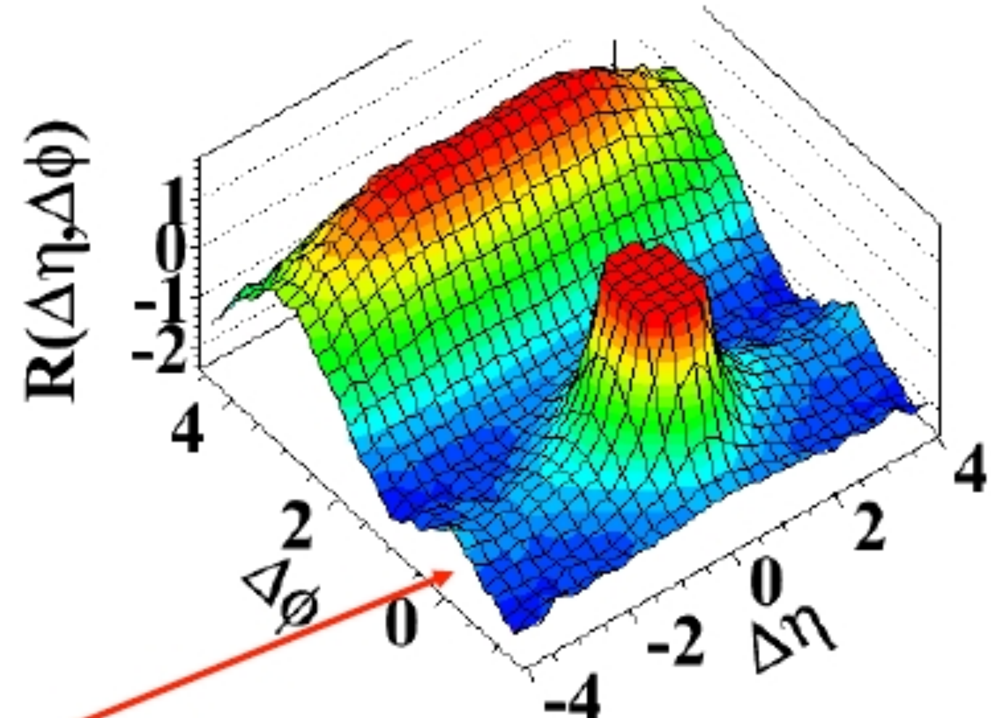

Pronounced structure at large $\Delta\eta$ around $\Delta\phi \sim 0$!

Multiplicity Evolution in pPb

PLB 718 (2013) 795

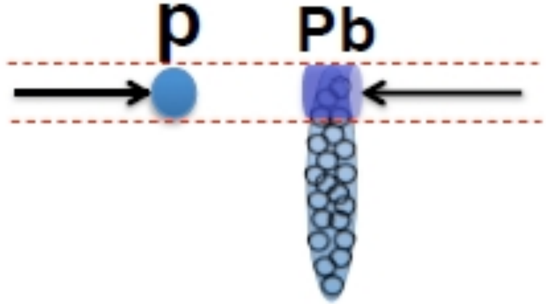

Low multiplicity

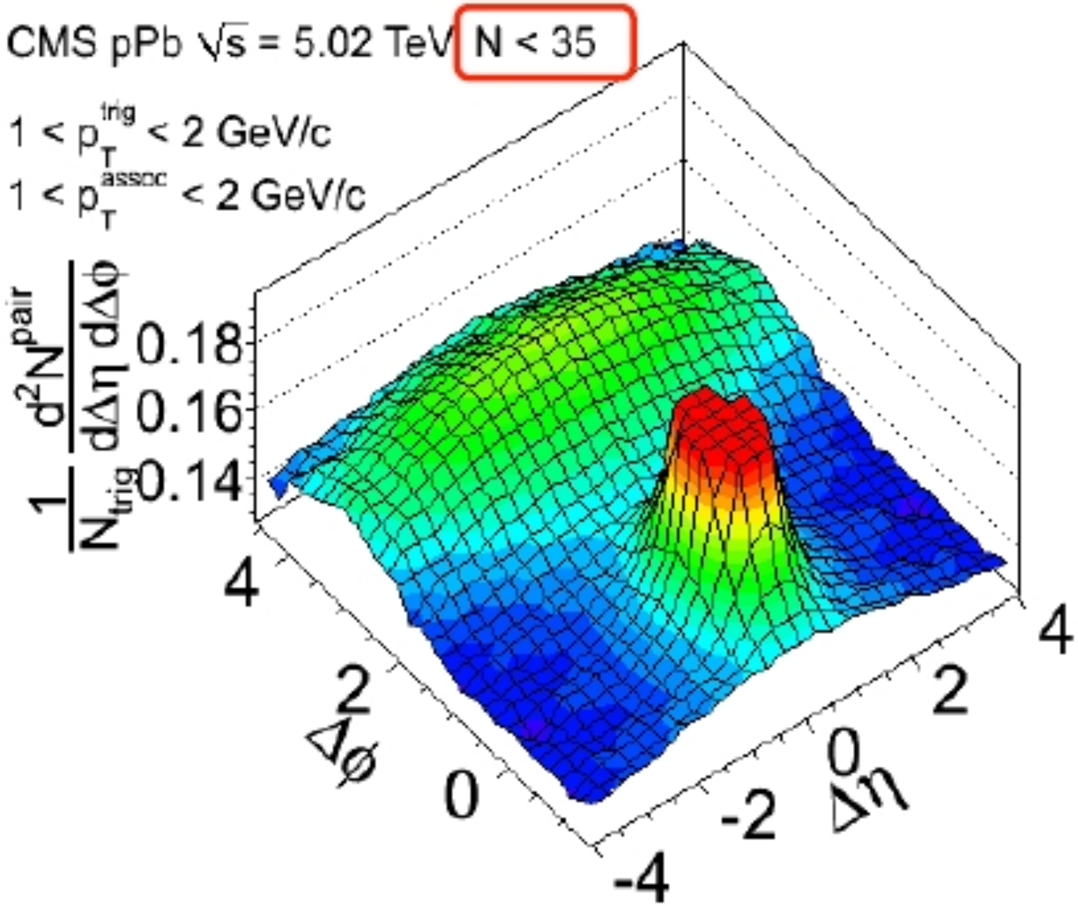

Divide into 4 multiplicity bins:

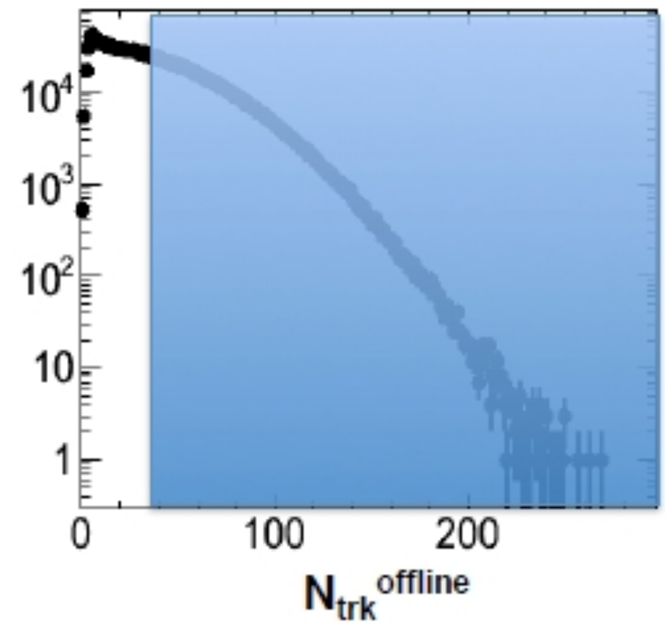

Multiplicity Evolution in pPb

PLB 718 (2013) 795

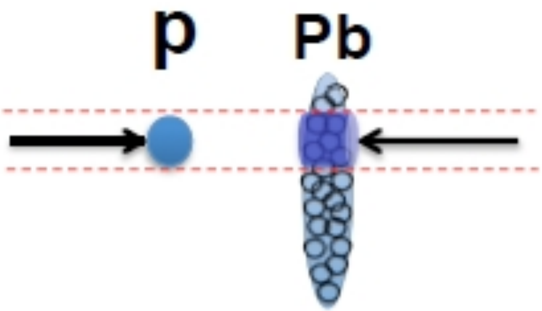

Increasing multiplicity

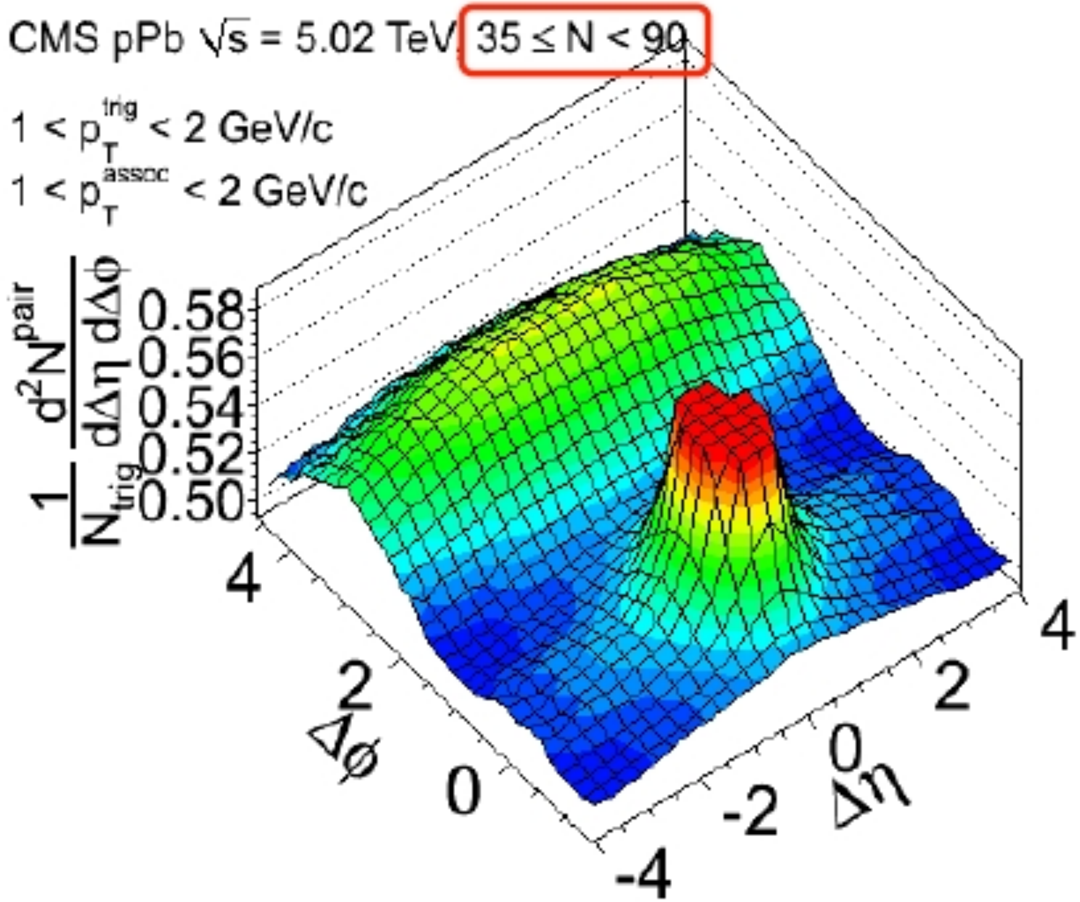

Divide into 4 multiplicity bins:

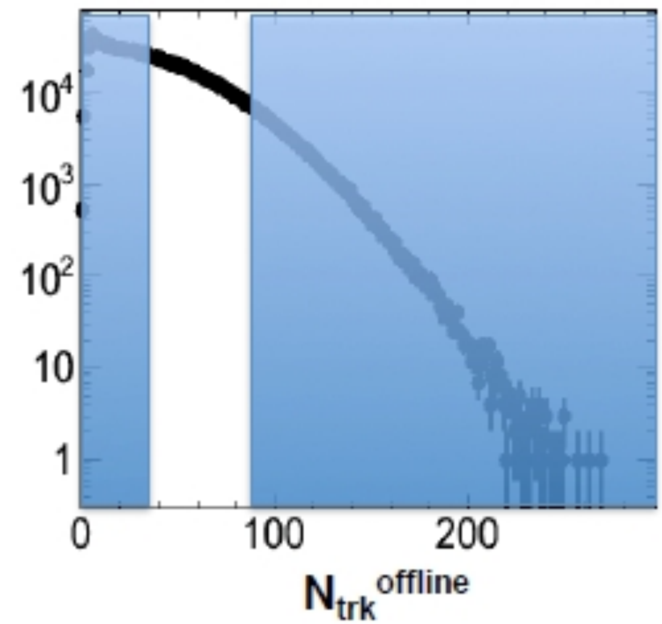

Multiplicity Evolution in pPb

PLB 718 (2013) 795

Increasing multiplicity

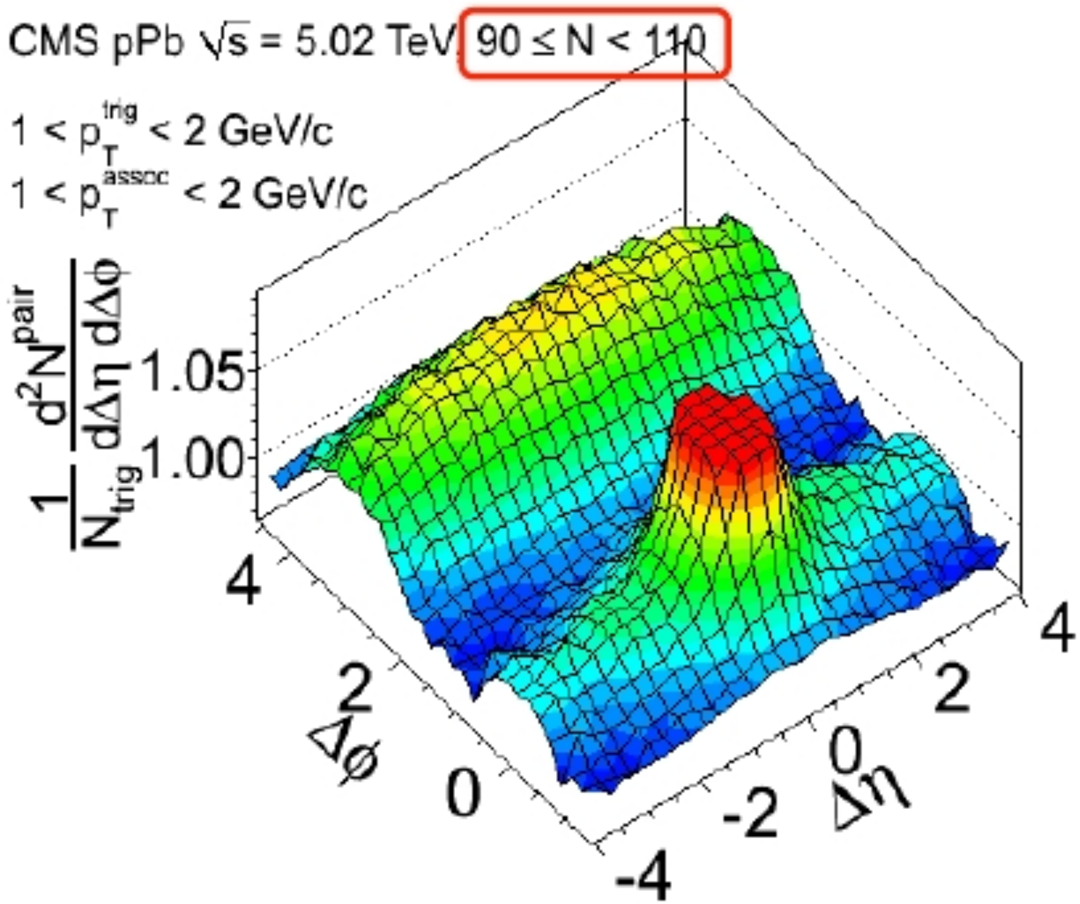

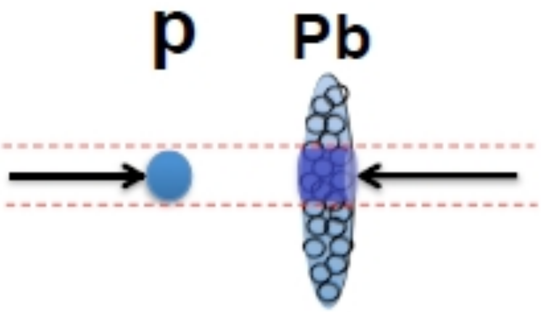

Divide into 4 multiplicity bins:

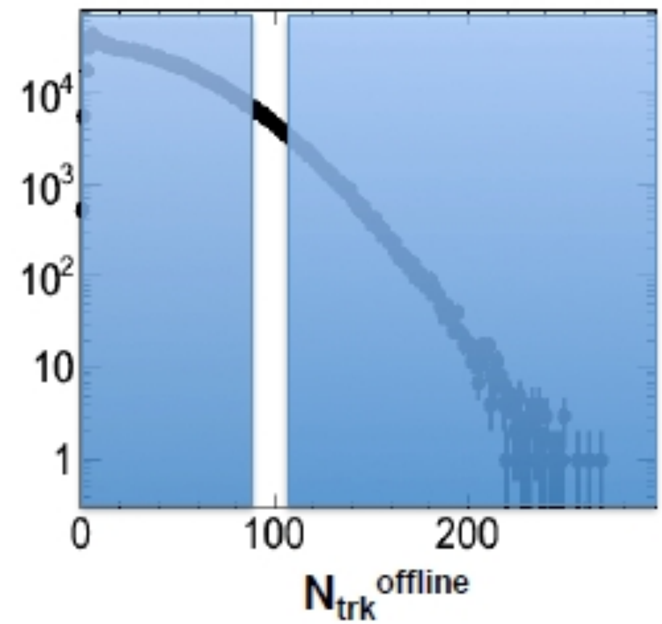

Multiplicity Evolution in pPb

PLB 718 (2013) 795

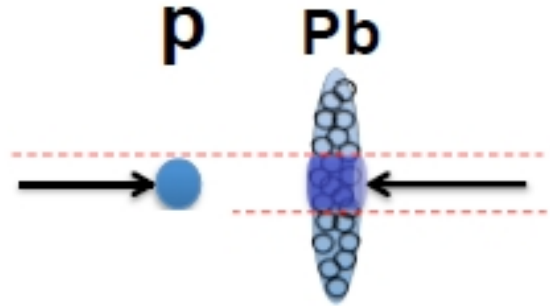

Increasing multiplicity

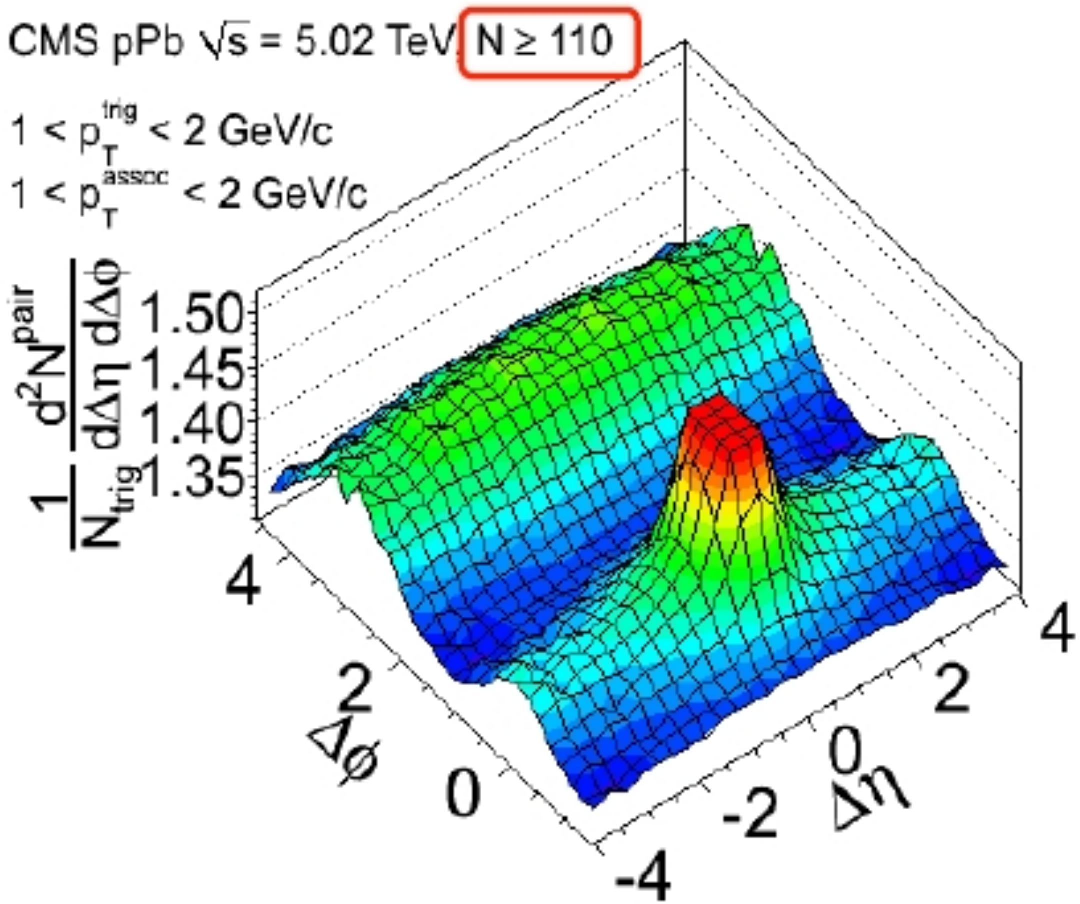

Divide into 4 multiplicity bins:

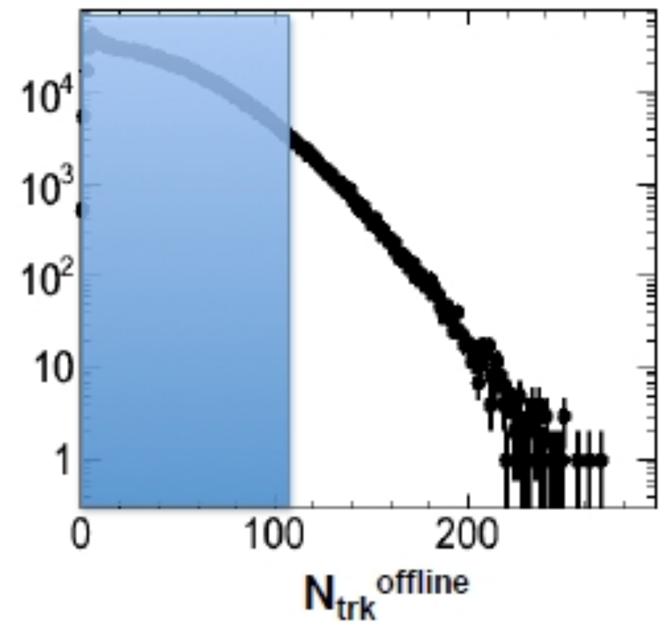

Subtracting the low-mult from the high-mult

- A double-ridge structure appears, with remarkable properties:
  - **Same yield near and away side for all classes of p_T and multiplicity: suggest common underlying process**
  - Width independent of p_T
  - Shape of the distributions decomposed into a Fourier series, in terms of the coefficients v_n of the corresponding single particle azimuthal distributions
    - v_2 is the dominant component
    - v_2 and v_3 increase with p_T and v_2 also with multiplicity
  - possible explanations? CGC?? Flow??

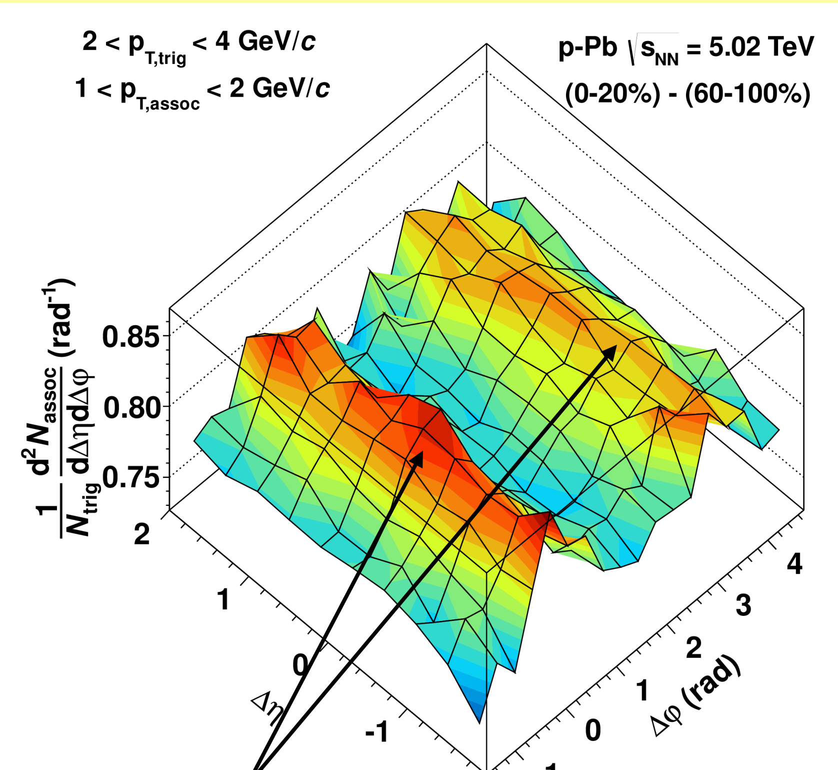

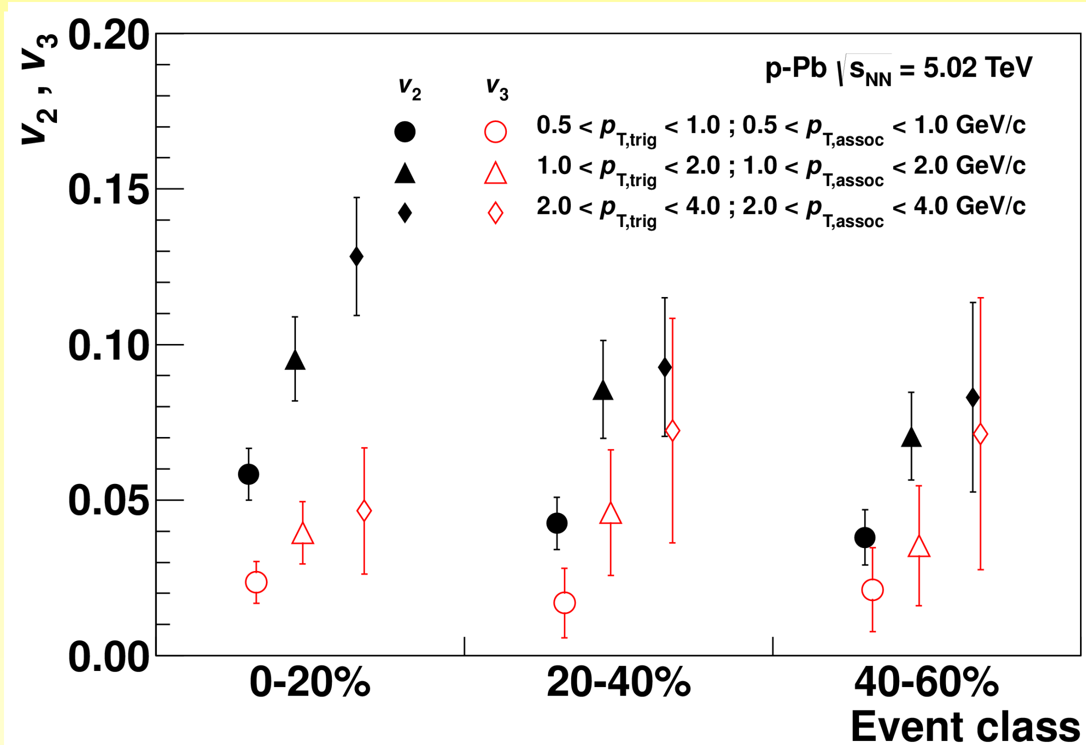

Double-ridge structure

Also observed by ATLAS, with the same method, and CMS

v_3 in PbPb and pPb

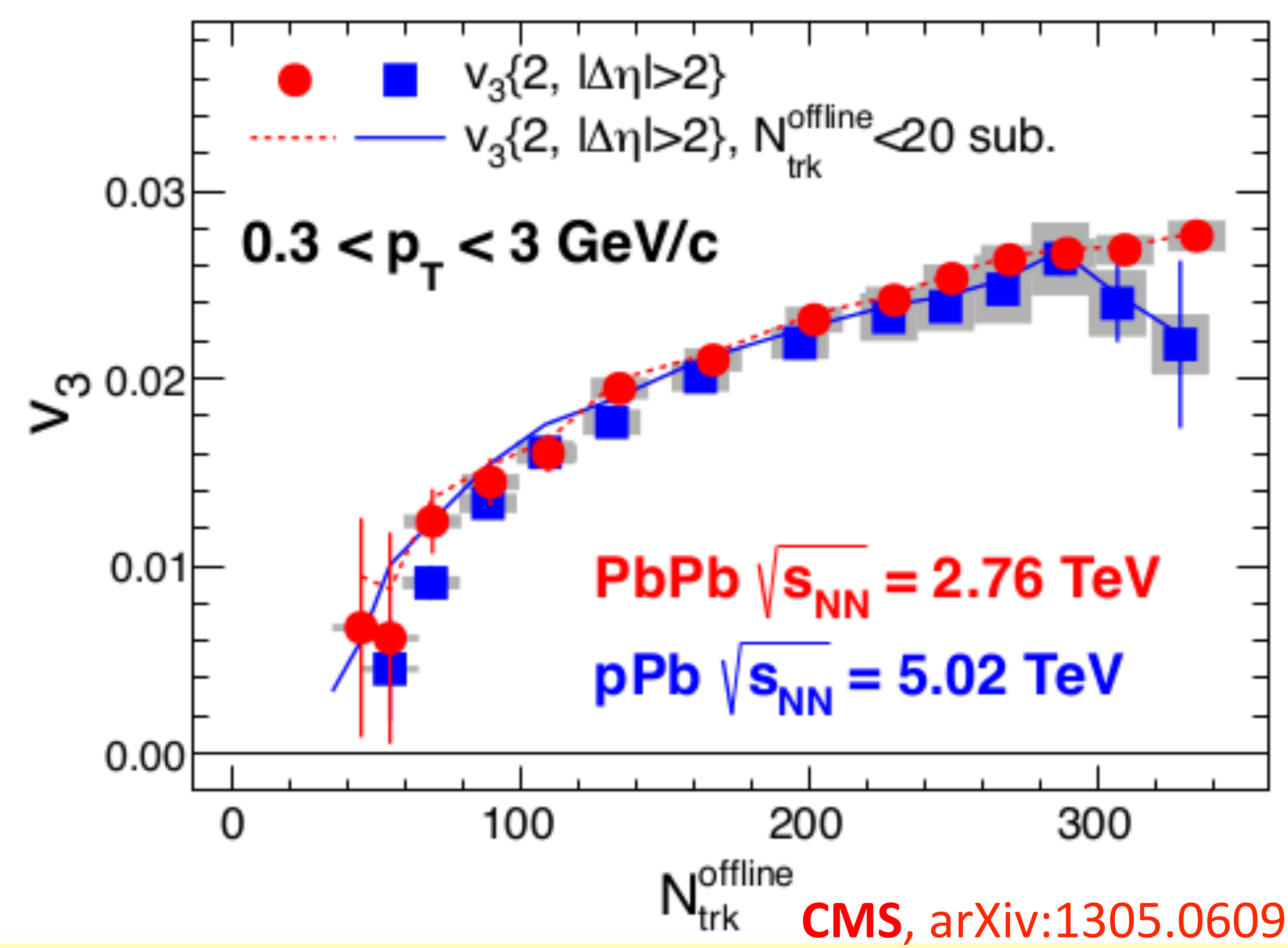

CMS, arXiv:1305.0609

- Observe essentially the same v3 in pPb as in PbPb
- Turn on at around M=50 tracks
- Established picture in PbPb
- Fluctuations of initial state are transformed into final state through interactions
- Hydrodynamical predictions (4.4 TeV, arXiv:1112.0915) consistent with pPb data

Nuclear Physics Based Applications

INPC 2013

INTERNATIONAL
NUCLEAR
PHYSICS
CONFERENCE

NUCLEAR PHYSICS AND NEW SYSTEMS FOR ENERGY PRODUCTION AND WASTE TRANSMUTATION

Sylvie Leray
CEA/Saclay, Irfu/SPhN

Sponsored by EPJ Plus
Recognized by European Physical Society

COUNTRY	NUCLEAR ELECTRICITY GENERATION 2011		REACTORS OPERABLE May 2013		REACTORS UNDER CONSTRUCTION May 2013		REACTORS PLANNED May 2013		REACTORS PROPOSED May 2013	
	billion kWh	% e	No.	MWe net	No.	MWe gross	No.	MWe gross	No.	MWe gross
Argentina	5.9	5.0	2	935	1	745	1	33	2	1400
Armenia	2.4	33.2	1	376	0	0	1	1060		
Bangladesh	0	0	0	0	0	0	2	2000	0	0
Belarus	0	0	0	0	0	0	2	2400	2	2400
Belgium	45.9	54.0	7	5943	0	0	0	0	0	0
Brazil	14.8	3.2	2	1901	1	1405	0	0	4	4000
Bulgaria	15.3	32.6	2	1906	0	0	1	950	0	0
Canada	88.3	15.3	19	13553	0	0	2	1500	3	3800
Chile	0	0	0	0	0	0	0	0	4	4400
China	82.6	1.8	17	13955	28	30550	49	56020	120	123000
Czech Republic	26.7	33.0	6	3766	0	0	2	2400	1	1200
Egypt	0	0	0	0	0	0	1	1000	1	1000
Finland	22.3	31.6	4	2741	1	1700	0	0	2	3000
France	423.5	77.7	58	63130	1	1720	1	1720	1	1100
Germany	102.3	17.8	9	12003	0	0	0	0	0	0
Hungary	14.7	43.2	4	1880	0	0	0	0	2	2200
India	28.9	3.7	20	4385	7	5300	18	15100	39	45000
Indonesia	0	0	0	0	0	0	2	2000	4	4000
Iran	0	0	1	915	0	0	2	2000	1	300
Israel	0	0	0	0	0	0	0	0	1	1200
Italy	0	0	0	0	0	0	0	0	10	17000
Japan	156.2	18.1	50	44396	3	3036	9	12947	3	4145
Jordan	0	0	0	0	0	0	1	1000		
Kazakhstan	0	0	0	0	0	0	2	600	2	600
Korea DPR (North)	0	0	0	0	0	0	0	0	1	950
Korea RO (South)	147.8	34.6	23	20787	4	5415	6	8730	0	0
Lithuania	0	0	0	0	0	0	1	1350	0	0
Malaysia	0	0	0	0	0	0	0	0	2	2000
Mexico	9.3	3.6	2	1600	0	0	0	0	2	2000
Netherlands	3.9	3.6	1	485	0	0	0	0	1	1000
Pakistan	3.8	3.8	3	725	2	680	0	0	2	2000
Poland	0	0	0	0	0	0	6	6000	0	0
Romania	10.8	19.0	2	1310	0	0	2	1310	1	655
Russia	162.0	17.6	33	24164	10	9160	24	24180	20	20000
Saudi Arabia	0	0	0	0	0	0	0	0	16	17000
Slovakia	14.3	54.0	4	1816	2	880	0	0	1	1200
Slovenia	5.9	41.7	1	696	0	0	0	0	1	1000
South Africa	12.9	5.2	2	1800	0	0	0	0	6	9600
Spain	55.1	19.5	7	7002	0	0	0	0	0	0
Sweden	58.1	39.6	10	9399	0	0	0	0	0	0
Switzerland	25.7	40.8	5	3252	0	0	0	0	3	4000
Thailand	0	0	0	0	0	0	0	0	5	5000
Turkey	0	0	0	0	0	0	4	4800	4	4500
Ukraine	84.9	47.2	15	13168	0	0	2	1900	11	12000
UAE	0	0	0	0	1	1400	3	4200	10	14400
United Kingdom	62.7	17.8	16	10038	0	0	4	6680	9	12000
USA	790.4	19.2	103	101570	3	3618	9	10860	15	24000
Vietnam	0	0	0	0	0	0	4	4000	6	6700
WORLD**	2518	c13.5	435	374,524	66	68,309	160	176,74	319	361,1
	billion kWh	% e	No.	MWe	No.	MWe	No.	MWe	No.	MWe
	NUCLEAR ELECTRICITY GENERATION		REACTORS OPERABLE		REACTORS UNDER CONSTRUCTION		ON ORDER or PLANNED		PROPOSED	

Source: World Nuclear Association (May 2013)

FUTURE OF NUCLEAR ENERGY

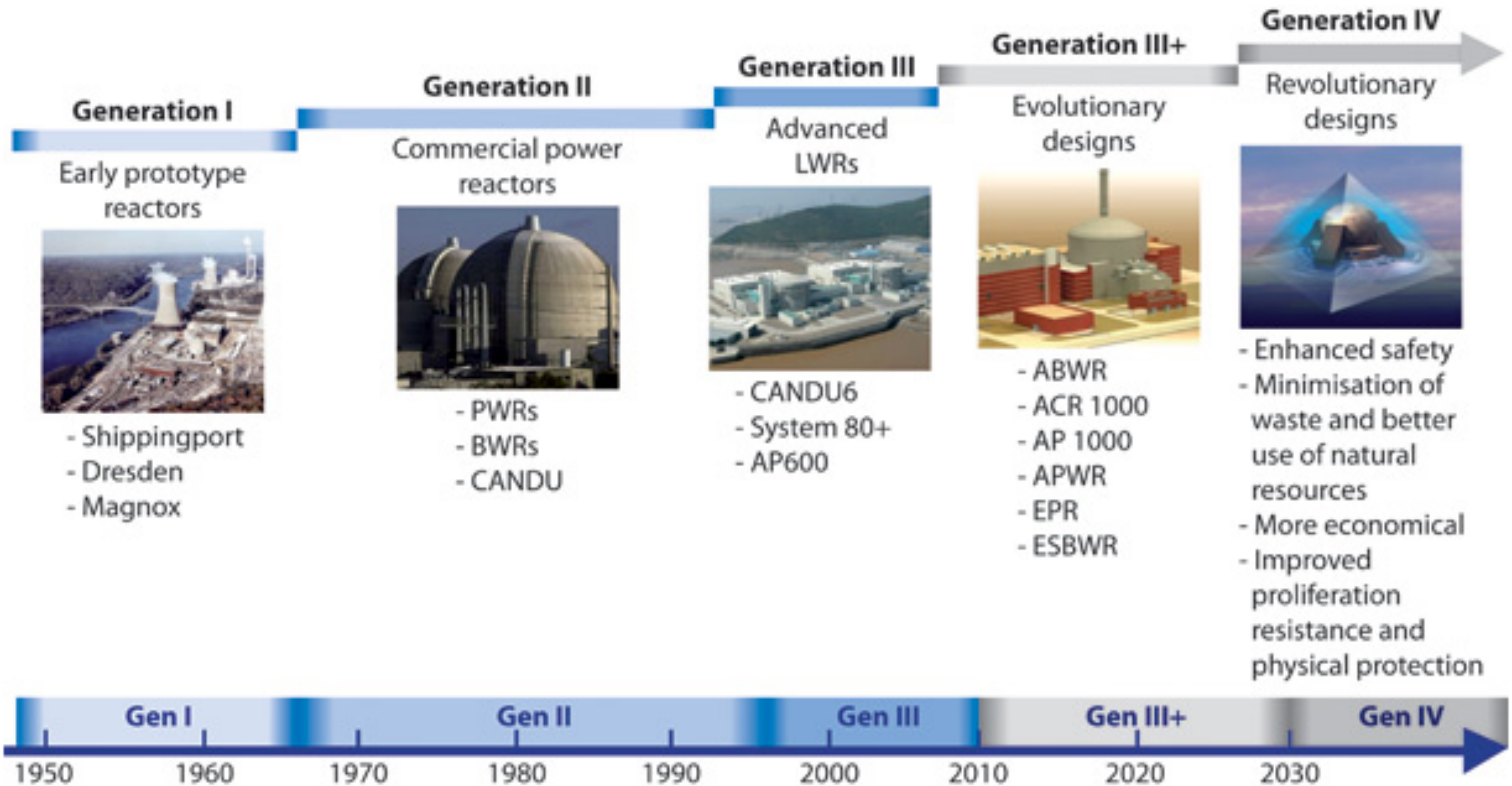

Source: Nuclear Energy Today © OECD/Nuclear Energy Agency 2012

NUCLEAR DATA NEEDS

- *Existing, Gen-III reactors*
  - *Optimization of fuel burn-up*
  - *Increase of life time*
  - *Safety margin reduction: decay heat, delayed n fraction*
- *Fast reactors (Gen-IV)*
  - *New fuel, cladding, coolant materials*
  - *Minor actinide transmutation*
- *ADS*
  - *Spallation target radioactive inventory*
  - *Material damage*

- *cross-sections*
  - *capture*
  - *fission*
  - *inelastic, (n,2n)*
- *multiplicities*
  - *prompt and delayed neutrons*
  - *delayed gammas*
- *characteristics of reaction products*
  - *Energy and angular distributions*
  - *fission fragments*
  - *spallation residues*

ANDES FP7 PROJECT

www.andes-nd.eu

ANDES main experimental facilities

Accurate Nuclear Data for nuclear Energy Sustainability

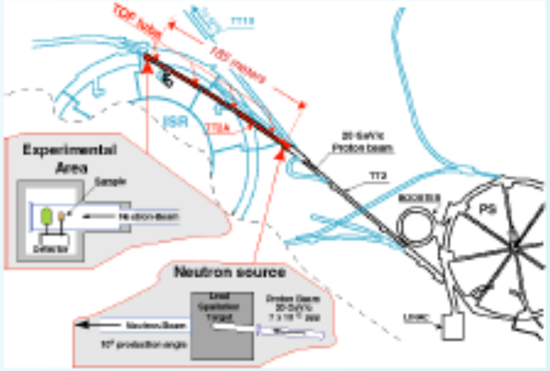

CERN n_TOF

IRMM in the JRC

GANIL

IFIN-HH

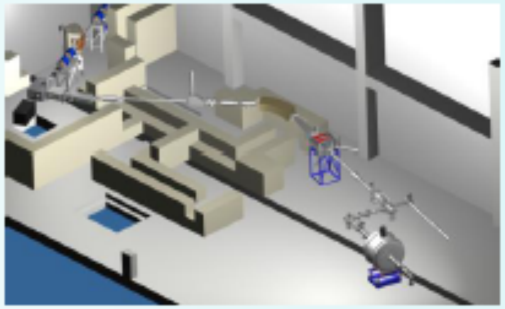

IGISOL at Jyväskylä

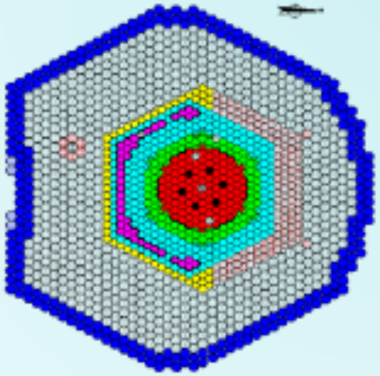

PROFIL at PHENIX

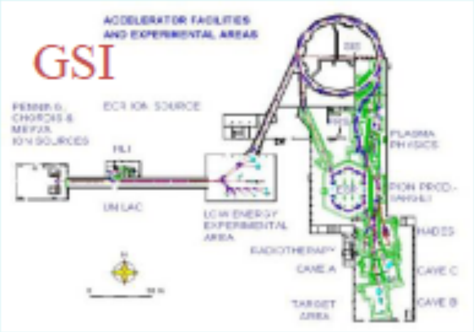

GSI

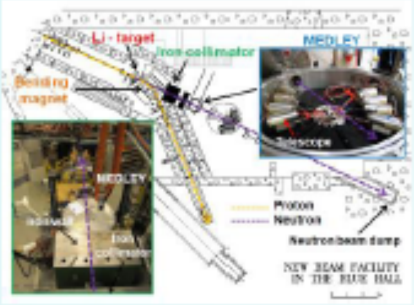

TSL

CAPTURE AND FISSION CROSS-SECTIONS

n_TOF CERN

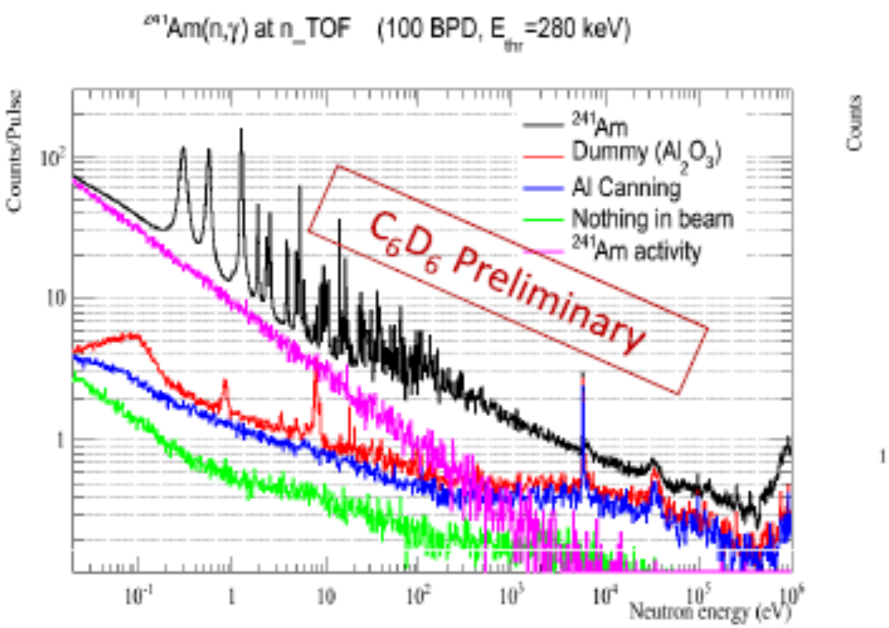

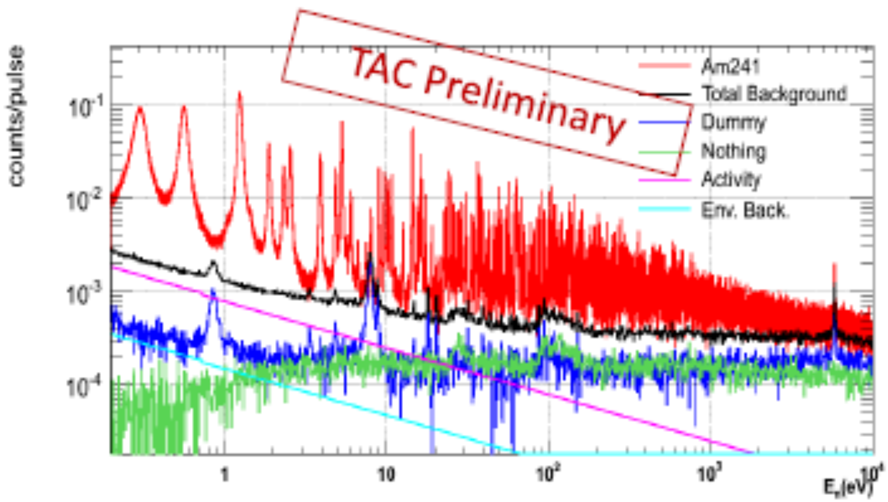

The ^{245}Cm(n,f) cross-sections

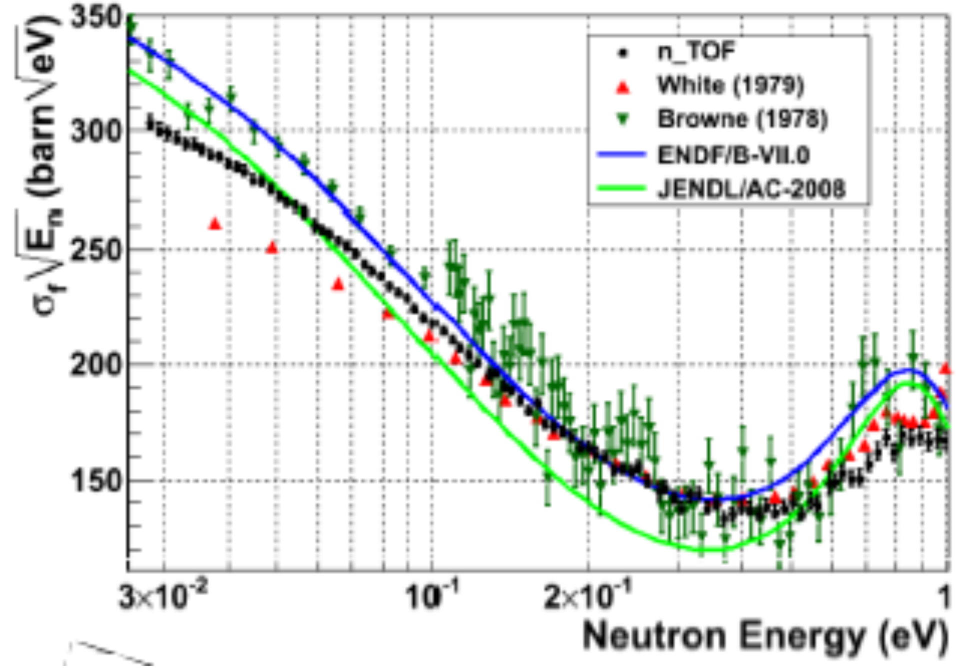

M. Calviani et al., PRC 85, 034616 (2012)

Modelling of spallation reactions

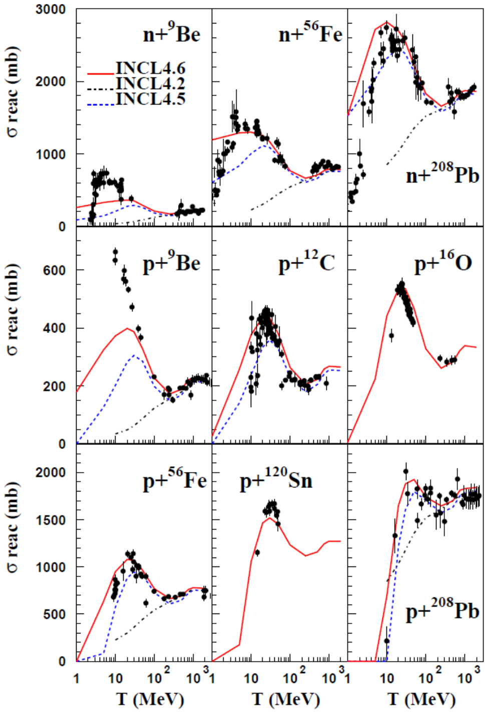

New high quality data

- isotopic distributions of residues at FRS
- excitation function measurements (Michel et al., Titarenko et al.)
- light charged particles DDXS and neutrons multiplicities by the NESSI / PISA collaborations

↪ **Highly predictive models for implementation into transport codes: INCL+ABLA, CEM, FLUKA…**

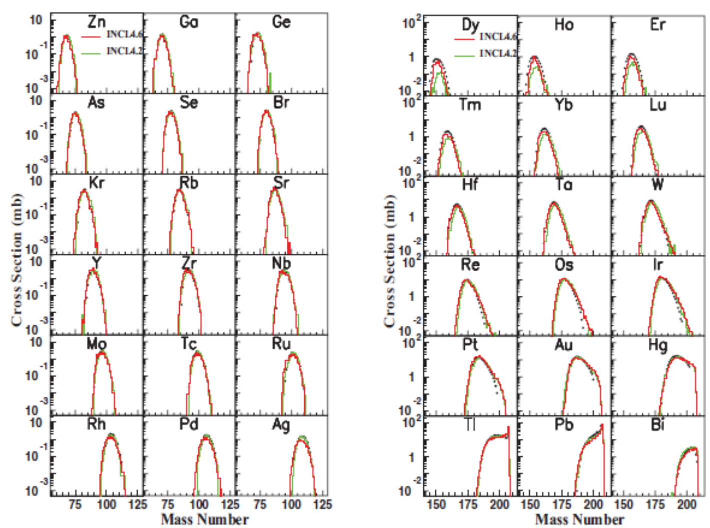

Data fromEnqvist et al.

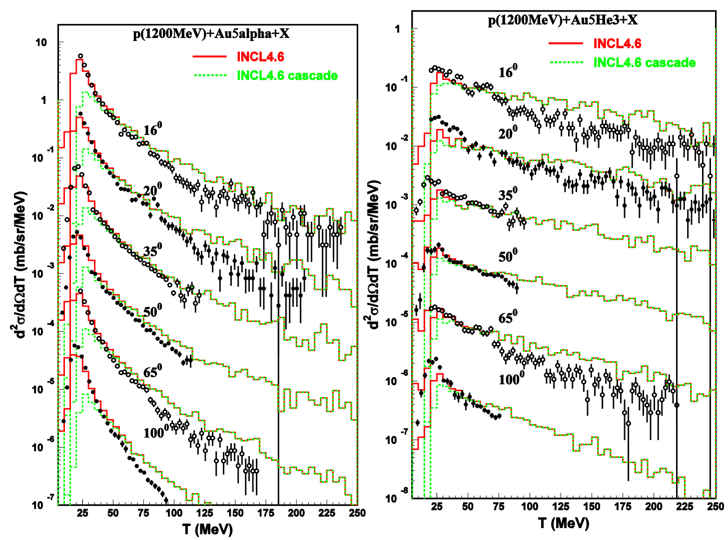

Data from Herbach et al.

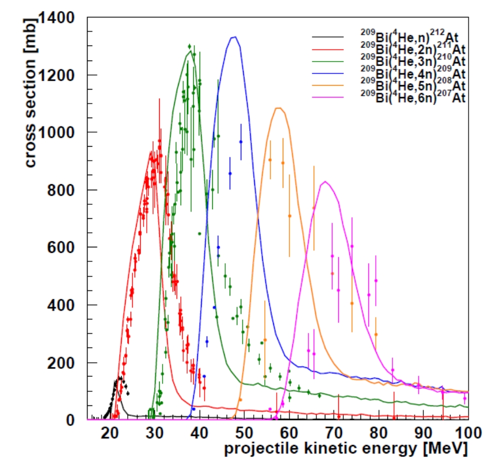

From A. Boudard et al., Phys. Rev. C 87, 014606 (2013)

New Facilities and Instrumentation

How to Polarize Antiprotons?

- Spin-1/2 particles ⟶ 2 states

selective removal

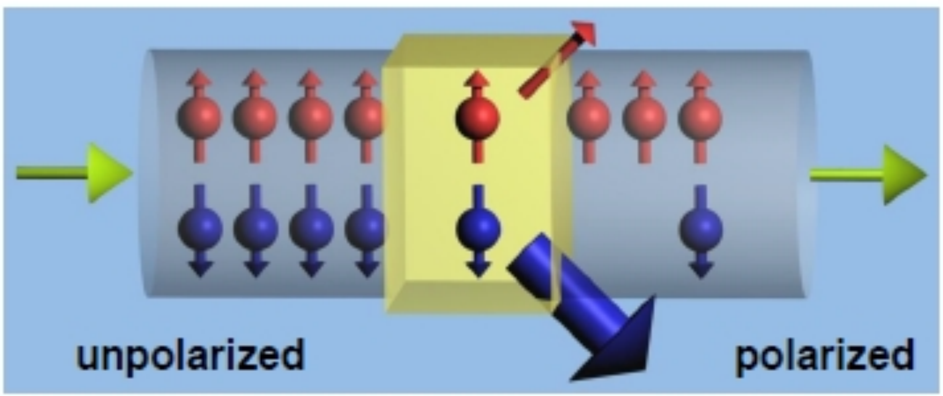

selective flip

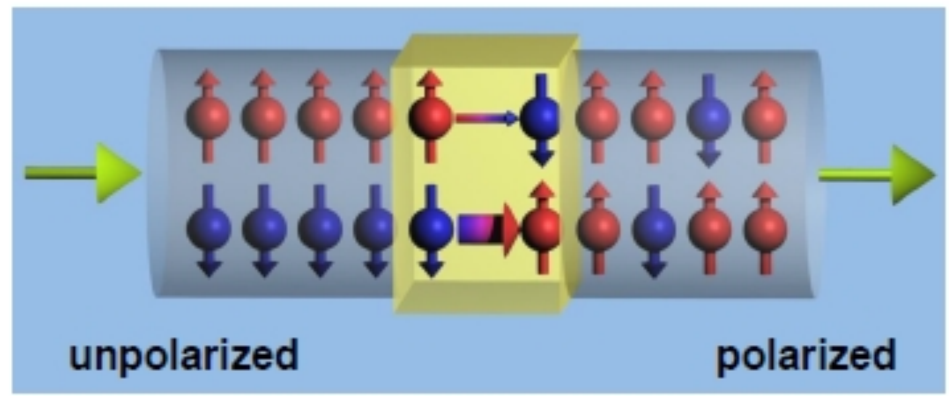

- Selective removal reduces beam intensity – Selective flip leaves intensity
- $e^+ \bar{p}$ spin-flip cross-section is too low to use selective flip

$\sigma_{\parallel} < 3.2 * 10^7$ b
$\sigma_{\perp} < 1.7 * 10^7$ b

D. Oellers. et al., Phys. Lett. B 674 (2009) 269

How to Polarize Antiprotons?

Spin filtering

Polarization build-up of a circulating particle beam by interaction with a polarized gas target

$$\sigma_{tot} = \sigma_0 + \sigma_1(\vec{P}\cdot\vec{Q}) + \sigma_2(\vec{P}\cdot\hat{k})(\vec{Q}\cdot\hat{k})$$

P…beam particle spin orientation
Q…target particle spin orientation
k || beam direction

$$P(t) = \frac{N_\uparrow - N_\downarrow}{N_\uparrow + N_\downarrow} = \tanh\left(\frac{t}{\tau_1}\right) \approx t \cdot \tilde{\sigma}_1 \cdot Q \cdot d_t \cdot f$$

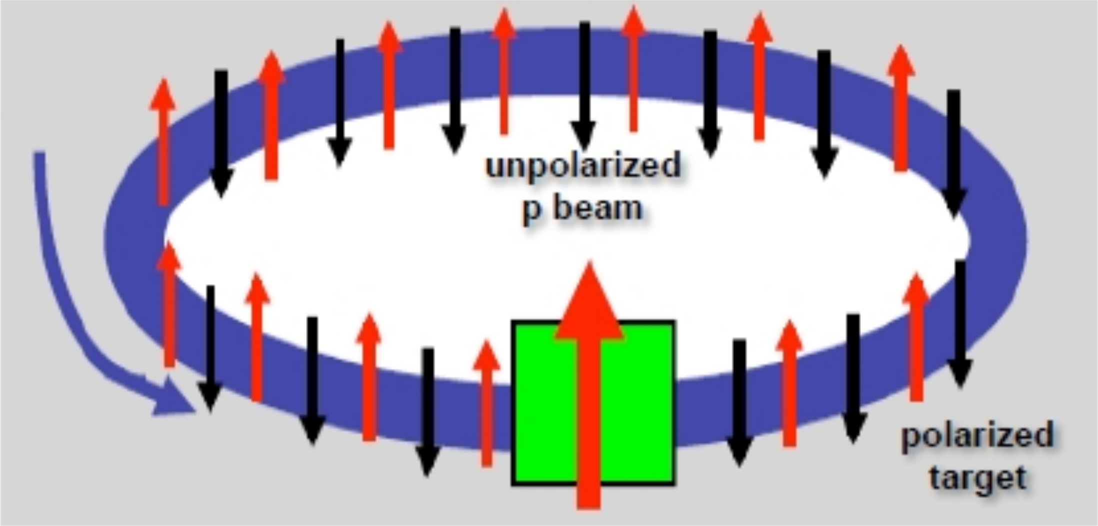

How to Polarize Antiprotons?

Spin filtering

Polarization build-up of a circulating particle beam by interaction with a polarized gas target

$$\sigma_{tot} = \sigma_0 + \sigma_1(\vec{P}\cdot\vec{Q}) + \sigma_2(\vec{P}\cdot\hat{k})(\vec{Q}\cdot\hat{k})$$

P…beam particle spin orientation
Q…target particle spin orientation
k || beam direction

$$P(t) = \frac{N_\uparrow - N_\downarrow}{N_\uparrow + N_\downarrow} = \tanh\left(\frac{t}{\tau_1}\right) \approx t\cdot\tilde{\sigma}_1\cdot Q\cdot d_t\cdot f$$

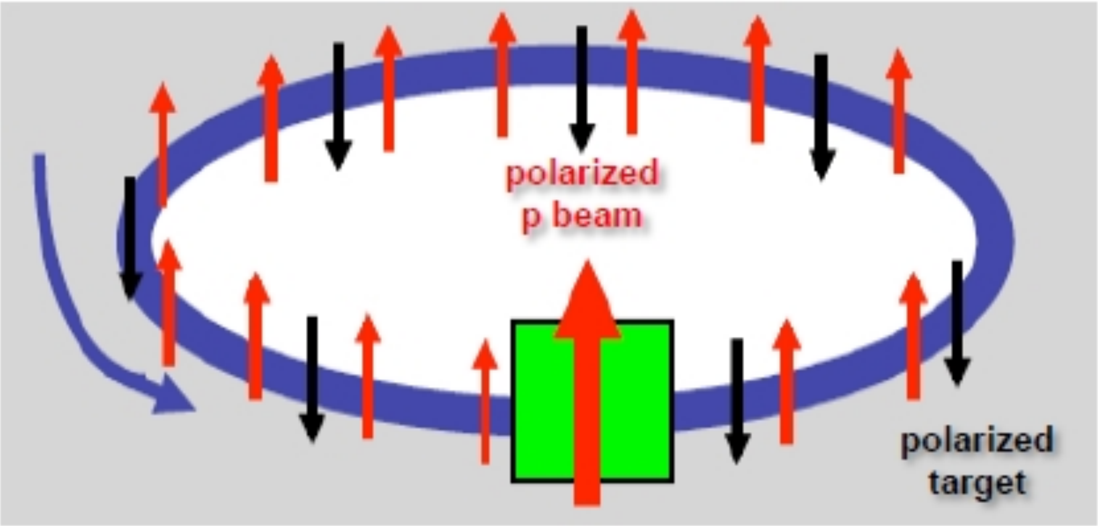

How to Polarize Antiprotons?

Spin filtering

Polarization build-up of a circulating particle beam by interaction with a polarized gas target

$$\sigma_{tot} = \sigma_0 + \sigma_1(\vec{P}\cdot\vec{Q}) + \sigma_2(\vec{P}\cdot\hat{k})(\vec{Q}\cdot\hat{k})$$

P…beam particle spin orientation
Q…target particle spin orientation
k || beam direction

$$P(t) = \frac{N_\uparrow - N_\downarrow}{N_\uparrow + N_\downarrow} = \tanh\left(\frac{t}{\tau_1}\right) \approx t\cdot\tilde{\sigma}_1\cdot Q\cdot d_t\cdot f$$

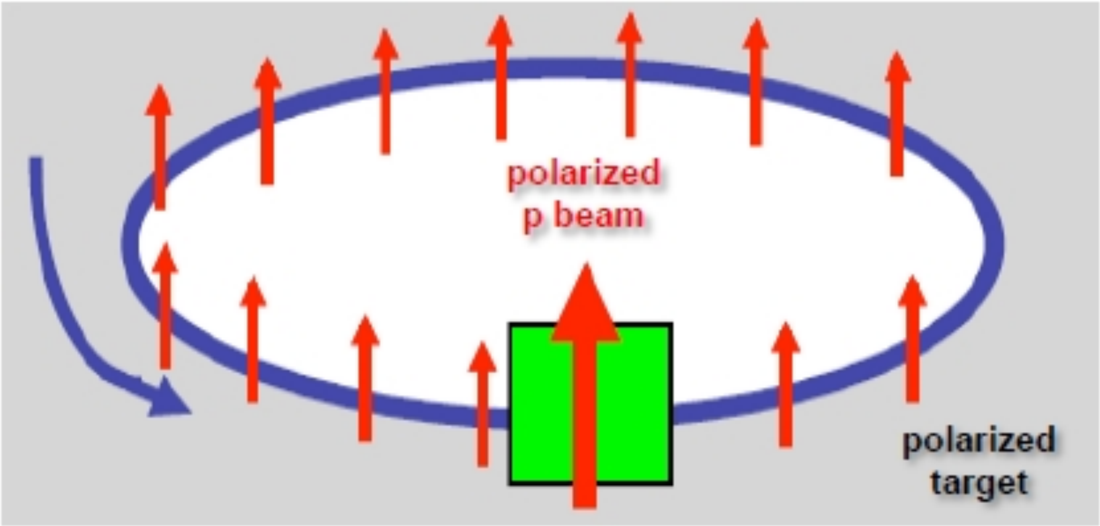

Results

- **P measured for 0s, 12000s and 16000s filtering time**

- **Polarization build with time:**

$$\frac{dP}{dt} = (4.8 \pm 0.8) \cdot 10^{-7} s^{-1}$$

- **Polarizing cross section:**

$$\boxed{\tilde{\sigma}_1 = -23.4 {\pm 3.9(stat.) \atop \pm 1.8(syst.)} mb}$$

W. Augustyniak. et al., Phys. Lett. B 718 (2012) 64

Theory: $\tilde{\sigma}_1 = -26.9\, mb$

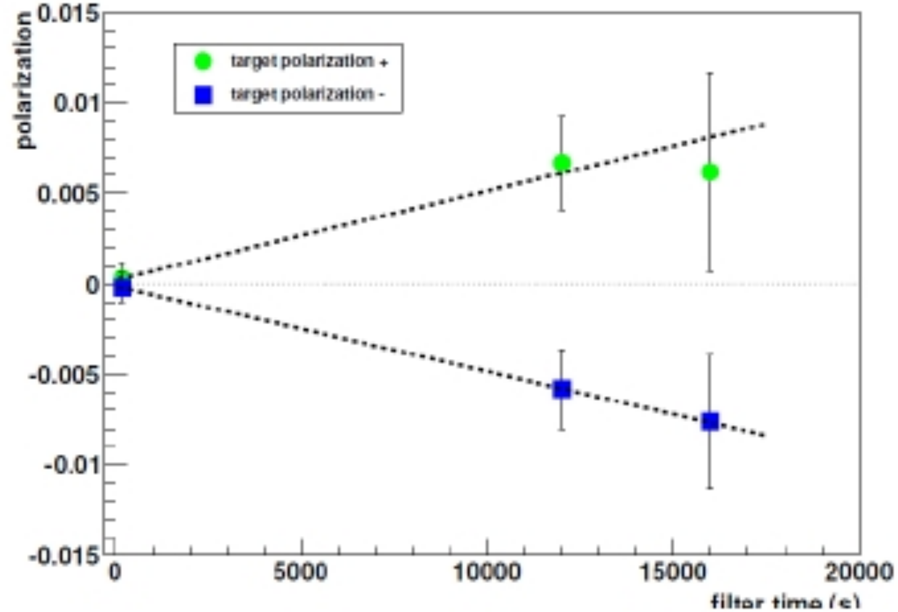

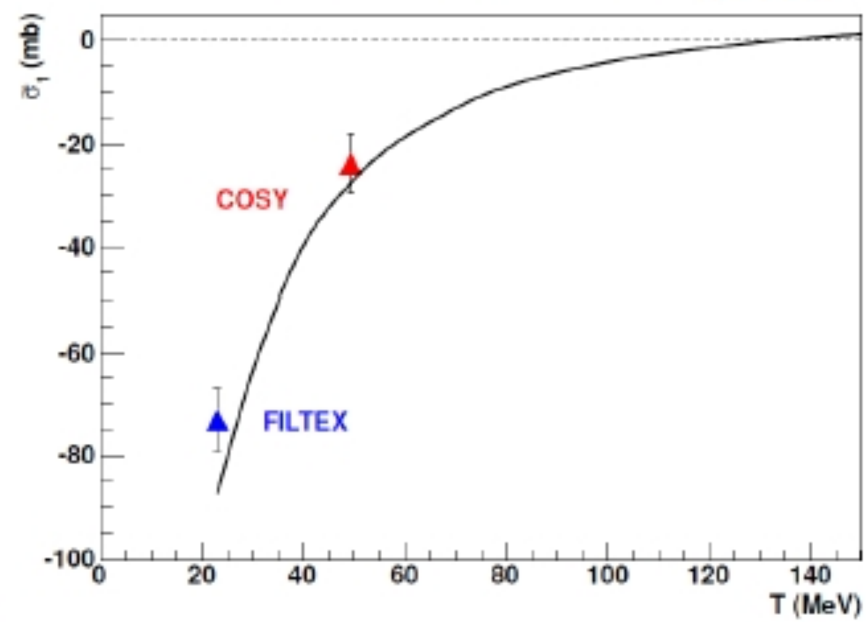

AFTER@LHC :
A Fixed-Target ExpeRiment at the LHC

Jean-Philippe Lansberg
IPN Orsay, Université Paris-Sud

on behalf of M. Anselmino (Torino), R. Arnaldi (Torino), S.J. Brodsky (SLAC), V. Chambert (IPNO), J.P. Didelez (IPNO), F. Fleuret (LLR), B. Genolini (IPNO), E.G. Ferreiro (USC), C. Hadjidakis (IPNO), C. Lorcé (IPNO),A. Rakotozafindrabe (CEA), P. Rosier (IPNO), I. Schienbein (LPSC), E. Scomparin (Torino), and U.I. Uggerhøj (Aarhus)

The beam extraction

★ The LHC beam may be extracted using "Strong crystalline field" **without any decrease in performance of the LHC !**

E. Uggerhøj, U.I Uggerhøj, NIM B 234 (2005) 31, Rev. Mod. Phys. 77 (2005) 1131

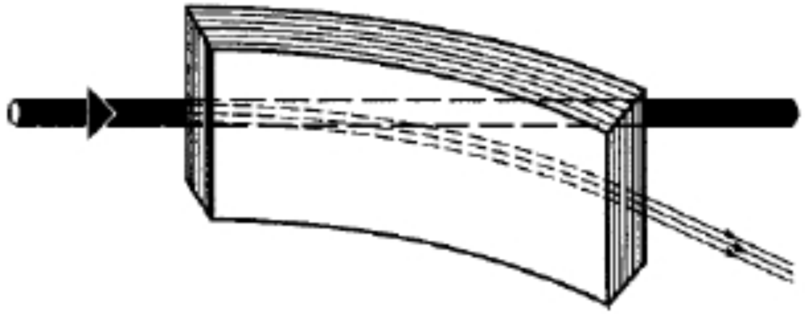

★ Illustration for collimation

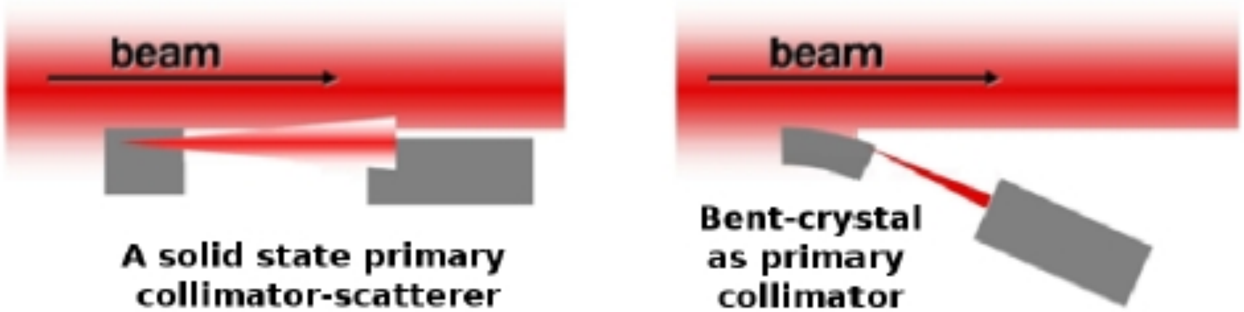

★ Tests will be performed on the LHC beam: LUA9 proposal approved by the LHCC

Key studies: gluons in the proton

Key studies: gluon contribution to the proton spin

Key studies: large-x gluon content of the nucleus

Key studies: precision heavy-flavour studies in Heavy-Ion Collisions

- Both p and Pb LHC beams can be extracted without disturbing the other experiments
- Extracting a few per cent of the beam $\to 5 \times 10^8$ protons per sec
- This allows for high luminosity pp, pA and PbA collisions at $\sqrt{s} = 115$ GeV and $\sqrt{s_{NN}} = 72$ GeV
- **Example**: precision quarkonium studies taking advantage of
  - high luminosity (reach in y, P_T, small BR channels)
  - target versatility (nuclear effects, strongly limited at colliders)
  - modern detection techniques (e.g. γ detection with high multiplicity)
- This would likely prepare the ground for $g(x, Q^2)$ extraction
- A wealth of possible measurements:
  DY, Open b/c, jet correlation, UPC... (not mentioning secondary beams)
- Planned LHC long shutdown (< 2020 ?) could be used to install the extraction system
- Very good complementarity with electron-ion programs

25th International Nuclear Physics Conference INPC2013
Firenze, June 4th 2013

Small-x Physics in eA at the LHeC: Understanding the Initial State of URHIC

Néstor Armesto

Departamento de Física de Partículas and IGFAE, Universidade de Santiago de Compostela

and

CERN, Physics Department, Theory Unit

nestor.armesto@usc.es

for the LHeC Study group, http://cern.ch/lhec

Relevance for the HI program:

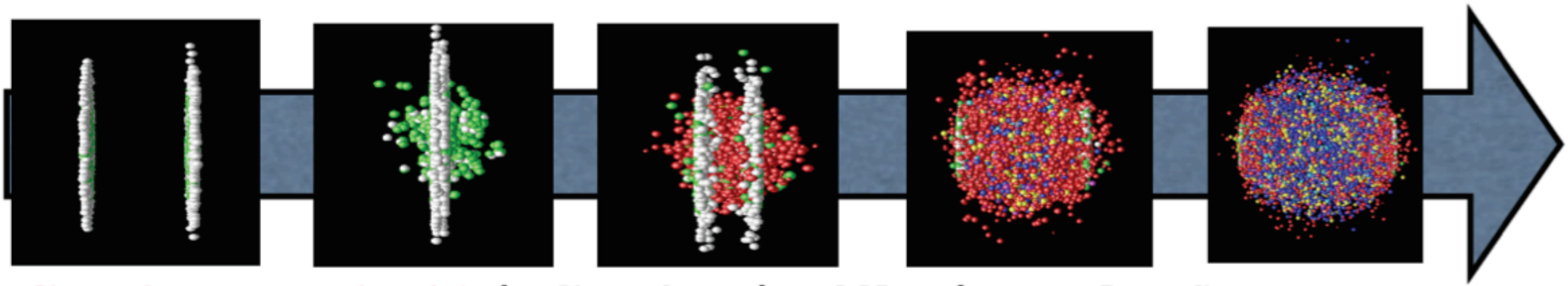

Gluons from saturated nuclei → Glasma? → QGP → Reconfinement

- Nuclear wave function at small x: nuclear structure functions.

- Particle production at the very beginning: which factorisation in eA?

- How does the system behave as ~ isotropised so fast?: initial conditions for plasma formation to be studied in eA.

- Probing the medium through energetic particles (jet quenching etc.): modification of QCD radiation and hadronization in the nuclear medium.

Accelerator:

electron beam	LR ERL	LR
e- energy at IP[GeV]	60	140
luminosity [10^{32} cm^{-2}s^{-1}]	10	0.44
polarization [%]	90	90
bunch population [10^9]	2.0	1.6
e- bunch length [mm]	0.3	0.3
bunch interval [ns]	50	50
transv. emit. $\gamma\varepsilon_{x,y}$ [mm]	0.05	0.1
rms IP beam size $\sigma_{x,y}$ [μm]	7	7
e- IP beta funct. $\beta^*_{x,y}$ [m]	0.12	0.14
full crossing angle [mrad]	0	0
geometric reduction H_{hg}	0.91	0.94
repetition rate [Hz]	N/A	10
beam pulse length [ms]	N/A	5
ER efficiency	94%	N/A
average current [mA]	6.6	5.4
tot. wall plug power[MW]	100	100

CDR numbers for luminosity, to be considered now as lower bounds.

$\sqrt{s} \simeq 0.8$ TeV/nucleon

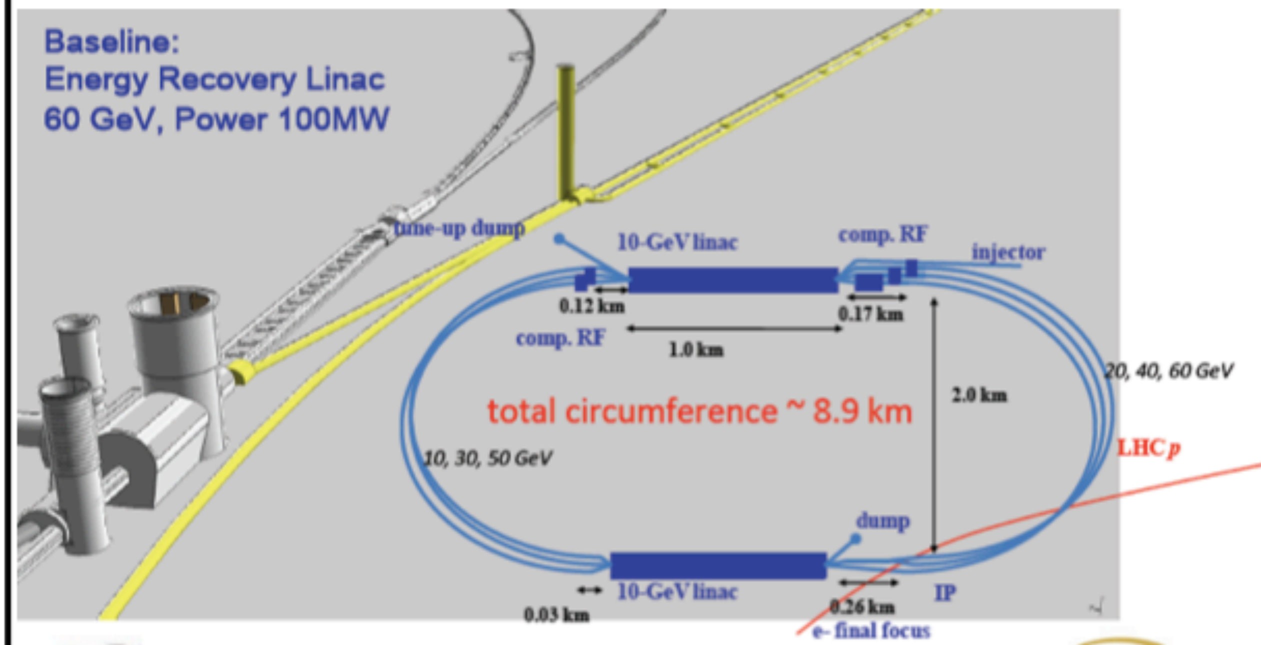

Luminosity per nucleon

$$L_{eN} = \begin{cases} 9 \times 10^{31}\ \mathrm{cm}^{-2}\mathrm{s}^{-1} & \text{(Nominal Pb)} \\ 1.6 \times 10^{32}\ \mathrm{cm}^{-2}\mathrm{s}^{-1} & \text{(Ultimate Pb)} \end{cases}$$

eD: $L_{eN} = AL_{eA} >\sim 3\times10^{31}$ cm^{-2}s^{-1}

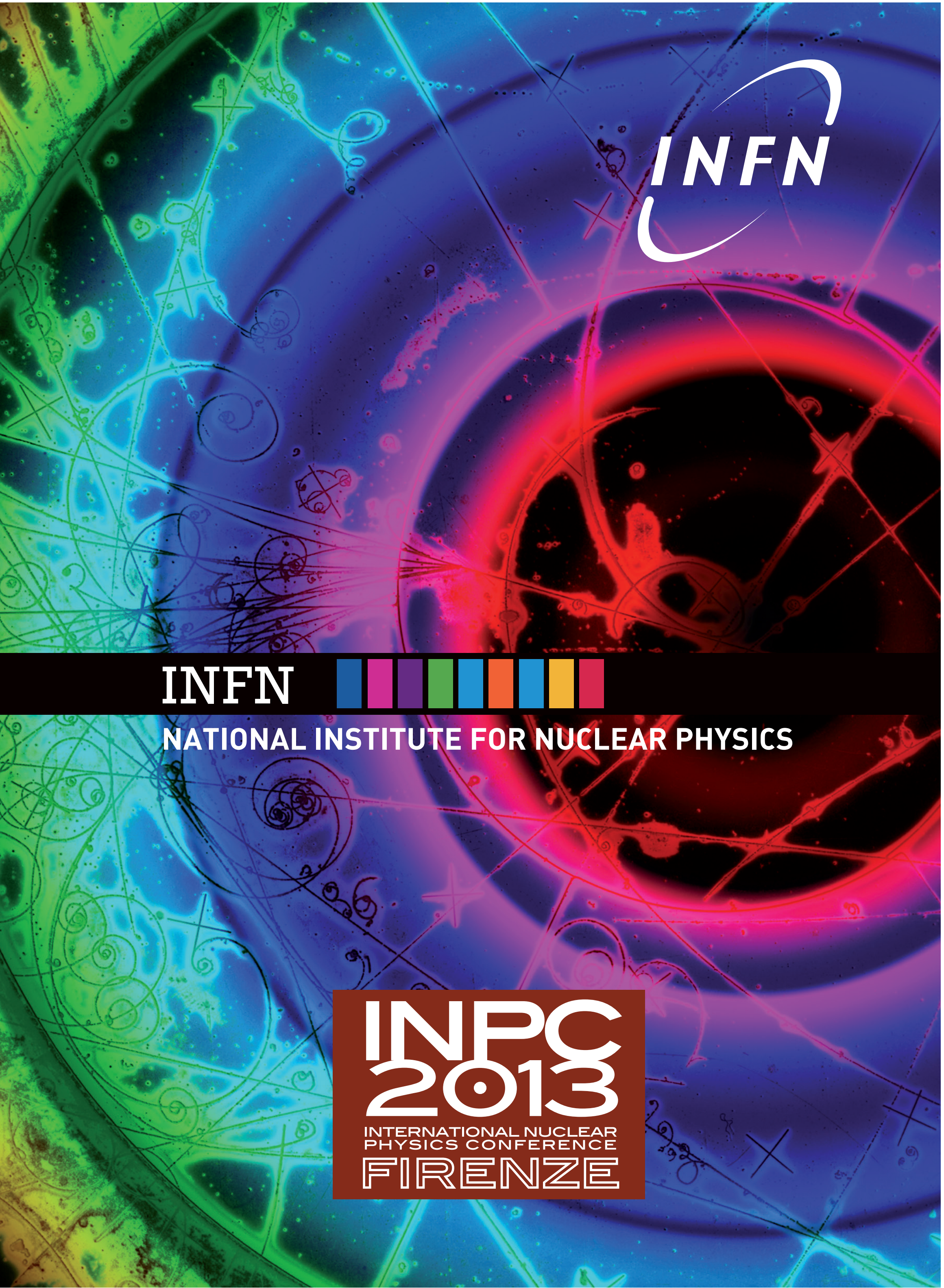

After a century, nuclear physics is a robust and vital science, motivated by the desire to account for the behavior of matter. Today, the frontiers of knowledge are much wider than in the previous golden decades, going from the nuclear structures, to the extremely hot matter passing through hadron structures and dynamics, double beta decay and the nature of the neutrino mass or the complex phenomena that emerge from the fundamental laws. INFN has nuclear physics in its DNA and everybody of us is proud to host such an important conference that - I'm sure - will give a wide world overview, indicating the future paths beyond the actual limit of our knowledge.

Fernando Ferroni
INFN President